UiT
THE ARCTIC UNIVERSITY OF NORWAY

Faculty of Science & Technology

Department of Geology

Mid Miocene – Early Pliocene depositional environment on the northern part of the Mid-Norwegian Continental Shelf

Bendik Skjevik Blakstad

Master thesis in Geology, GEO-3900
May 2016

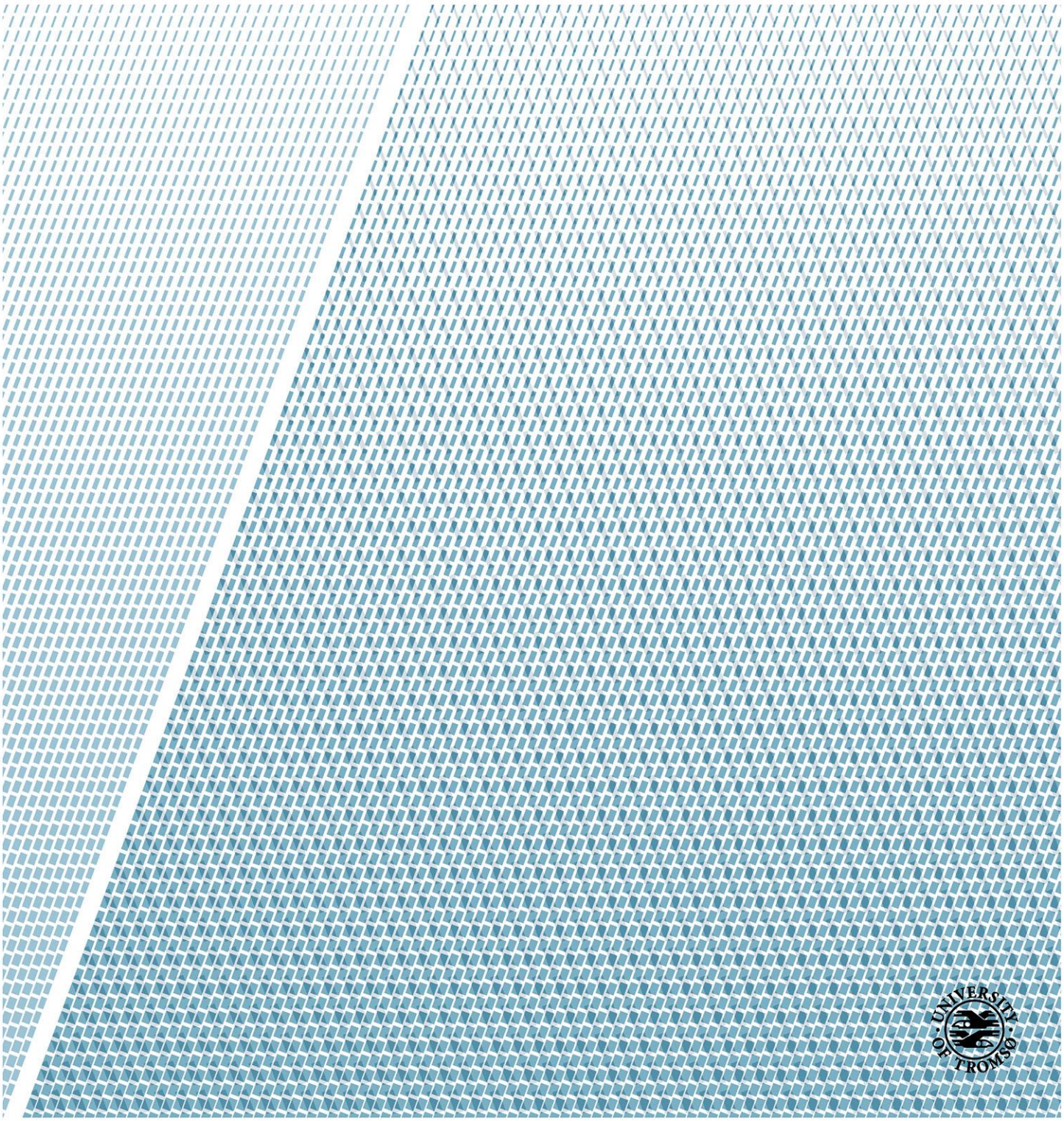

Abstract

Based on the study of 2D seismic data, this thesis have focused on the depositional environment during the deposition of the Kai formation (Mid-Miocene – Early Pliocene) on the Mid-Norwegian continental margin, in order to increase our knowledge of the evolution of the paleo-environment in the time-period right before the development of the large Northern Hemisphere ice sheets. Based on a seismic stratigraphic analysis, correlated to selected well logs, the deposits comprising the Kai formation were divided into seismic sub-units. The stratigraphy of the formation and the sub-units, as well as the geometry of multiple paleo-sea-floor surfaces have been described and discussed in relation to the development of the ocean circulation pattern in the Norwegian Sea during this time.

The study area were subdivided into an inner- (Trøndelag Platform) and outer (Vøring Basin) part of the continental shelf. The Kai formation is dominated ooze sediments in the deeper basins, and mainly clayey sediments on the inner shelf. Multiple anticlinal highs and structures can be observed within the study area. Based on observations near the flanks of these highs, it is evident that the highs have played a larger role in the distribution and flow pattern of ocean currents under the deposition of the Kai formation. The largest high is the Helland-Hansen Arch, which separates the Kai formation on the inner and outer shelf by an area of non-deposition, located on top of the arch. The relation between the Kai formation and the Molo formation have been included in the study, with alternative interpretations of an undecided sediment package located between the Brygge and Molo formations proposed.

Contouritic deposits, interpreted to be mounded elongated contourite drifts with associating moat structures, were observed within the Kai formation on both the inner and outer part of the shelf, suggesting ocean current activity in the Vøring basin, as well on the Trøndelag Platform. The contourite drifts suggest a north/northeast ocean current pattern, entering the study area from the south, and exiting in the north/northeastern part of the study area. Multiple generations of contourite deposits were found, some separated by unconformities, suggesting changes in current strength and –pattern, as well as possible sea-level oscillation.

Polygonal fault systems have been observed within the Kai formation in the Vøring Basin. The polygonal faults occur in connection with the expulsion of fluids within the ooze sediments in the Vøring Basin, as well as overpressure from the overlying Naust formation.

Acknowledgements

Da var det snart slutt på livet som student ved Universitetet i Tromsø, og etter 5 år med studier føles det veldig godt, men også litt rart at masteren endelig er på plass. Det har vært en utfordrende periode som har resultert i mange gode minner, og ikke minst fantastiske venner.

Jeg vil først og fremst takke mine to veiledere for å ha støttet og hjulpet meg gjennom det siste året. Professor Jan Sverre Laberg har alltid tatt seg tid til oppfølging og spørsmål, og ikke minst kommet med beroligende ord i stressende perioder. Geolog Bjarne Rafaelsen har gjennom året kommet med gode tips til hvordan jeg kunne produsere et bra sluttresultat. Jeg setter stor pris på all hjelpen jeg har fått, og jeg takker for at jeg fikk muligheten til å jobbe med et så spennende prosjekt. Jeg vil også takke TGS-NOPEC for tilgang til seismiske data.

Jeg har fått mange gode venner gjennom min tid i Tromsø, og vil takke alle som har vært med på den fem år lange reisen. Jeg vil spesielt si takk til Andreas og Frank som alltid har fått meg til å le, både gjennom stressende kvelder på universitetet og glade kvelder på byen. Vi holder kontakten!

Jeg vil også takke familien min for å ha støttet meg gjennom tiden i Tromsø. Dere var alltid bare en telefonsamtale unna, og sørget for at jeg kom meg hjem og fikk ladet batteriene når jeg trengte det.

Spesielt vil jeg takke Sandra for at hun alltid har vært der for meg, og at hun alltid har fått meg til å smile, selv i de travleste eksamensperioder. Du betyr veldig mye for meg, og jeg gleder meg til Oktober når to blir til tre!

Bendik Skjevik Blakstad

Tromsø, May 2016

Table of contents

1. Introduction and objectives

The objective of this thesis is to describe the deposits comprising the Kai Formation on the Mid-Norwegian continental margin using 2D seismic data, discussing the origin of the deposits, as well as derive the paleo-environment under deposition.

The Kai Formation is located mostly on the outer part of the continental shelf, and is dated to mid Miocene – early Pliocene (Eidvin et al., 2007). Based on seismic stratigraphic analysis, the deposits of the Kai formation will be divided into seismic sub-units. The geometry and internal seismic reflection pattern of the sequence will then be described and discussed. The deposits will further be discussed in relation to the development of oceanic circulation in the Norwegian Sea and contribute to an increased understanding of the paleo-climate in the time period, the period before the evolution of the large ice sheets on the Northern Hemisphere. In addition, seismic anomalies will be described and interpreted.

The relation between the Kai and Molo formations towards mainland Norway will also be interpreted and discussed. In addition to this, polygonal fault systems within the Kai formation will be described.

2. Geological background

2.1 Study area

The study area comprises of the northern part of the Mid-Norwegian continental margin, including the Vøring Basin to the west and the surrounding areas of Trøndelag Platform at the inner part of the shelf (Fig. 2-2-1). The 2D seismic lines used are located between 64º50' – 67º50' N and 1º00' – 12º00' E (Fig. 2-1-1).

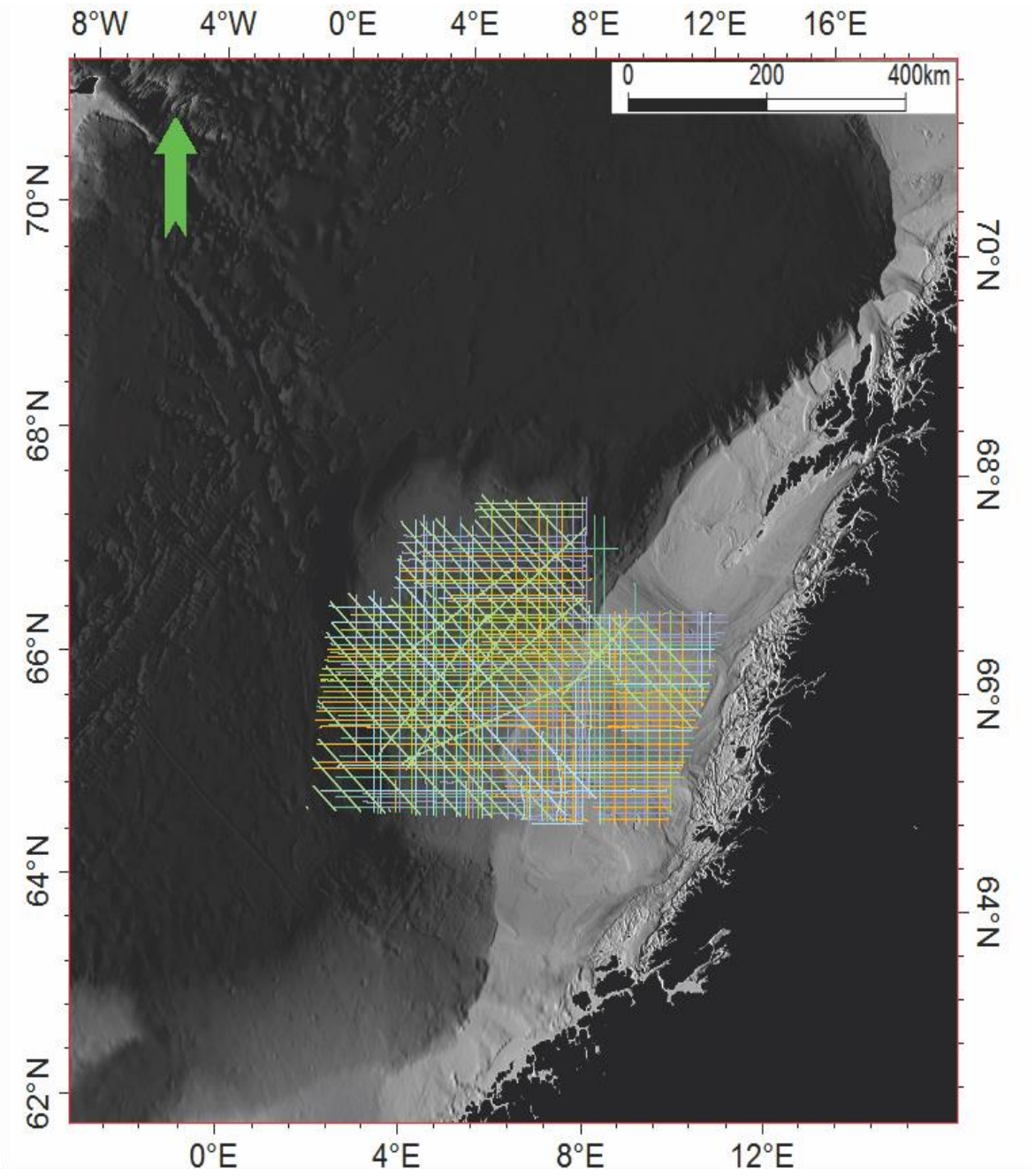

Figure 2-1-1: Overview map of the Mid-Norwegian continental margin, and the location of the 2D-seismic lines constituting the study area.

2.2 Morphology of the Mid-Norwegian continental margin

The present-day morphology of the Mid-Norwegian continental margin is mainly a product of the progradation of the shelf during the last ~3 million years (Rise et al., 2005). The Mid-Norwegian continental margin can be divided into three main provinces; Møre-, Vøring- and Lofoten-Vesterålen Margin (Faleide et al., 2008) *(Fig. 2-2-1).*

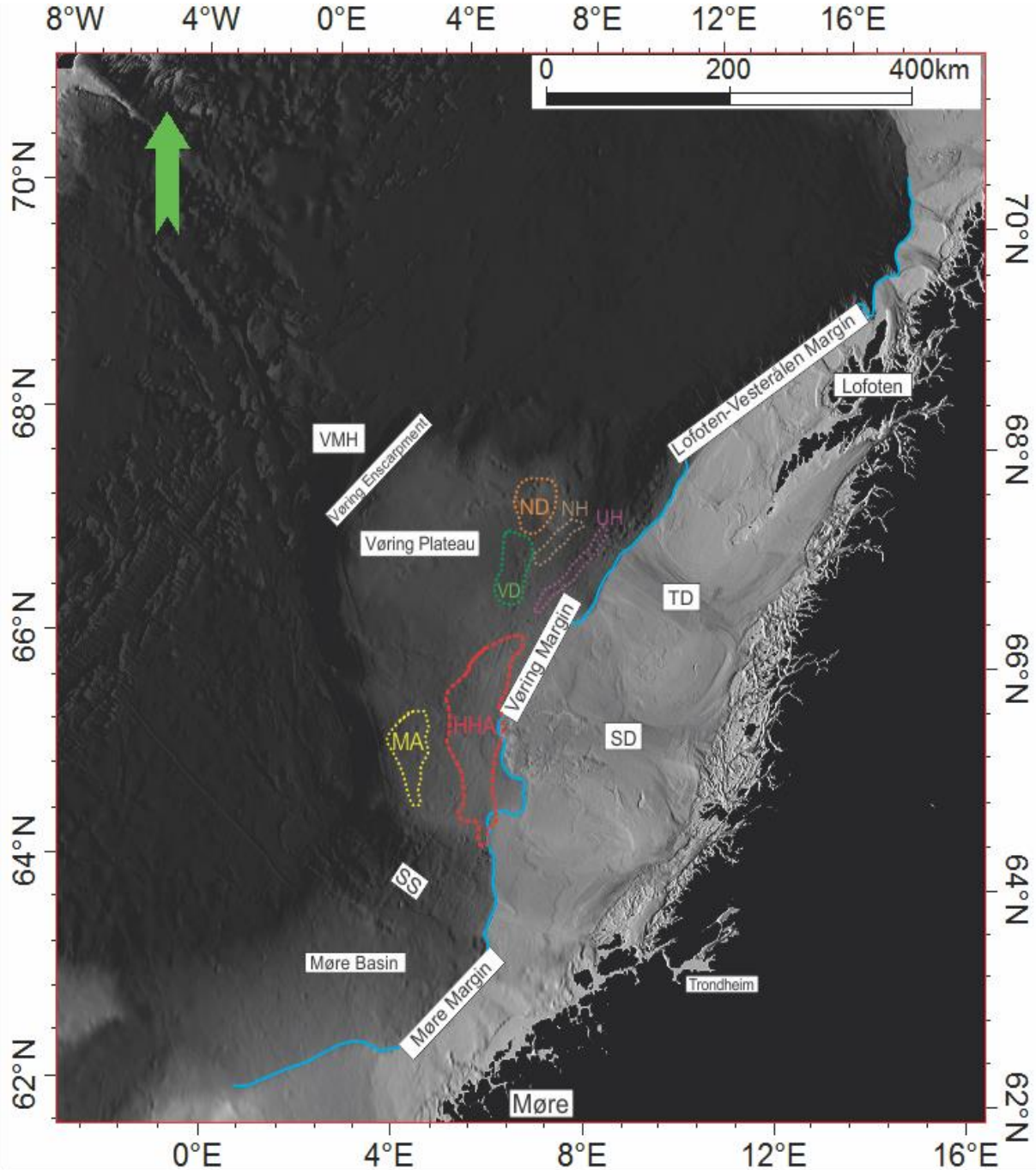

Figure 2-2-1: Overview map of the mid-Norwegian Margin with location of structural elements. VMH: Vøring Marginal High; ND: Naglfar Dome; UH: Utgard High; NH: Nyk High; VD: Vema Dome; TD: Trænadjupet; SD: Sklinnadjupet; HHA: Helland Hansen Arch; MA: Modgunn Arch; SS: Storegga Slide. Blue line displaying the Shelf edge.

The Møre Margin is located in the southwestern part of the Mid-Norwegian continental margin, the Vøring Margin comprise the middle part, and the Lofoten-Vesterålen margin is located towards the north-east (Faleide et al., 2008). Faleide et al. (2008) describes the three main provinces each to be approximately 400-500km long. The continental margin is less than 100 km wide at the Møre margin, and expands to 250 km at Vøring margin, before it narrows northwards. Outside Lofoten, the margin is found to be only 60-80 km wide (Ottesen et al., 2009). The Norwegian continental slope is found to be steepest where the margin is narrow. The continental slope on the Lofoten-Vesterålen margin can reach a gradient of 5º, while the central parts of the Vøring Plateau only reaches a gradient of 1º (Dahlgren et al., 2002). The mid-Norwegian shelf is characterized by shallow banks which are separated by deeper troughs. The banks are located at water depths between 50 and 300 meters, while the troughs can be found between 150 and 550 meters (Ottesen et al., 2005; Rise et al., 2005). These troughs may have played an important part in the development of the margin, as they can represent pathways for enhanced glacial transport by paleo ice-streams during the late Quaternary (Ottesen et al., 2001).

The Møre margin is underlain by the Møre Basin (Fig. 2-2-1). The basins sediment succession is thickest in the western part, and decreasing toward the mainland of Norway. The Møre margin is characterized by a thick Cretaceous basin fill and a gentle slope (Faleide et al., 2008). **The Vøring Margin** is underlain by the Vøring basin to the northwest (Fig. 2-2-1), ending with the Vøring Marginal High (VMH) (Fig. 2-2-1). The Vøring Basin can be subdivided into a number of smaller basins and highs, reflecting differential vertical movements during the Late Jurassic-Early Cretaceous basin evolution (Faleide et al., 2008). Southeast of the Margin, the Trøndelag Platform is located. The outer part of VMH has an abnormally thick oceanic crust, while the inner part has a stretched continental crust, which is covered by Early Eocene basalts and is underplated by mafic intrusions (Faleide et al., 2008). During Mid-Miocene the VMH experienced a renewed uplift episode, due to compression. This also affected the Vøring basin, where further doming and elevation of the highs is inferred (Brekke, 2000; Laberg et al., 2005a). The Vøring Margin is located in the middle of the study area (Fig. 2-2-1). The northern part of the continental margin is **the Lofoten-Vesterålen margin** (Fig. 2-2-1). This part of the margin is also underlain by sedimentary basins, but the basins here are narrower and shallower than the sedimentary basins located underneath the Vøring and Møre margins (Faleide et al., 2008).

The mid-Norwegian Margin comprises three phases of tectonic-magmatic segmentation (Faleide et al., 2008): (1) Lithospheric extension during the rifting episodes in the latest Cretaceous-Paleocene, leading to breakup and separation of tectonic plates. (2) Central rift, uplift and an increase in igneous activity during the late rifting episode and a few million years after breakup. (3) Change to normal accretionary magma volumes with subsequent continental margin subsidence and maturation from middle Eocene to present day.

2.3 Pre-glacial development of the Norwegian continental margin

2.3.1 Pre-breakup basin formation

Before the continental breakup, the margins bordering the Norwegian-Greenland Sea evolved within a region (Fig. 2-3-1), which have been through periods of regional lithospheric extension over the last 350 Ma. This includes Devonian collapse of the Caledonia mountain chains and Early Eocene continental breakup, as well as subsequent sea-floor spreading. These periods were followed by subsidence and basin formation leading to a series of pre-opening sedimentary basins within the North Atlantic-Arctic region (Lundin et al., 2002).

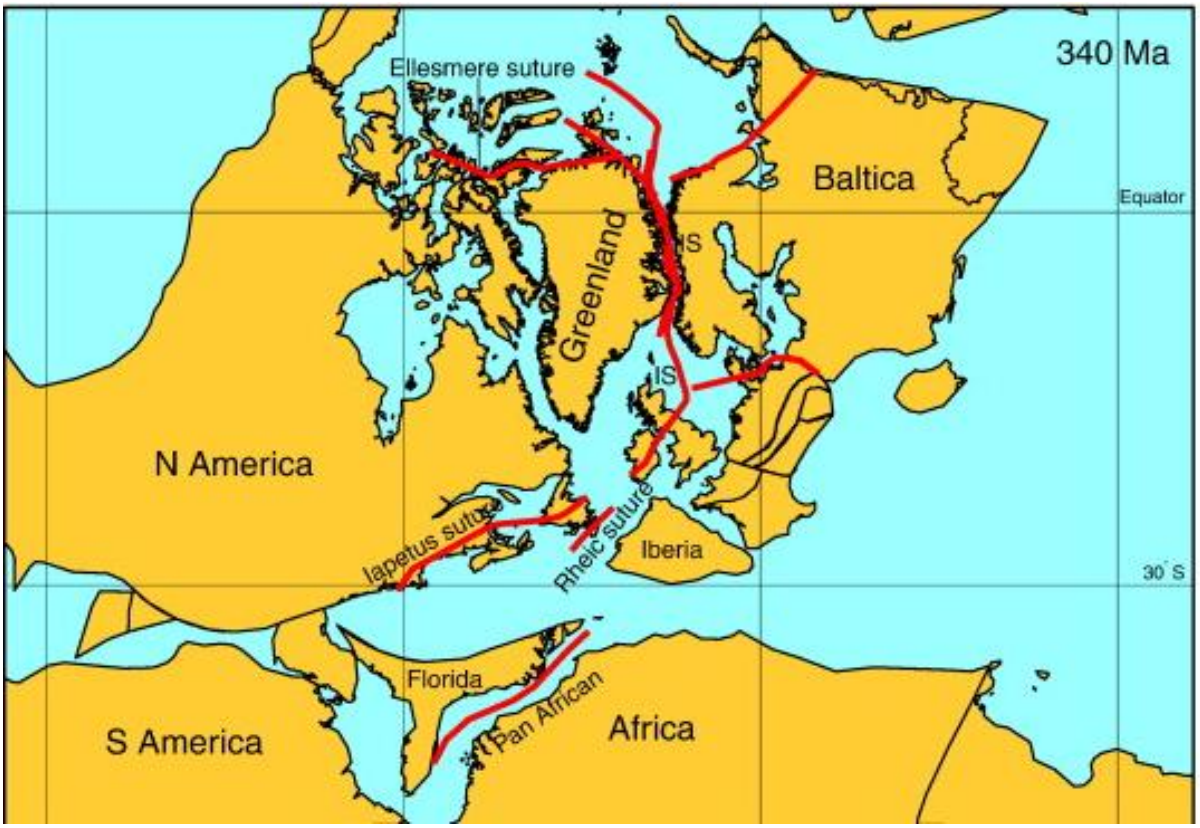

Figure 2-3-1: Map displaying the pre-opening paleo-geography of the Norwegian-Greenland Sea at about 340 Ma, before the periods of regional lithospheric extension. Figure modified from Buiter et al. (2014).

The pre-opening development is dominated by the prominent North East Atlantic-Arctic Late Jurassic-Early Cretaceous rift episode making the foundation for the development of major Cretaceous basins such as the Møre and Vøring basins off Norway (Eldholm et al., 2002). A similar tectonic evolution is recognized in the Barents Sea, where Faleide et al., (1993); Eldholm et al (2002) also separate the main development into Middle/Late Jurassic and Early Cretaceous phases.

2.3.2 Post-breakup basin formation

After 350 million years of being connected, ever since Baltika came together with Laurentia under the creation of the Caledonians, the continents main break up sequence started in the early Eocene (ca. 55 Ma), forming the Norwegian-Greenland Sea, with seafloor spreading and the creation of new seabed in between. The seafloor spreading at the mid-oceanic ridge is an ongoing process today (Martinsen et al., 2007). The cycle where there is opening and closing of ocean basins, caused by movement by tectonic plates, is called the Wilson cycle, and describes the making of oceans and mountains, as well as graben-structures (Martinsen & Nøttvedt, 2007).

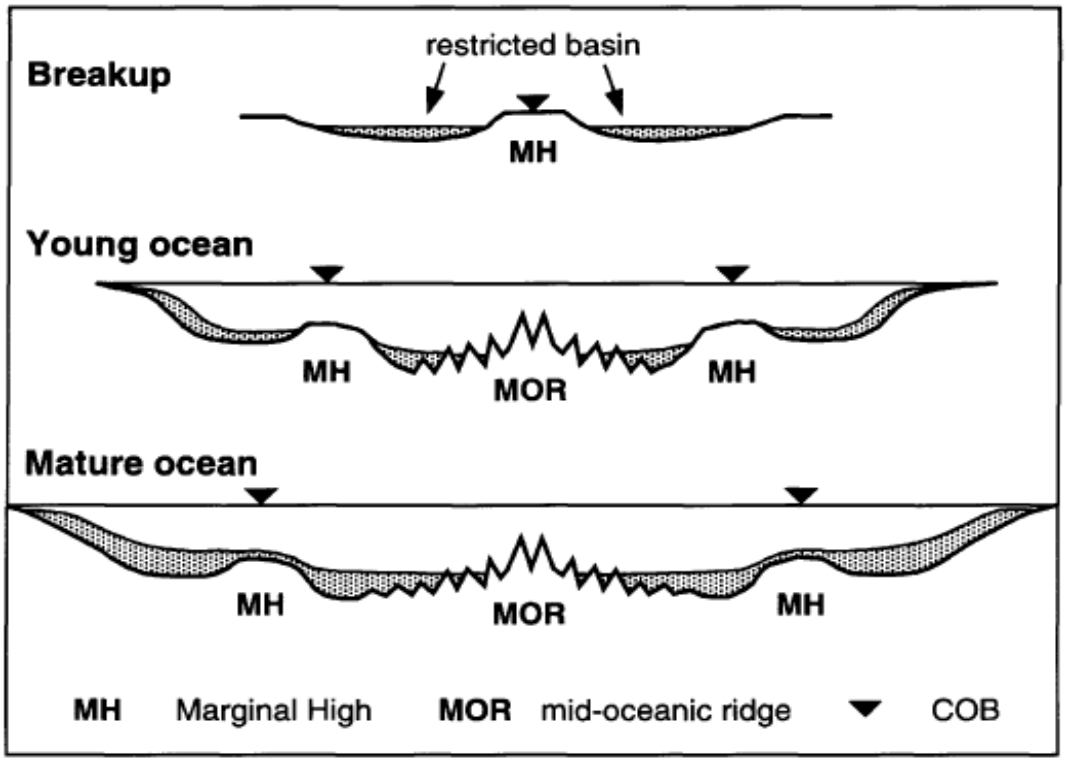

Figure 2-3-2: Schematic illustration of a volcanic margin basin segmentation creating across-margin barriers for water mass circulation caused by late rift uplift and construction of extrusive edifices along the continent-ocean boundary (COB). Figure added from Eldholm et al. (2002).

The main break-up culminated in a 3–6 Ma period of massive magmatic activity during breakup and onset of early sea-floor spreading. At the outer Møre and Vøring margins, the lavas form characteristic seaward dipping reflectors (SDR) sequences that drilling has demonstrated to be subaerially and/or neritically erupted basalts (Faleide et al., 2008). These seaward dipping reflections became diagnostic features for the volcanic margins. During the main igneous episode at the Paleocene to Eocene transition, sill intruded into the thick Cretaceous successions throughout the NE Atlantic margin, including the Vøring and Møre basins (Faleide et al., 2008).

The depositional margin evolution in Cenozoic time comprises three main stages (Hjelstuen et al., 1999; Eldholm et al., 2002); (1) Paleocene-early Eocene uplift of rift provinces, breakup volcanism and restricted basin sedimentation during a climatic maximum culminating during the early Eocene. (2) Middle Eocene-Early Pliocene margin subsidence and little sedimentation during a period of climatic decline. (3) Late Pliocene-Pleistocene Northern Hemisphere glaciation resulting in deep continental erosion, as well as very high sedimentation rates and the development of large-scale sedimentary fans.

The mid-Norwegian marginal basins have experienced compressional deformation, including domes, reverse faults, and broad-scale inversion (Some examples displayed in Fig. 2-2-1). These types of deformation is well documented on the Vøring margin, but its timing and significance are highly debated (Stoker et al., 2005; Faleide et al., 2008). Lundin & Dore (2002) suggest that the stratigraphy revealed by seismic data shows that the compressions occurred in pulses between Middle Eocene and Early Miocene.

2.4 Glacial history of Fennoscandia

There is a distinct unconformity, stretching out over the entire Mid-Norwegian continental shelf shelf, which changes on the slope to a downlap surface for large prograding wedges of sandy and silty muds originating from the mainland. This horizon marks the transition to glacial dominated sediment deposition on the Northern Hemisphere, and are dated to be about 2,6 Ma (Faleide et al., 2008). Indication of regional cooling and the formation of glaciers have been found during Pliocene, with sedimentation interspersed by ice-rafted debris (Faleide et al., 1996; Laberg et al., 1996; Dahlgren et al., 2005; Nygard et al., 2005; Rise et al., 2005; Faleide et al., 2008). During the last ca. 2.7 Ma, huge quantities of glacially derived material were transported out from the Norwegian mainland and the inner part of the shelf.

At ca. 2.7 Ma there was a large increase in the IRD flux in the Norwegian – Greenland Sea (Fig. 2-4-1). This is, according to Hjelstuen et al., (2005), most likely a reflection of a significant ice volume expansion around the Nordic Seas in connection with the onset of the Northern Hemisphere glaciations. The age-estimate is supported by Dahlgren et al., (2005), who found that glacigenic wedge-growth began around 2,74Ma. Sejrup et al., (2005) also supported this age-estimate, due to the marked increase in the accumulation of IRD in deep-sea sediments in the Norwegian Sea, found in their studies. These climatic conditions lasted until ca. 1.1 Ma, when there was a shift in the climate, which caused glacial periods of longer duration and warmer interglacial periods (Hjelstuen et al., 2005). This is confirmed by the interpretation of a number of till units, where the lowermost unit is dated to 0.90-1.1 Ma.

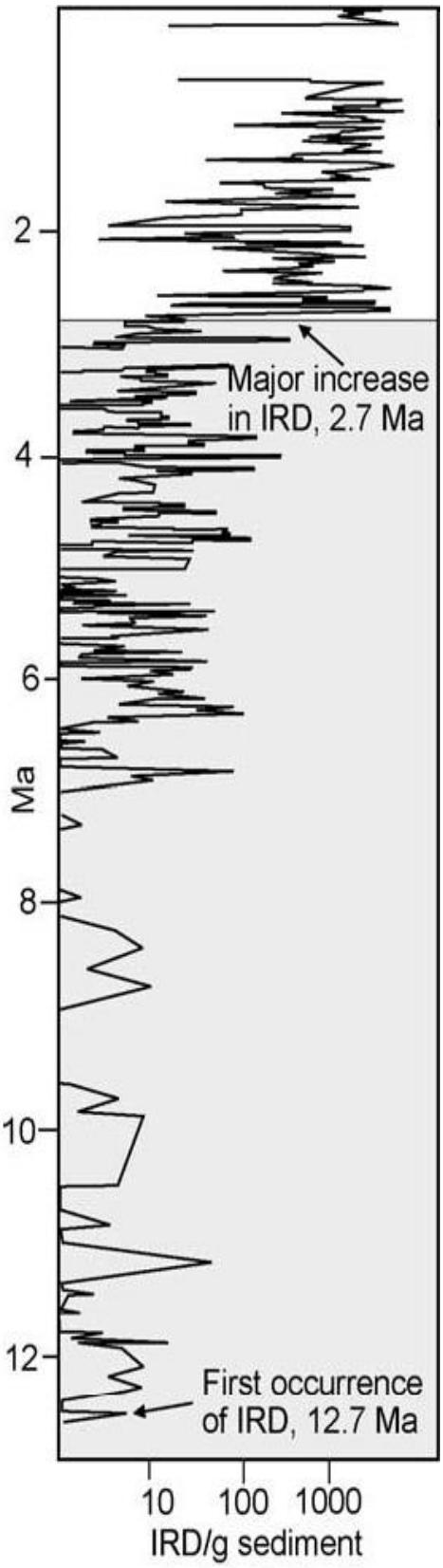

Figure 2-4-1: Compiled IRD records from the Vøring Plateau. Modified from Fronval, and Jansen (1996); Hjelstuen et al. (2005).

Both this and the increase in IRD suggest that the first occurrence of an ice stream in the Norwegian Channel occurred at ca. 1.1 Ma (Hjelstuen et al., 2005). Dahlgren et al., (2005) suggested that a change in glaciation style were present at approximately the same time, due to a change in glacial transport routes.

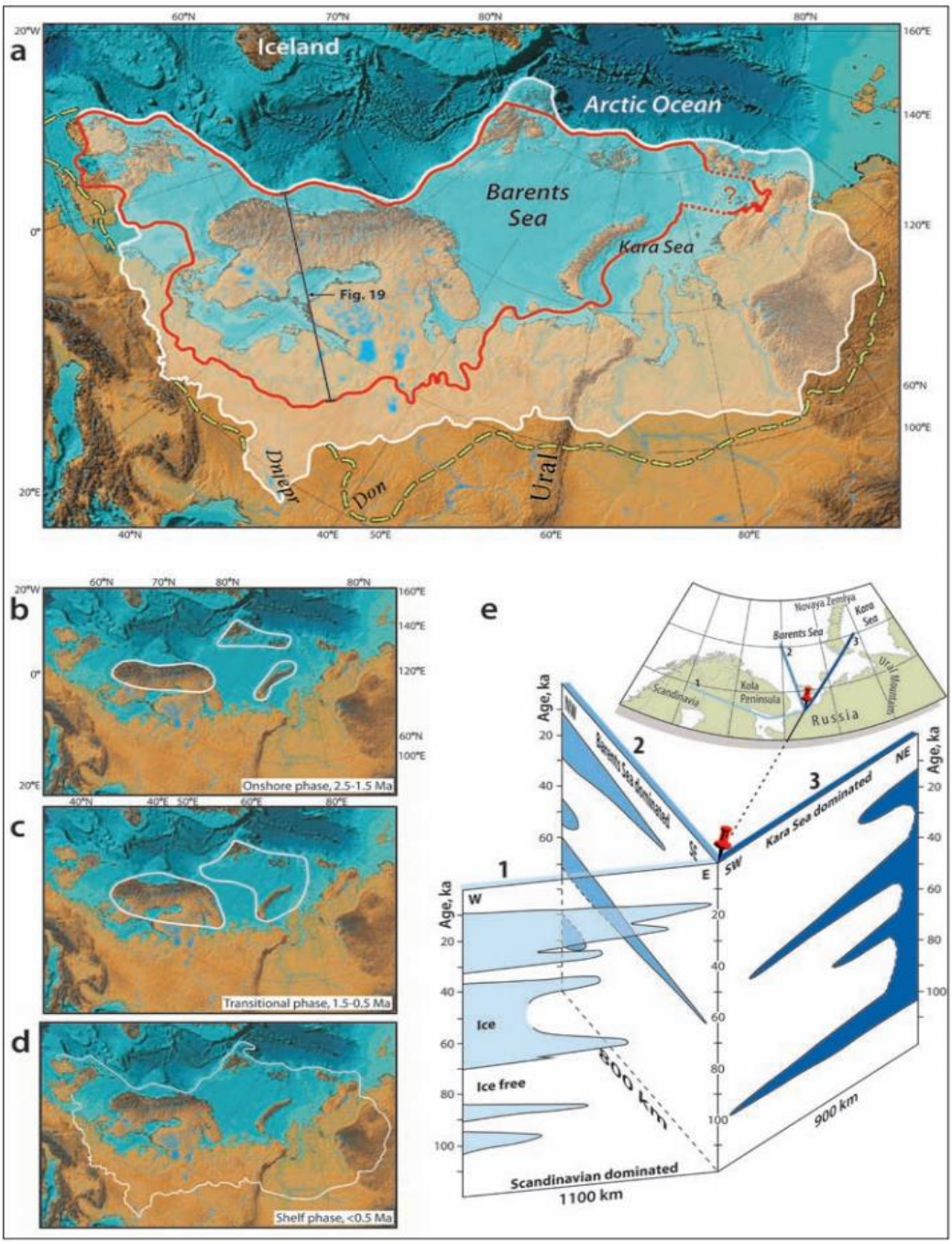

Figure 2-4-2: Glaciations/glacial extension in northern Europe. Image (a) displays LGM (red line) and previous major glaciations (white line) while (b), (c) and (d) displays the extension of maximum glaciations within three periods of the Pleistocene (to 2.7 Ma). (e) Weichselian glaciation curves depicting Scandinavian ice sheet dominance. Figure added from (Olsen et al., 2013).

The glacial sediments were deposited mainly as prograding sediment wedges into a basin of intermediate depth offshore Mid-Norway. The thickness of the deposits can be up to 1000 m (Rise et al., 2005; Rise et al., 2010). Due to the glacial-interglacial cycles in Scandinavia, in addition to elevation of the mainland, the Norwegian continental margin had a huge increase in sediment deposition in relation to the earlier, non-glacial sediment accumulation (Faleide et al., 2008). Interglacial periods with contouritic and hemipelagic processes is present within the last 3 million years, suggesting more bottom-current affected periods (Dahlgren et al., 2002).

The most extensive progradation occurred in the Lofoten–Haltenbanken area (Rise et al., 2005). Less sedimentary material was supplied to the Møre shelf, but the narrow shelf in this area is mainly the result of a steeper dip of the existing slope towards a much deeper basin, causing a larger proportion of sediments to be dispersed towards the deep ocean. The importance of glaciations at the Møre shelf and further south increased through the Pleistocene period. The Norwegian Channel Ice Stream transported enormous amounts of glacigenic debris to the North Sea Fan during the last 3–4 glaciations (ca. 400,000 years) (Rise et al., 2005).

Due to the eroding-ability of glacial cycles, most of the evidence from past glaciations on land have been removed. To find complete records of these glaciations, sedimentary records located at the glacial continental margins have to be looked upon (Mangerud et al., 2011). The present interglacial may serve as an example of previous interglacial periodes, which is characterized by low sedimentation rates, where the topography and ocean currents control the surficial sediment distribution (Hjelstuen et al., 2005).

Previous studies of sediment cores indicate that the mid-Norwegian margin was characterized by high sedimentation rate during Late Weichselian (Dowdeswell et al., 2002; Dowdeswell et al., 2010). The glacial maximum ice sheets in the artic advanced across the continental shelf to reach the shelf break during Late Weichselian (Svendsen et al., 2004; Rydningen et al., 2013).

The last glacial maximum (LGM) (Fig. 2-4-2a) is assumed to have had its peak at different times along the Norwegian coast. At the Vøring Margin Hjelstuen et al. (2008) suggest this to be approximately 22,000 years ^{14}C BP, continued by an ice-free period till 19,100 years ^{14}C BP. This suggest a withdrawn ice sheet position, allowing for deposition of glacial-marine sediments on the slope.

2.5 Cenozoic evolution and stratigraphy of the Mid-Norwegian Margin

In the deep basins of the Norwegian Sea, the Eocene to Oligocene Brygge Formation and the middle to late Miocene Kai Formation consist mainly of biogenic ooze (Eidvin et al., 2014). After the onset of the glaciations in the Late Pliocene, these several hundred meters thick ooze deposits were overlain by glacigenic deposits of the Naust Formation which prograded from the shelf towards the deep sea (Riis et al., 2005).

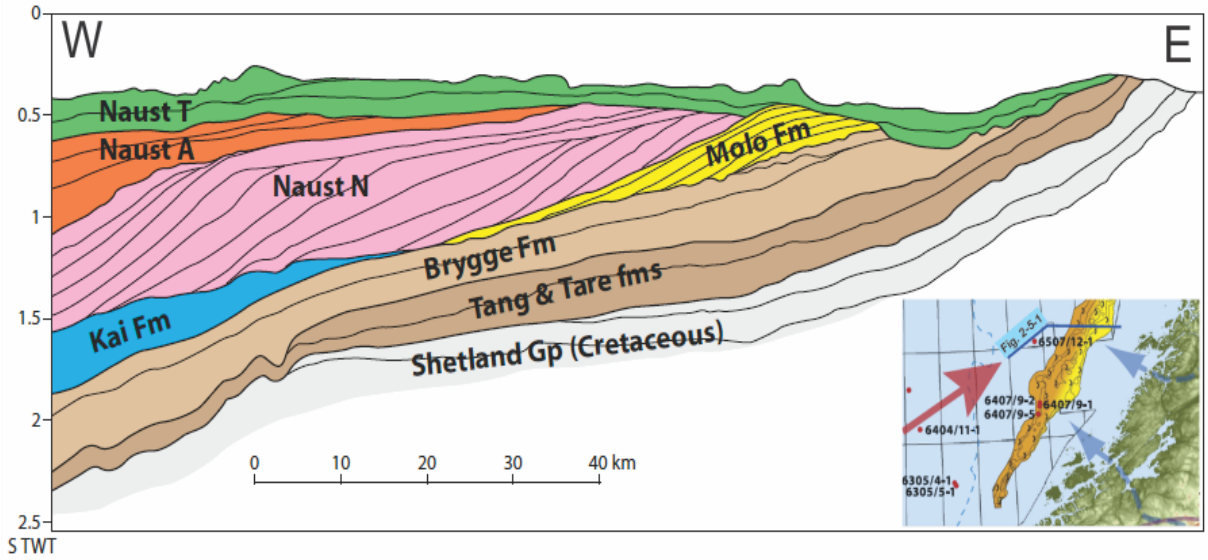

Figure 2-5-1: Geoseismic section displaying the location of the different sequences on the mid-Norwegian margin. Also showing that Kai and Molo formations are proximal and distal equivalents with each other Figure modified from Eidvin et al, (2007).

2.5.1 Tang and Tare formation

Below the Paleocene succession ooze was deposited in major parts of the Norwegian Sea, including the Møre and Vøring Basins. The material was mostly derived from the Norwegian mainland, although there has been found deposits from East-Greenland in the western part of the basins. These ooze deposits are called the Tang formation (Fig. 2-5-1). In the formation above, the ooze includes a lot of volcanic material, which constitutes the Tare formation (Martinsen & Nøttvedt, 2007). During Paleocene there was regional uplift resulting in shallow marine conditions and subaerial exposure of large regions. The margin later subsided and the Norwegian Sea transgressed the margin and parts of the mainland. Overlying the Tang & Tare formations there are three main sequences, on the Norwegian margin, which were deposited after the margin subsided and the sea transgressed. These are the Brygge, Kai/Molo and Naust formations (Eidvin et al., 2007).

2.5.2 Brygge formation

The Brygge formation is the oldest of the main sequences on the margin, and were deposited just after a transgression occurred. The formation is clay dominated on the present day shelf, whilst in the deeper Møre and Vøring basins it is ooze dominated. In the Møre basin the thickness of the unit were 600-1000m. The outer part of the Vøring basin has a thickness of 500-700m (Eidvin et al., 2007). For the outer part of the slope of the Vøring Marginal High, Laberg et al., (2005a) suggest that the deposits have been influenced by ocean currents. This may imply that most of the sediments found on the outer part of the margin are of contouritic origin.

The ooze sediments in the Brygge formation is characterized by small-scale polygonal faulting. This can be interpreted to be the result of compaction and water escaping from the sediments during the Pliocene/early Pleistocene because of the increase in pore pressure, due to rapid loading of glacial sediments in this time period (Bryn et al., 2005). The sediments deposited in the Brygge formation have in some areas been remobilized by different processes. Within the Storegga slide, liquefaction and vertical squeezing have been observed in crater-similar forms, like for example the Vema Dome area (Riis et al., 2005). This reactivations has, according to Eidvin et al, (2007), occurred during or after deposition of the glacially influenced sediments of the Naust formation (Fig. 2-5-1). Sliding has also been observed occasionally on the slope, while diapirism are more dominant in the basins.

2.5.3 Kai/Molo formation

During the Oligocene there were tectonic activity affecting the margin, which resulted in compression and elevation of the basin-flanks, and parts of the continental margin. This led to a regional elevation on the Mid-Norwegian continental margin in the middle of the Miocene which created a unconformity called the mid-Miocene unconformity (Brekke, 2000). This unconformity separate the Brygge formation from the overlying Kai and Molo formations (Fig. 2-5-1).

After the creation of the mid Miocene unconformity, sedimentation resumed on the outer and middle part of the Norwegian continental margin. The Kai formation is mostly clay dominated, while the Molo formation is mostly sand-dominated (Eidvin et al., 2014). The two formations are both dated as late Middle Miocene and younger. The Molo formation may lack the oldest part (middle Miocene) (Eidvin et al., 2007; Eidvin et al., 2014). Rise et al. (2010) confirms this, and indicates that the stratigraphic position and dating results strongly suggests

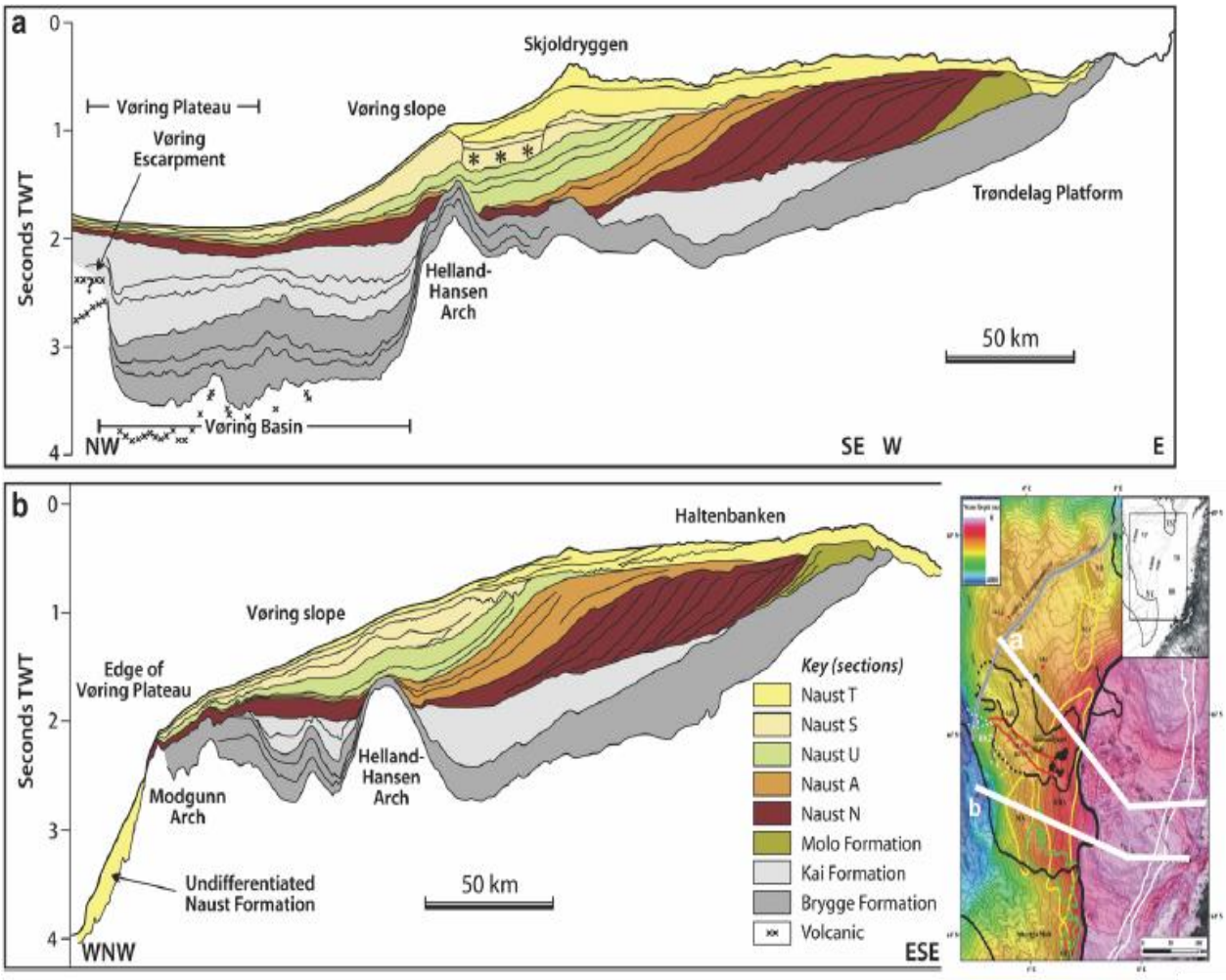

Figure 2-5-2: Two seismic sections offshore mid-Norway form the coast and extending to the Vøring Plateau. The figure displayed the general stratigraphy of the region, as well as the difference in thickness and distribution of the Kai formation. The location of the two seismic sections are shown on the map. Figure modified from (Rise et al., 2010).

that the sand-dominated and coast-parallel Molo formation is a proximal equivalent to the deeper marine-dominated Kai formation. The Kai formation varies greatly in thickness and distribution (Fig 2-5-2) being thickest in the widest areas of the Vøring basin. The formation is thinner in the southern and northern part of the study area, while the distribution of sediments varies a lot landwards, east of the margin (Rise et al., 2010).

The sediments belonging to the Kai formation were mostly deposited on the middle and outer part of the continental margin. The Kai formation is clay dominated on the outer shelf and slope down to the deeper basins, with ooze in the basinal areas (Eidvin et al., 2014). The Kai formation has a similar polygonal fault pattern as the Brygge formation, but are separated due to differences in the seismic facies between the two formations (Eidvin et al., 2007). As in the underlying Brygge formation, Laberg et al (2005a) suggest that the Kai deposits have also been influenced by ocean currents. At this time, the currents as well as the seafloor bathymetry were affected by the large domes and depressions, which were a result of the

Middle Miocene compressional tectonic phase (Eidvin et al., 2014). Rise et al (2010) confirms that the environment was greatly affected by bottom currents, based on the absence of the Kai formation in the upper part of the Helland-Hansen- and Modgunn arches (Fig 2-2-1).

The Molo formation was deposited from the coast off Møre (63º15'N) to the Lofoten Islands (67º50'N), a distance over 500km. The Molo formation comprises of a fairly steep clinoform system (Fig.2-5-1). This suggests a fairly high-energy environment, which can be confirmed by the sandy lithology in the area (Eidvin et al., 2007).

2.5.4 The Naust formation

After the deposition of the Kai and Molo formations, the climate cooled, glaciers started to grow and the glaciation of Scandinavia were introduced. The glaciation, combined with the uplift of the mainland resulted in a pronounced increase in erosion of the mainland and sediment deposition along the margin (Ottesen et al., 2009; Rise et al., 2010). Based on glacial debris in deep sea cores, the Naust formation is normally interpreted to be of late Pliocene time, at ca. 2.7 – 2.8 million years BP (Eidvin et al., 2007; Rise et al., 2010; Eidvin et al., 2014). The age estimate and classification of the different units in Naust formation in highly debated, as displayed in Figure 2-5-3. This section will use the age estimate from Rise et al. (2006), which also was adapted by Rise et al. (2010).

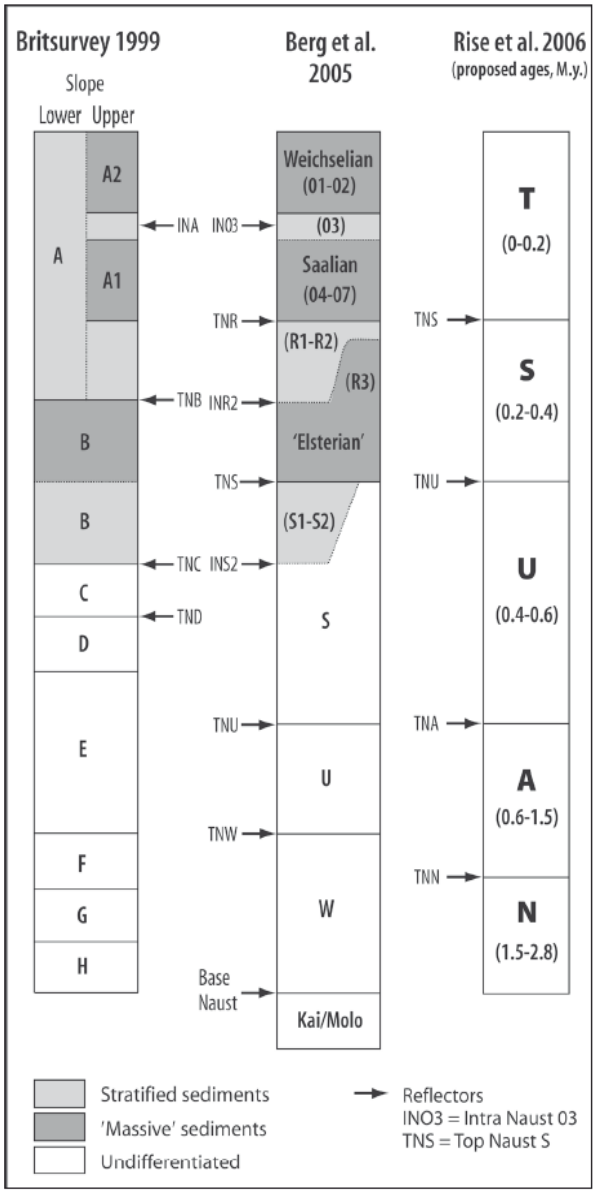

Figure 2-5-3: Diagram showing the Naust stratigraphic scheme, including the ages of the different units in the Naust formation. Figure added from (Rise et al., 2006).

The erosional products from mainland Mid-Norway and the inner part of the continental shelf, was under Naust time transported westwards, which resulted in a

rapid outbuilding of the shelf (Rise et al., 2005). The Naust formation comprises thick sequences of low angled glacial sediment deposits, and sheet-like units. In seismic sections, it is clear that most of the sediments comprising the Naust formation is located west of the Molo formation (Fig. 2-5-1). The base of the Naust formation marks the transition to the underlying Kai formation (Rise et al., 2010). Because of the major increase in sediment accumulation, due to change in deposition pattern and uplift of the mainland, the Naust formation has a thickness that is mostly greater than the underlying Brygge, Kai and Molo formations (Rise et al., 2005) (Fig. 2-5-4)

The Naust formation can be divided into five different units (Fig. 2-5-3), from oldest to youngest are called N, A, U, S and T, from oldest to youngest. The two oldest and bottommost units, the **N and A sequences** (Fig. 2-5-4e) are westerly prograding, and are mostly wedge-formed. The units are massive and Rise et al (2010) infer that they comprise sediments transported beyond the palaeo-shelf edge, as various types of mass wasting and down-slope gravity currents. **Naust U** have different slope-building units and aggradation, which may indicate glacial-interglacial cycles, with a maximum sediment deposition on the present shelf edge (Ottesen et al., 2009). **Naust S** is a representative for the third last glaciation. The unit was mostly deposited seaward of the present shelf (Ottesen et al., 2009). During Naust S, the paleo-shelf migrated to its westerly position, covering the shallow crest of the HHA with more than 200m of sediments. The glacial debris were transported to the shelf edge, as a result of paleo-ice streams routed through the Sklinnadjupet paleo-trough (Rise et al., 2010). **Naust T** consists mostly of massive units with layered sediment sequences from the two last glacial-interglacial cycles. Naust T comprises of two major units of till and glacial debris, as a result of the two Saalian and Weichselian glaciations (Rise et al., 2010).

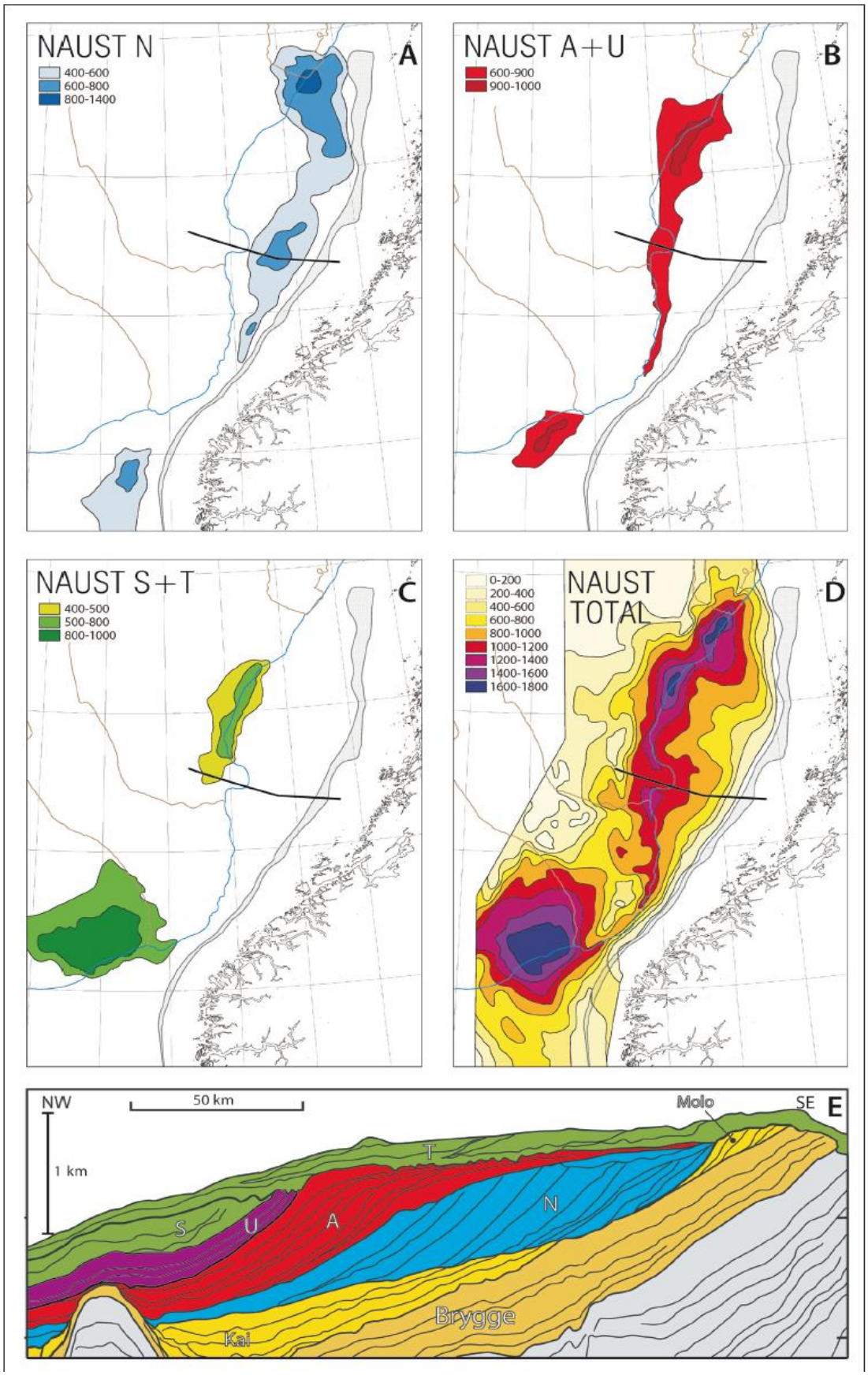

Figure 2-5-4: Time thickness maps in milliseconds (two-way travel time) of the Naust formation and equivalent sediments and the depocentres of the Naust sequences (A-D). E displays the overall thickness in a seismic section. Figure added from Ottesen et al (2009).

2.6 Oceanography

The Norwegian Atlantic Current (NAC) is presently flowing northeastwards along the continental margin. This current is, as Fig 2-6-1 displays, a continuation of the Continental Slope Current moving from offshore Ireland and Northwestern Britain through the Faroe-

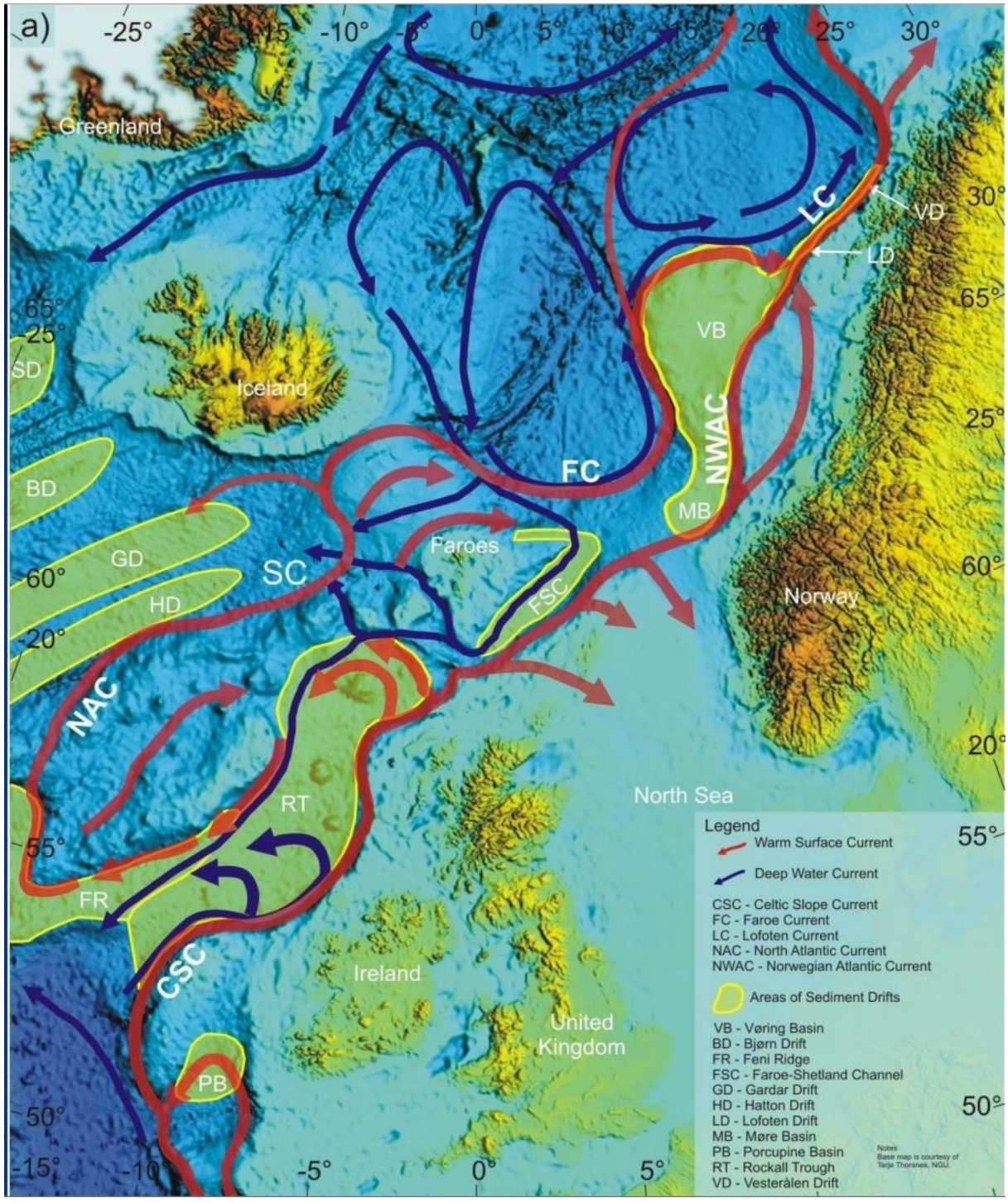

Figure 2-6-1: Map displaying the modern ocean circulation and the general location of contouritic sediments on the Atlantic margin. Warm saline Atlantic surface water is indicated by red arrows, while cold and dense deep water by blue arrows. Modified from (Laberg et al., 2005b).

Shetland Channel. The current is at present influenced by north-eastward-flowing, warm, saline surface water (Laberg et al., 2005b). The surface circulation system consists in general of saline, warm Atlantic water going north as the Norwegian Atlantic Current (NAC), which sinks due to temperature reduction, and forms the Norwegian Sea Deep Water (NSDW). This deep water returns south, and are mostly transported into the Atlantic Ocean by deep-water passageways, such as the Faroe Conduit. The deepest flowing water of the NSDW can be reflected back north, due to not being able to traverse to the shallower parts of the passage-ways (Bryn et al., 2005).

The NAC can be divided into two different north-flowing paths, which both are adjacent to the continental margin. Figure 2-6-1 displays the two different paths, west/north and south/east of the Faroes Island. The western path flows between Iceland and the Faroe Islands, and continues north adjacent to the continental margin, into the Storegga area, and further along the outer part of the Vøring Plateau. The eastern path passes through the Faroe-Shetland region and into the upper part of the Storegga slide area (Bryn et al., 2005).

The morphological evolution during Cenozoic time had a profound effect on the palae-oceanographic circulation, as well as the deep-water sedimentation patterns (Laberg et al., 2005b). Laberg et al., (2005a) suggested that there are indications of Paleogene ocean current affected sediments in the Vøring Plateau succession. Because of the upslope progradation during the late Eocene, there is reason to believe that there is sediments influenced by ocean currents on the outer part of the Vøring Plateau slope, while the inner part were mostly sub-aerially exposed. Sediments deposited in Oligocene were mostly the result of the influence of ocean currents on the northeastern, inner high. Laberg et al., (2005a) further suggested that during late Miocene to early Pliocene a change to more hemipelagic dominated sedimentation occurred. This may indicate that the topographic control of the Vøring Plateau on the ocean currents was reduced. Figure 2-6-2a displayes four seismic units identified by Laberg et al., (2005b), classified as current-influenced sediments.

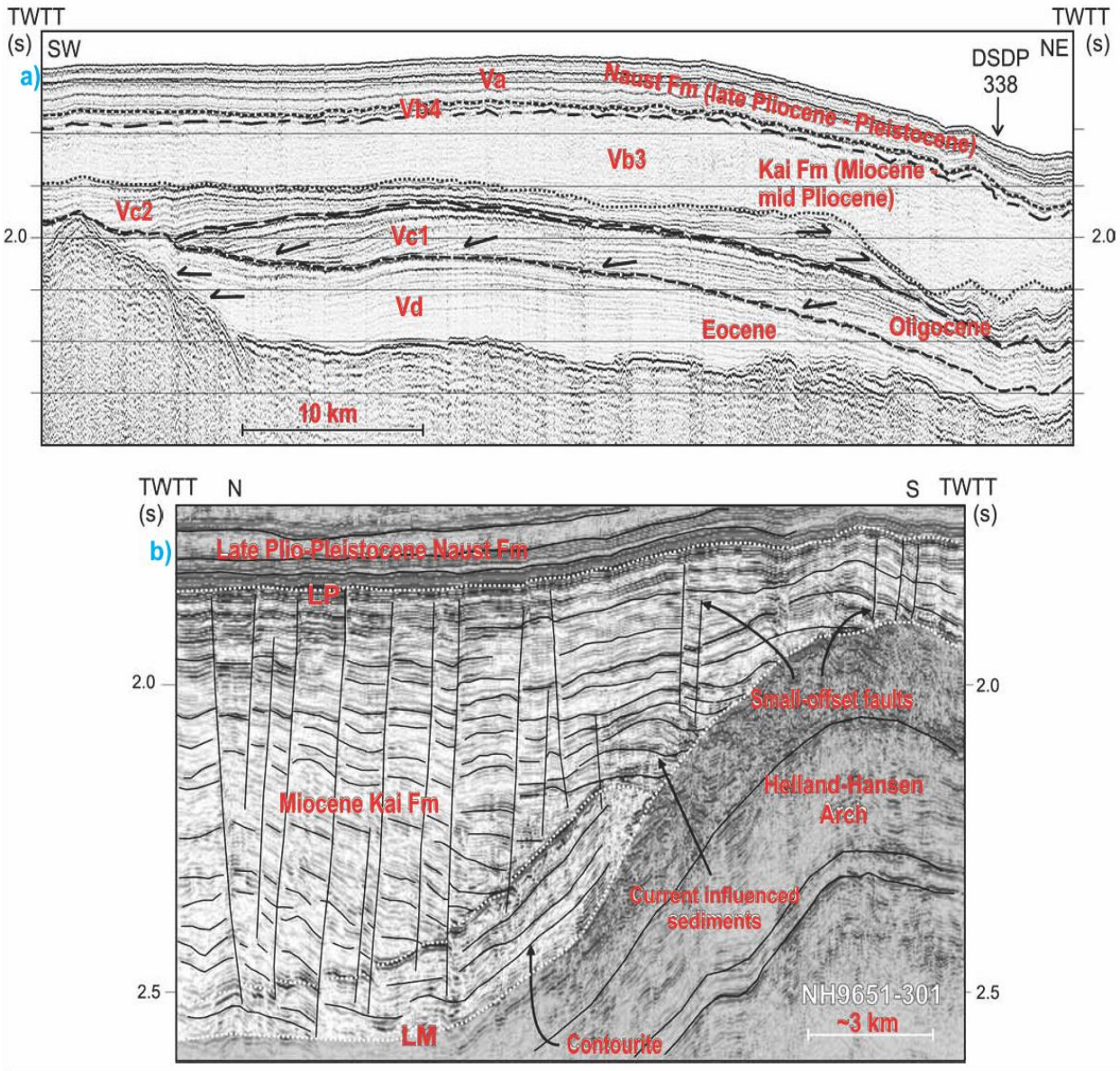

Figure 2-6-2: a) Seismic profile eon the inner Vøring Plateau. Displaying the identified four different seismic units Vd, Vc1, Vc2 and Vb3, and the acoustic signature showing onlapping, downlapping and reflection truncation within the units. b) Example of current influenced sediments on the Vøring Plateau deposited during the Miocene Kai formation. Figure modified from (Laberg et al., 2005b).

Within the Vøring basin, there are depositional patterns which indicate that the Miocene sediments had current influenced deposition (Fig. 2-6-2). The mid-Norwegian continental shelf were in Miocene time, characterized by elevated anticlinal structures (Laberg et al., 2005b). These elevated structures may have interfered with the bottom currents, since the currents followed the flanks of the structures, causing a Miocene non-deposition along the structures surrounding the Helland Hansen Arch (Hjelstuen et al., 2004).

2.7 Contourites

Contourites can be defined as sediments deposited by, or affected by the action of bottom currents. Bottom currents can often be divided into two different types; Thermohaline currents and tidal currents. Most bottom currents are "semi-permanent parts" of thermohaline circulation, while some are influenced by tides (Stow et al., 2002). Bottom currents and deposition of contourites can be classified as an along-slope process. Stow et al (2002) showed that a wide range of contourite facies can be found in muddy to gravel-lag facies, dependent on the supply of sediments and strength of the ocean current; In general, weak bottom current leads to the deposition of fine-grained sediments, while strong bottom currents leads to coarse grained deposits. Because of the interaction and variant sediment supply during deposition of the contourites, transitional facies can occur.

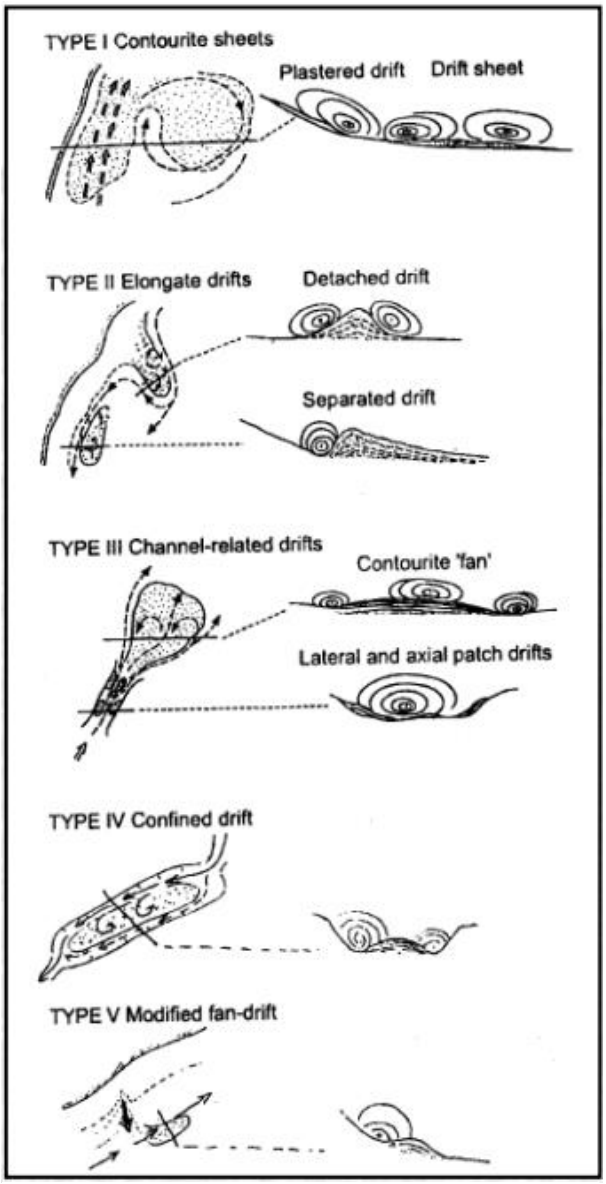

Figure 2-7-1: Contourite drift models, with illustrations of the deposition around the drifts. Added from Stow et al (2002).

Contourite drifts are a type of sediment drift (sediments accumulated by currents) which occur below a water depth of 300 meters. The sediment drifts found above this depth is referred to as shallow water drifts. Stow et al, (2002) divide the contourite drifts into six main classes; (1) contourite sheet drifts, (2) elongate mounded drifts, (3) channel-related drifts, (4) confined drifts, (5) infill drifts, and (6) modified drift-turbidity systems. The five first is represented in Fig. 2-7-1. The different types are controlled by morphology, current velocity, sediment supply, duration and interaction from downslope processes (Stow et al., 2002).

According to Laberg et al (2001), most of these contourite drift types can be recognized at the Atlantic margin of northwestern Europe. Offshore mid Norway, two types has been accounted for. This includes contourite sheet drifts in the Møre basin, and elongate

mounded drifts which are normally developed in palaeo-slide scars at the Vøring and Lofoten margins, as well as the Storegga area (Bryn et al., 2005).

The Kai formation is found to be dominated by contourite drift deposits (Hjelstuen et al., 2004; Bryn et al., 2005; Laberg et al., 2005a; Laberg et al., 2005b). These sediments has been developed with little to no interaction from downslope processes that are commonly featured in the Naust formation. Because of this, the Kai formation consists mainly of deep-water basinal sedimentation on-lapping the adjacent continental slope and the Paleogene domes in the Vøring plateau, as well as the Storegga slide area (Fig. 2-7-2) (Bryn et al., 2005). The thickest contouritic sedimentation sequence of the Kai formation is found on the Vøring Basin

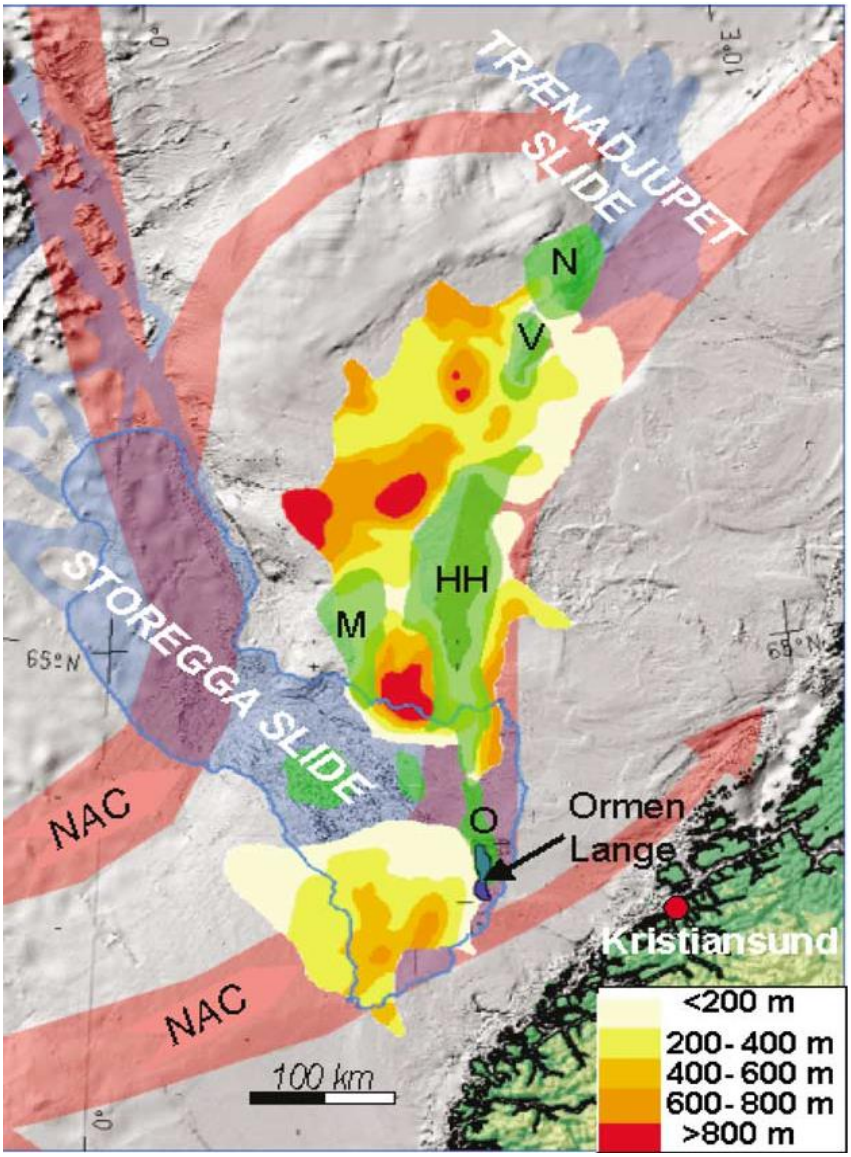

Figure 2-7-2: Thickness map if the Kai formation displaying the contouritic drift depocenters. The green structures indicate topographical highs which influenced the path of the currents. NAC: Norwegian Atlantic Current, N: Naglfar Dome, V: Vema Dome, HH: Helland Hansen Arch, M: Modgunn Arch, O: Ormen Lange Dome. Modified from Bryn et al., (2005).

(Fig 2-7-2). According to Bryn et al, (2005) the preserved thickness of sediment drift deposits can here come up to 1000 m. There is samples of these deposits, form the southern part of the Vøring plateau, which reveals that the deposits in the Kai formation have the characteristics of biogenic ooze with a water content of 70-80%. The contourite drifts of the Kai formation are not much effected by mass wasting processes, but paleo-slides have cut into these deposits at the southern part of the Vøring area. In addition of this, there have been identified ooze sediments in huge crater structures within the Kai and Brygge formations (Riis et al., 2005).

Instabilities have been found in areas of contouritic deposits on continental slopes, ocean gateways and on some of the biggest submarine landslides known (Laberg et al., 2008). Contouritic sediments on the mid-Norwegian margin are probably prone to failure because of the following four factors (Laberg & Camerlenghi, 2008); (1) the composition of the well sorted muddy or sandy sediments make them weaker compared with poorly sorted sediments, and they can be exposed to liquefaction in response to cyclic loading. (2) High sedimentation rate resulted in high water content and low shear strength due to under-consolidation. (3) Their location on continental slopes can be affected by rapid loading; on high-latitude margins excess pore pressure can be developed in contourites with glacigenic sediments under and over. (4) Gas migration and gas-hydrate dissociation can also develop excess pore pressure, due to a high organic-carbon content, which are often found along continental margins.

Slides with contouritic instability can become very large since the contourites may have a large distribution area, due to the possible vast size of the bottom current systems (Laberg & Camerlenghi, 2008).

2.8 Polygonal Faults and their relation to fluid flow

Polygonal fault systems consists of non-tectonic faults, which often occur in fine-grained fill of sedimentary basins. Cartwright et al., (2003) define polygonal faults to be an array of layer-bound extensional faults within a fine-grained stratigraphic interval which exhibit a diverse range of fault strikes that partially or fully intersect to form a polygonal pattern when seen in map view. Studies have shown growth-related sedimentary successions at the top of the polygonal faults, which indicates that the development of the faults started during early burial of the host sediments (Berndt et al., 2003).

How polygonal fault systems occur in the subsurface is widely debated (Cartwright et al., 2003). The most accepted theory is the relation to sediment contraction and fluid expulsion (Berndt et al., 2003; Cartwright et al., 2003; Gay et al., 2007) (Fig. 2-8-1). All genetic models for polygonal fault systems involve fluid expulsion from the host rock, which makes it reasonable to anticipate that the fault systems creates a major source for the fluid flows observed in areas dominated by polygonal fault systems (Berndt et al., 2003) (Fig. 2-8-2).

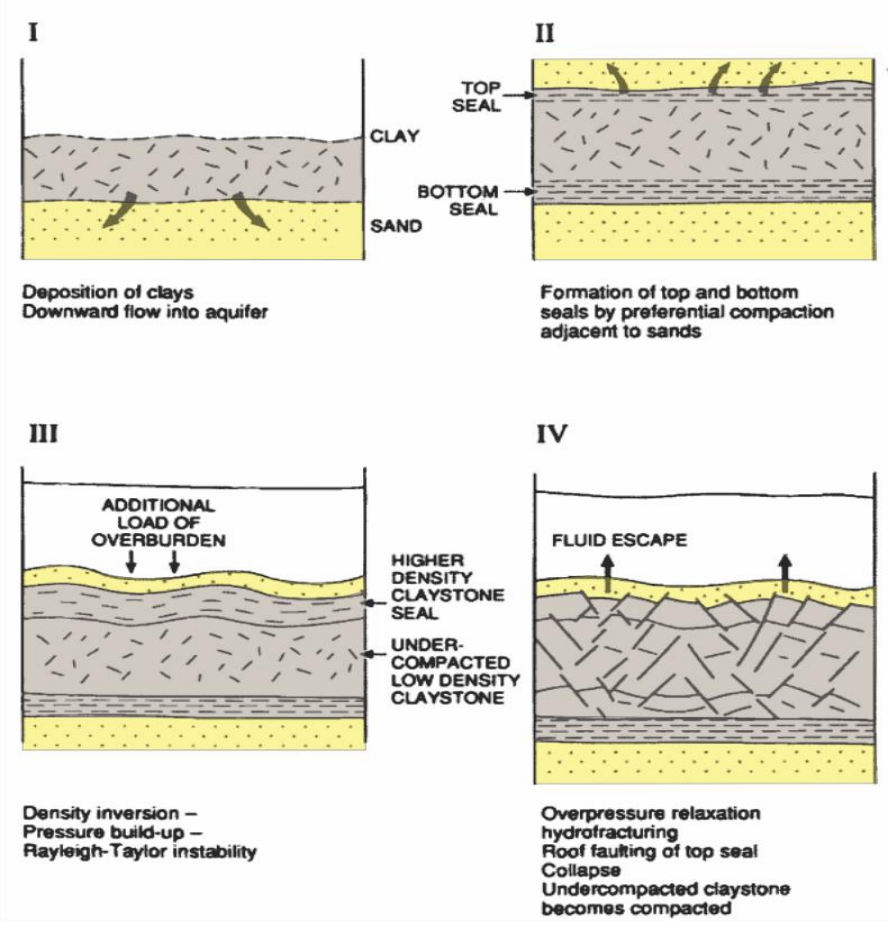

Figure 2-8-1: Four-step model displaying the development of polygonal fault system. I: Deposition of clays. II: Self-sealing and overpressure buildup. III: Density inversion folding. IV: Faulting and pore pressure collapse with fluid escape. Figure modified from Cartwright et al (2003).

The Kai Formation in the outer part of the Vøring basin is characterized by polygonal fault systems. Stratigraphically the faults are located in the fine-grained ooze sediments found in the Kai formation (Berndt et al., 2003; Bryn et al., 2005; Chand et al., 2011). Assuming that fluid flow seismic indicators can be used as a proxy for active fluid flow, it may be possible to quantify the duration of the development of the polygonal fault systems. The stratigraphic position of where the fluid flow indicators ends, implies that the processes causing fluid expulsion have been active on the Mid-Norwegian margin since Miocene time. If polygonal faults are related to the expulsion of fluids, the development of polygonal faults have been active since Miocene as well (Berndt et al., 2003).

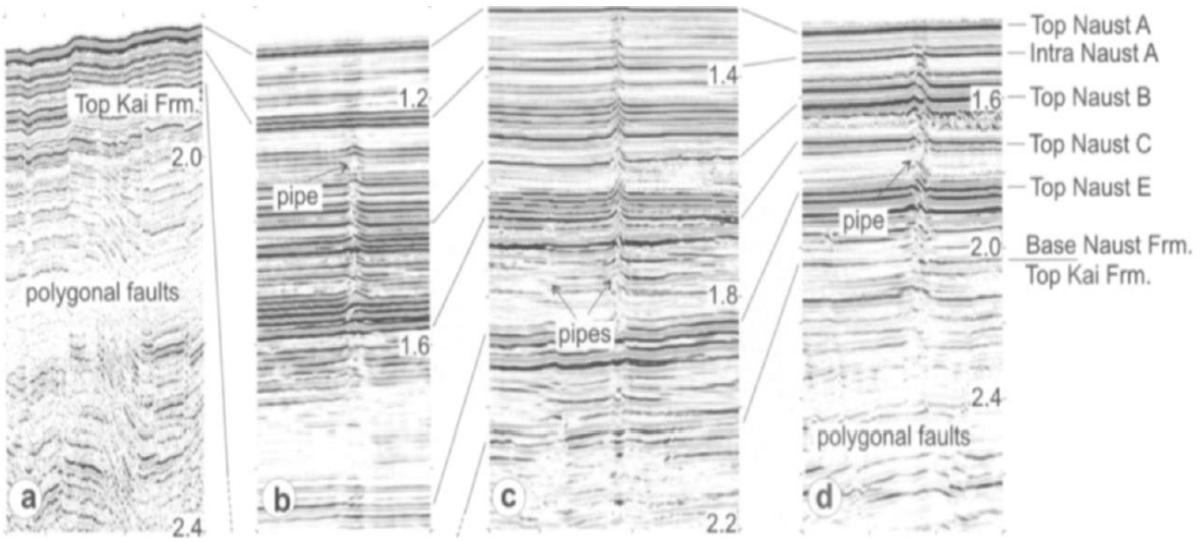

Figure 2-8-2: Seismic evidence for prolonged polygonal fault system development, and polygonal faults relation to fluid flow. Figure modified from Berndt et al (2003).

3. Data material and methods

3.1 Seismic dataset

The study is based on 2D-seismic surveys located on the Vøring Plateau to the inner part of the mid-Norwegian margin. The seismic lines used have been obtained from eight different surveys (MNR04 to MNR11), which have been provided by TGS. The seismic surveys consists of over 200 separate lines (Fig. 3-1-1). The quality of the seismic dataset is overall very high, but differs a lot between the different surveys. The frequency in the seismic lines differs, but is mostly lying between 30 and 40 Hz.

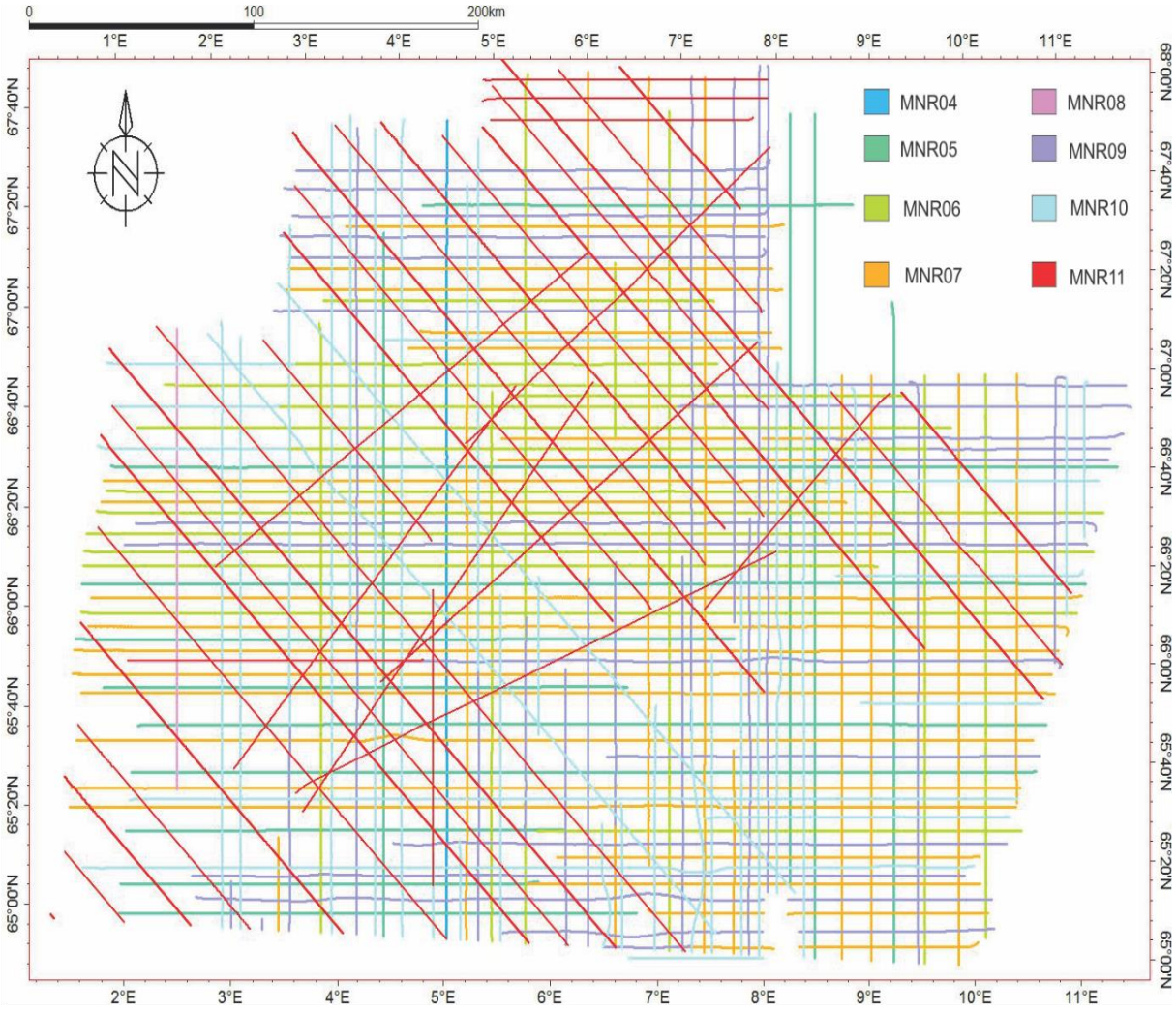

Figure 3-1-1: The seismic data used in the study, with the eight different surveys displayed. The surveys are illustrated with different colors to separate them.

The polarity and phase of the seismic datasets have been determined by a seismic cross section of the wiggles on the seafloor (Fig. 3-1-2). The seafloor was used since there always is

an increase in acoustic impedance when the seismic reflection goes from a fluid to a solid interface (water-seafloor). The wiggles in Figure 3-1-2 displays the traces showing a strong maximum peak, in the middle of two minimum (negative) troughs. This applies to every survey used in this study. According to the standard Sheriff (2006) SEG polarity, all the 2D surveys have been processed to zero-phase signal, with a normal polarity.

The seismic lines used in the study have been modified and cut, only to display the study area. The original surveys stretches south covering some of the Møre Margin as well. In the study well data retrieved from NPD's homepage have been used to correlate the seismic data (See chapter 3.3.4).

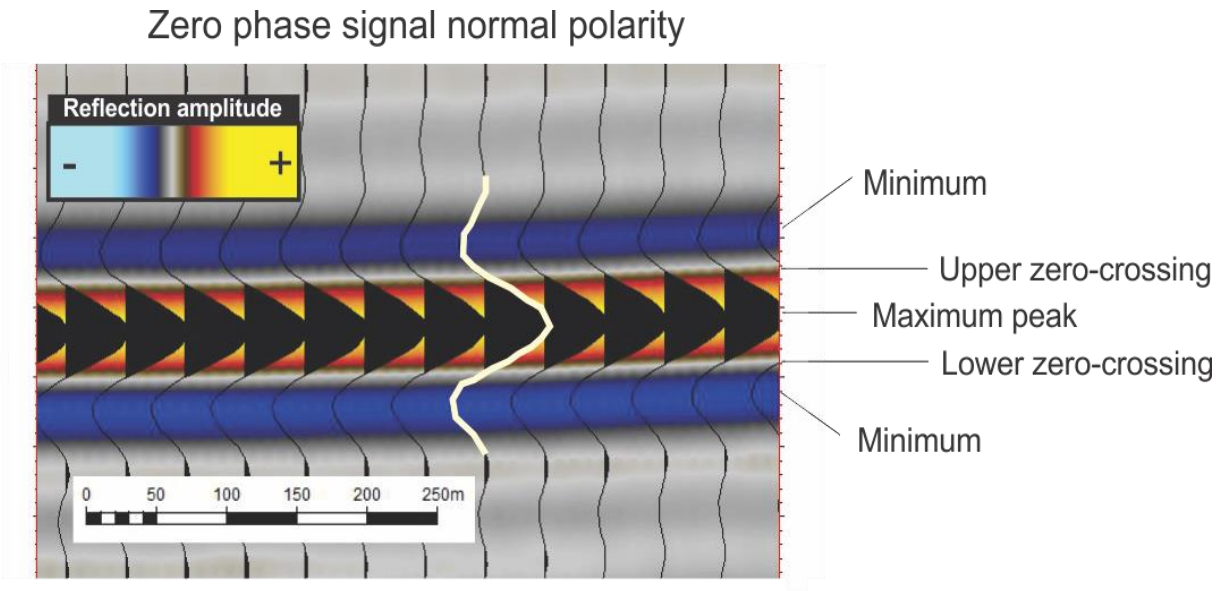

Figure 3-1-2: Seismic cross section displaying the wiggles on the seafloor of seismic line MNR10_90568M, as well as confirming the zero-phase signal with a normal polarity from Sheriff (2006).

3.2 Seismic resolution

Seismic resolution is a measure of how large a structure, or object need to be in order to be displayed in a seismic section. The seismic resolution can be divided into horizontal and vertical resolution, and are dependent on two factors; the P-wave velocity (v) of the sediments/rocks penetrated by the seismic signal and frequency (f) of the wave. These factors can define the wavelength (λ) of a seismic signal, which is given as the relationship between the two factors. Seismic resolution is proportionally decreasing with depth, while the wavelength is increasing. This is the result of the increase in velocity as we go deeper into the ground, due to heavier compaction of older, underlying rocks. In addition to this, higher frequencies are absorbed more easily than lower frequencies with increasing depth (Badley, 1985; Brown, 1999).

3.2.1 Vertical resolution

The vertical resolution is the minimum thickness a layer must have to appear as a separate layer in a seismic section, and is defined by the wavelength as (Badley, 1985; Brown, 1999);

Equation 1: $\boldsymbol{Vertical\ resolution = \frac{\lambda}{4}}$

The thickness must therefore be at least ¼ of the wavelength for layers to appear as separate elements in the subsurface. According to Brown (1999) a subsurface structure must be at least 1/30 λ to be displayed in a seismic section, and ¼ λ to be displayed as a separate structure. The wavelength can be calculated as a function of the velocity and the frequency;

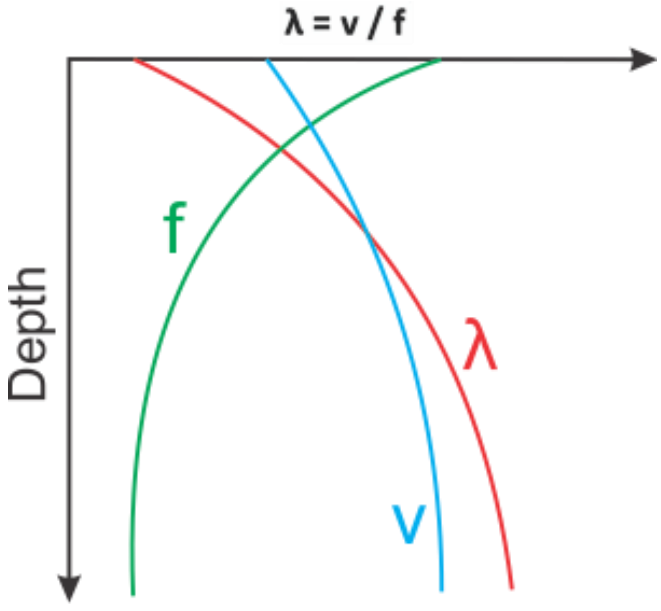

Figure 3-2-1: Figure displaying how the different factors react to an increase in depth. Velocity increases, frequency reduces, which leads to an increase in wavelength and a reduction to seismic resolution at greater depths. Figure modified from Brown (1999).

Equation 2: $\boldsymbol{\lambda = \frac{v}{f}}$

λ is the wavelength (m)

f is the dominating frequency (Hz)

v is the velocity (m/s).

3.2.2 Horizontal resolution

The horizontal resolution for seismic data pre-migration can be defined by the size of the Fresnel zone (Fig. 3-2-2). This represent the smallest horizontal distance two reflection points can have in order to be seen as two separate objects in the seismic profile. This is due to how the wave front moves downward. The wave front is propagating downward spherically. This result in the reflected signals from a reflector is not coming from only one point, but from multiple points within a circular zone, which is the Fresnel zone. The Fresnel zone therefore displays a limit of how large structures have to be to be displayed separately in the seismic (Badley, 1985; Brown, 1999; Andreassen, 2009). The resolution can, as Figure 3-2-2 displays, be improved by migration, since the Fresnel zone decreases after migration. Since 2D seismic only migrates along a seismic line, it will only decrease in one direction. 3D seismic on the other hand can be migrated in every direction, resulting in a decrease in the Fresnel zone in every direction (Fig 3-2-2). The Fresnel zone increases in depth because the velocity also increases downwards (Brown, 1999);

Equation 3: $Fresnel\ zone\ before\ migration = r(f) = \frac{v}{2}\left(\frac{t}{f}\right)^{0,5}$

Equation 4: $Fresnel\ zone\ after\ migration = \frac{\lambda}{4} = \frac{v}{4f}$

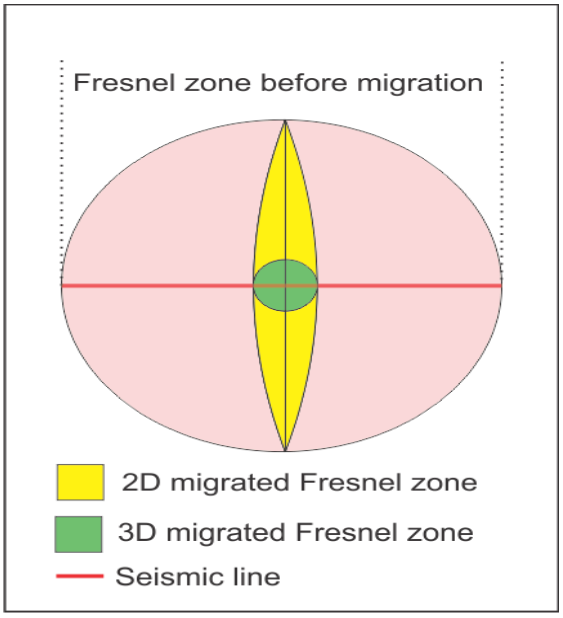

Figure 3-2-2: Figure displaying the Fresnel zone before and after migration, and how the Fresnel zone differs from 2D to 3D seismic after migration. Figure is modified from Brown (1999).

r(f)	=	Radius of the Fresnel zone (m)
v	=	Average velocity (m/s
t	=	Two-way-traveltime (s)
f	=	Dominating frequency (Hz)
λ	=	Wavelength (m)

3.2.3 Resolution of the dataset in this study

As explained earlier, the P-wave velocity is needed to calculate the resolution. The most relevant velocity model found, is from the inner part of the southern Vøring margin (Storvoll et al., 2006) (Fig. 3-2-3). The relevant resolution of the Kai formation would be top and bottom of the formation. From Figure 3-2-3, an average velocity can be identified.

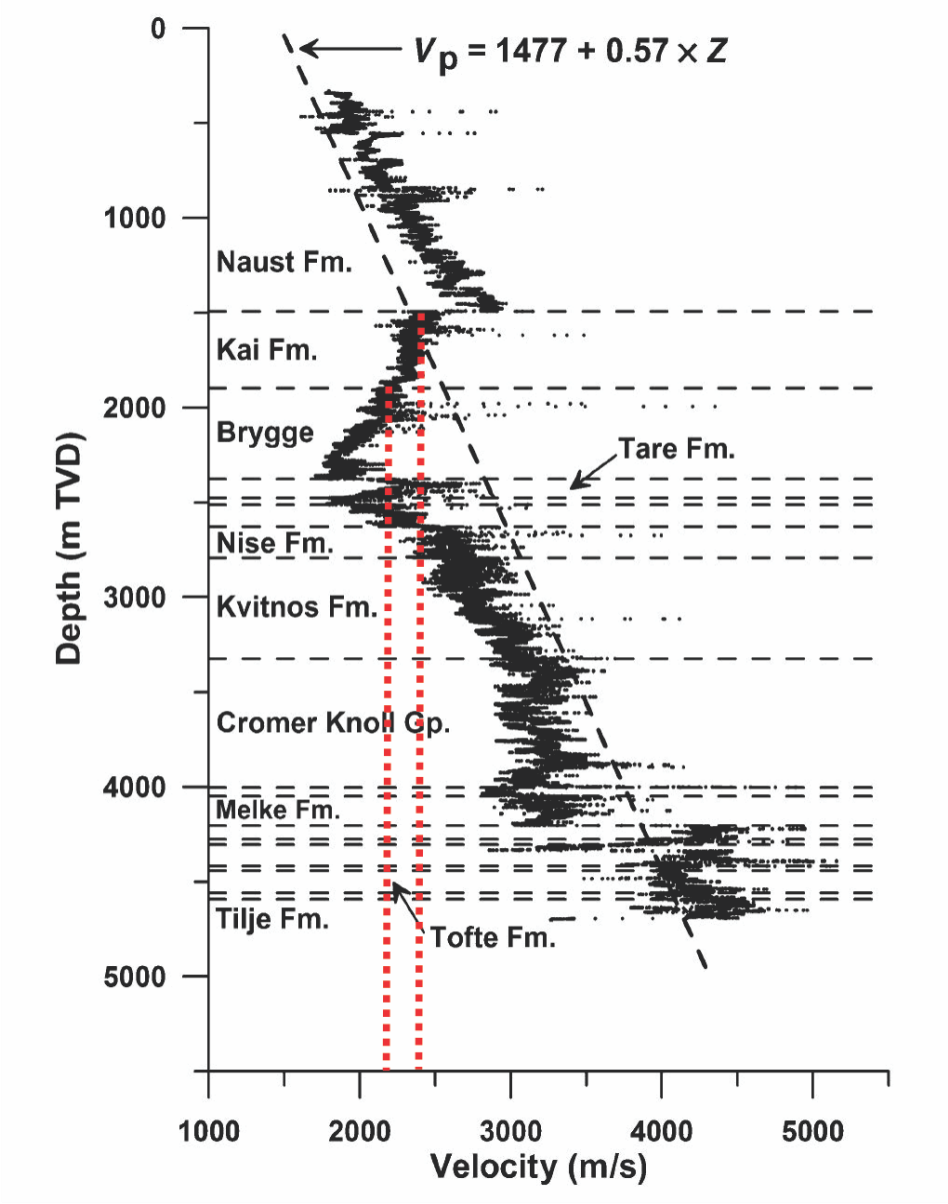

Figure 3-2-3: Velocity model based on studied wells, correlated by data from various publications. The Figure was modified from Storvoll et al., (2006).

The velocity is approximately 2400 m/s for the top of the Kai formation, and 2200 m/s at the base of the formation. This is an unusual trend when it comes to velocity values downwards into a sediment package. Normally the velocity in sediments increases downwards in relation to the increase in density, due to compaction. Storvoll et al., (2006) suggest that this has a connection to the decrease in density, related to the change in mineralogy from the Naust to

the Kai and Brygge formations. The frequency of the seismic data has earlier been given as 30-40Hz. For simplicity the frequency will be set as 35. The resolution of the dataset will be calculated by using Equation 1-4.

Top Kai formation

Wavelength: $\lambda = \frac{v}{f} = \frac{2400\ \mathrm{m/s}}{35\ Hz} = 68{,}6\ m$

Vertical resolution: $\frac{\lambda}{4} = \frac{68{,}6\ m/s}{4} = 17{,}2\ m$

Fresnel zone before migration: $r(f) = \frac{v}{2}\left(\frac{t}{f}\right)^{0,5} = \frac{2400m}{2}\left(\frac{1{,}5\ s}{35\ Hz}\right)^{0,5} = 248\ m$

Fresnel zone after migration: $r(f) = \frac{\lambda}{4} = \frac{v}{4f} = \frac{2400m/s}{4 * 35Hz} = 17{,}2\ m$

The vertical resolution of Top kai formation is 17,2 m, the radius of the Fresnel zone before migration is 248 m and the radius of the Fresnel zone after migration is 17,2 m.

Bottom Kai formation

Wavelength: $\lambda = \frac{v}{f} = \frac{2200\ \mathrm{m/s}}{35\ Hz} = 62{,}9\ m$

Vertical resolution: $\frac{\lambda}{4} = \frac{62{,}9\ m/s}{4} = 15{,}7\ m$

Fresnel zone before migration: $r(f) = \frac{v}{2}\left(\frac{t}{f}\right)^{0,5} = \frac{2200m}{2}\left(\frac{1{,}9\ s}{35\ Hz}\right)^{0,5} = 256\ m$

Fresnel zone after migration: $r(f) = \frac{\lambda}{4} = \frac{v}{4f} = \frac{2200m/s}{4 * 35Hz} = 15{,}7\ m$

The vertical resolution of Top kai formation is 15,7 m, the radius of the Fresnel zone before migration is 256 m and the radius of the Fresnel zone after migration is 15,7 m.

3.3 Methods

3.3.1 Software used

In this study the seismic interpretation and visualization program **Petrel 2014** has been used. The program is developed by Schlumberger and is used to interpret the 2D seismic data, as well as creating seismic thickness maps. The seismic stratigraphic analysis (See chapter 3.3.2) will include the creation of isochrone and isopach maps. Petrel can be used to track horizons manually as well as automatically (tracked by the program) along a reflection. At noisy, and discontinues parts of the seismic, manual tracking of the reflection had to be done.

Most of the figures have been modified by using **CorelDRAW X6**, a vector based image editor program.

3.3.2 Isopach and Isochrone map

Isochrone maps are contour maps that display variation in time between two seismic reflectors. **Isopach maps** display thickness variations in a formation, and will be used to identify the geometry of the formation. The isopach map is created by using horizons created by tracking in Petrel.

3.3.2 Seismic Sequence Stratigraphic Analysis

Seismic stratigraphy analysis can be defined as the study of stratigraphy and depositional sequences and facies, interpreted from seismic data, and are often used for recognition and correlation of depositional sequences, as well as interpretation of depositional environment and lithofacies (Mitchum et al., 1977). A depositional sequence is a defined stratigraphic unit, which is composed of genetically related strata and bounded by unconformities. The deposition of most sequences can be related to cycles of regional and global change in sea level. Seismic stratigraphic analysis can be divided into two different steps; **(1) Seismic sequence analysis** – Subdividing a seismic section into packages (concordant reflections separated by surfaces of discontinuity), and interpreting them as depositional sequences. **(2) Seismic facies analysis** – analyzing the seismic reflection patterns within the seismic sequences (Mitchum et al., 1977).

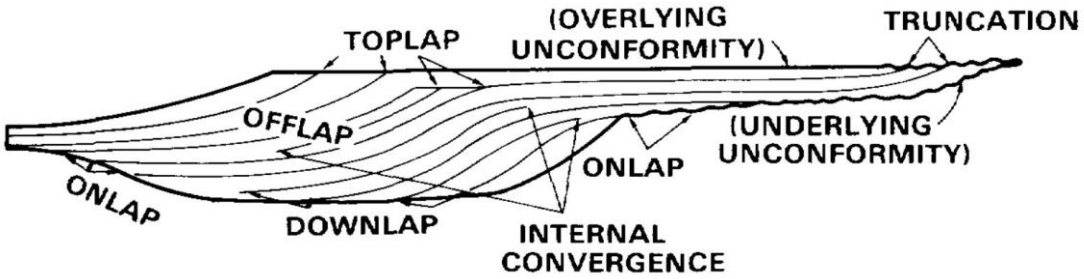

Figure 3-3-1: Seismic stratigraphic reflection terminations within a seismic sequence. Figure is added from Mitchum et al. (1997).

Seismic sequence analysis are classified in terms of reflection terminations, which are based on types of stratal terminations. These types of terminations are illustrated in Figure 3-3-1. The terminations including top-discordant relations is erosional truncation and toplap. **Erosional truncation** implies the deposition of strata and their subsequent removal along an unconformity surface (strata against an overlying erosional surface). **Toplap** can be classified as strata against an overlying surface as a result of non-deposition (sedimentary bypassing). Of the two, erosional truncation is generally the most reliable top-discordant criterion of a sequence boundary (Mitchum et al., 1977).

The terminations including base-discordant relations is onlap and downlap. **Onlap** is in general horizontal strata, terminated progressively against an initial inclined surface, or in which already inclined strata is terminating progressively updip against a surface of greater initial inclination. **Downlap** is a relation that in many ways are the opposite of toplap, where seismic reflections are interpreted as initially inclined strata terminating downdip against a horizontal surface. The two terminations are similar, and sometimes hard to differ. If this is the case, the term baselap is used. Out of the two, true onlap is normally the most reliable base-discordant for a sequence boundary (Mitchum et al., 1977).

Terminations not related to boundaries between sequences, but rather within a sequence can be identified as internal convergence and offlap (Mitchum et al., 1977). **Internal convergence** is used when strata is thinning out, and becoming smaller than the seismic resolution (not showing as a separate structure in the seismic). **Offlaping** terminations can be used for reflection patterns from prograding strata into basins (Mitchum et al., 1977).

After the seismic sequences are defined, environment and lothofacies within the sequences are interpreted. This is called seismic facies analysis, and are interpreted and described by looking at configuration, continuity, amplitude frequency and interval velocity. Seismic sequences are

interpreted in relation to environmental setting, depositional processes, and estimates of lithology (Mitchum et al., 1977).

The Kai formation in confined by the mid-Miocene unconformity at the base, and the Naust unconformity at the top. Firstly these two will be mapped and interpreted, secondly possible internal sub-horizons will be mapped. The horizons will be displayed using isochrone maps, while the deposits between will be displayed using isopach maps.

SEISMIC FACIES PARAMETERS	GEOLOGIC INTERPRETATION
REFLECTION CONFIGURATION	• BEDDING PATTERNS • DEPOSITIONAL PROCESSES • EROSION AND PALEOTOPOGRAPHY • FLUID CONTACTS
REFLECTION CONTINUITY	• BEDDING CONTINUITY • DEPOSITIONAL PROCESSES
REFLECTION AMPLITUDE	• VELOCITY-DENSITY CONTRAST • BED SPACING • FLUID CONTENT
REFLECTION FREQUENCY	• BED THICKNESS • FLUID CONTENT
INTERVAL VELOCITY	• ESTIMATION OF LITHOLOGY • ESTIMATION OF POROSITY • FLUID CONTENT
EXTERNAL FORM & AREAL ASSOCIATION OF SEISMIC FACIES UNITS	• GROSS DEPOSITIONAL ENVIRONMENT • SEDIMENT SOURCE • GEOLOGIC SETTING

Table 3-1: Seismic reflection parameters used in seismic stratigraphy, and their geologic significance. Table added from Mitchum et al. (1977).

Each parameter displayed in Table 3-3-1 provides information on the geology of the subsurface. **Reflection configuration** can show gross stratification patterns, which can be used to interpret depositional processes, erosion and paleotopography. **Reflection continuity** can be used to determine continuity of strata, which can suggest a widespread, uniformly stratified deposits. **Reflection amplitude** may display information on the velocity and density contrasts, which can be used to predict lateral bedding changes, as well as hydrocarbon occurrences. **Frequency** is related to geologic factors as the spacing of reflectors, and lateral changes in **interval velocity**, associated with gas occurrence (Mitchum et al., 1977). Using these reflection parameters together allows interpretation of the depositional environment and the geological setting within a sequence (Mitchum et al., 1977). The general geometry of a seismic unit consists of the external shape of the unit, as well as the internal reflection configuration of the unit (Table 3-3-2). Both must be described and interpreted to understand the geometric internal relation and depositional setting of the units (Mitchum et al., 1977).

REFLECTION CONFIGURATIONS (WITHIN SEQUENCES)		EXTERNAL FORMS (OF SEQUENCES AND SEISMIC FACIES UNITS)
PRINCIPAL STRATAL CONFIGURATION		
PARALLEL		SHEET
SUBPARALLEL		SHEET DRAPE
DIVERGENT		WEDGE
PROGRADING CLINOFORMS		BANK
SIGMOID		LENS
OBLIQUE		MOUND
COMPLEX SIGMOID-OBLIQUE		FILL
SHINGLED		
HUMMOCKY CLINOFORM		
CHAOTIC		
REFLECTION-FREE		
MODIFYING TERMS		
EVEN	HUMMOCKY	
WAVY	LENTICULAR	
REGULAR	DISRUPTED	
IRREGULAR	CONTORTED	
UNIFORM		
VARIABLE		

Table 3-2: Geological interpretation of seismic facies parameters. Table modified from Mitchum et al. 1997.

3.3.3 Seismic expression of contourites.

Seismic studies of contourites can be used to predict lithology and reconstructing the geological and (palaeo) oceanographic history. Other studies have identified the deposits in the Kai formation to be off contouritic origin (Laberg et al., 2005a). Therefore the knowledge of contourite characteristics in reflection-seismic is important. This characterization of contourites can be divided into three 'orders of seismic sediments', called large-, medium- and small scale (Nielsen et al., 2008) (Fig. 3-3-2).

The first order of seismic elements, classified as large scale, can be based on the overall architecture of the deposited contourite drift system. This includes the external geometry, finding upper and lower boundaries of the drift, and configuration of larger internal seismic units (Nielsen et al., 2008). The external geometry comes down to that contourite drifts can be classified as either sheeted or mounded, which further can be divided into five main types based on different geological and oceanographic settings; Sheeted drifts, Giant elongated drifts, Channel-related drifts, Confined drifts and Mixed drift systems (Nielsen et al., 2008). Differentiate between a contourite drift and other deep-sea deposits may be difficult, but contourites drifts can be recognized by having a unique geometry. Contourite deposits is normally the result of elongated along-slope processes, following the direction of the bottom currents (Nielsen et al., 2008). The top and base boundaries of a drift are important factors since they often create records of larger changes in the depositional environment, from a current-affected regime to a non-current-affected regime (Nielsen et al., 2008). This can result

in regional unconformities, confining the drift system. In the seismic, the unconformity can be revealed as a high amplitude reflector of semi-regional to regional extent. Internally the reflectors often show a low-angle downlap onto the unconformity (Nielsen et al., 2008). The internal seismic character of a contourite drift is overall a uniform pattern of continuous, low and medium amplitude reflectors that normally follows the gross drift morphology (Nielsen et al., 2008). **The second order of seismic elements (medium scale)** is based on the internal drift architecture of the sub-units, commonly displaying; (1) a lens-shaped, upward-convex geometry, (2) a uniform stacking pattern (normally intervals of stable conditions), (3) a progradational stacking pattern that shows migration in a down-current direction or an aggrading stacking pattern (common in sheeted drifts), and (4) downlapping reflector terminations. Second order of seismic sediments of contourites differs from the first order by being the result of smaller fluctuations causing variations in sediment characteristics like bedding, bioturbation, compaction and composition. **The third order of seismic elements can be classified as small scale**, and cannot alone be used as a diagnostic tool, but may be useful in combination with geometry of seismic units, or correlated with cores (Nielsen et al., 2008). In small scale contourite drifts, the most common seismic facies configurations are; (1) Continuous, (sub)parallel reflection configurations, (2) Wavy reflection configurations, (3) structureless or non-reflection configurations. Seismic attributes can be a tool to map current-induced bedforms like sediment waves and ripples, as well as channels etc. (Nielsen et al., 2008).

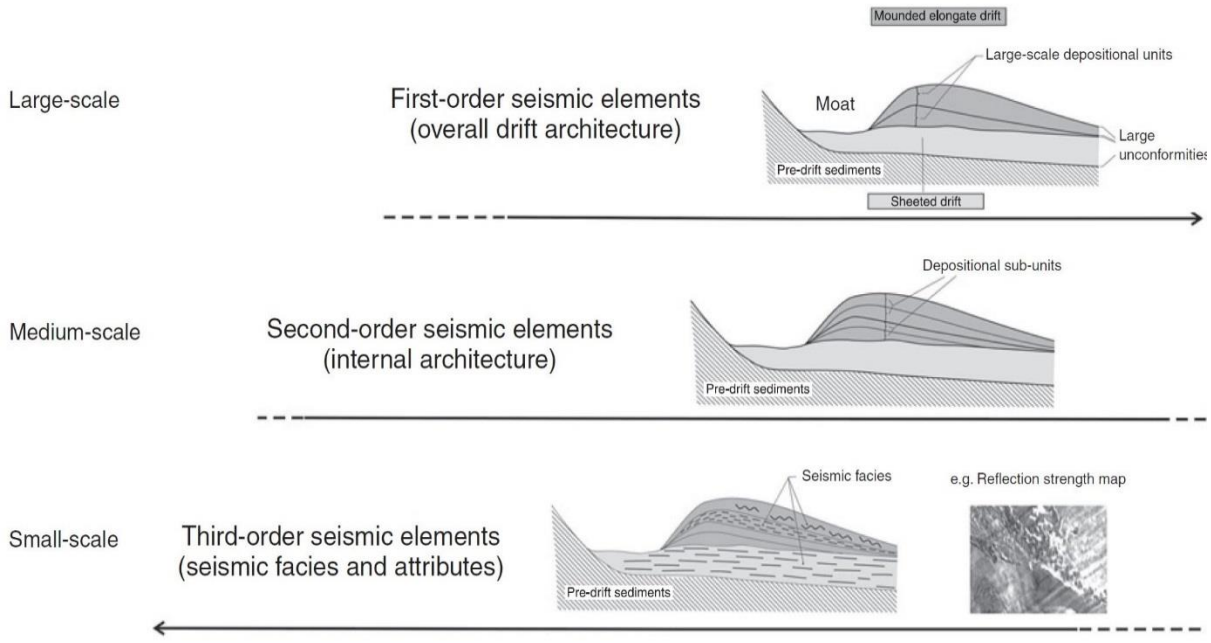

Figure 3-3-2: Seismic characteristics of contourite deposits, separating the different order of seismic elements. Figure added from Nielsen et al. (2008).

3.3.4 Correlating with well data

The well log data used in this study (Fig. 3-3-3) are retrieved from NPD's database (http://factpages.npd.no/factpages/Default.aspx?culture=no). The logs are named and described by NPD, and has been used to identify the depth to the main seismic reflectors form the depth of the Kai formation in the wells and to compare the depth to and estimated thickness of the Kai formation from the seismic stratigraphic analysis. This is done by calculating the depth of the top and base of the Kai formation in TWTT, and compare it with the interpreted TWTT depth. When calculating the different depths, mean slowness (used to find mean velocity) were conducted from NPD composite logs. The mean velocity and the depth in TWTT can be found by using equation 5 and 6 (Rider et al., 2011).

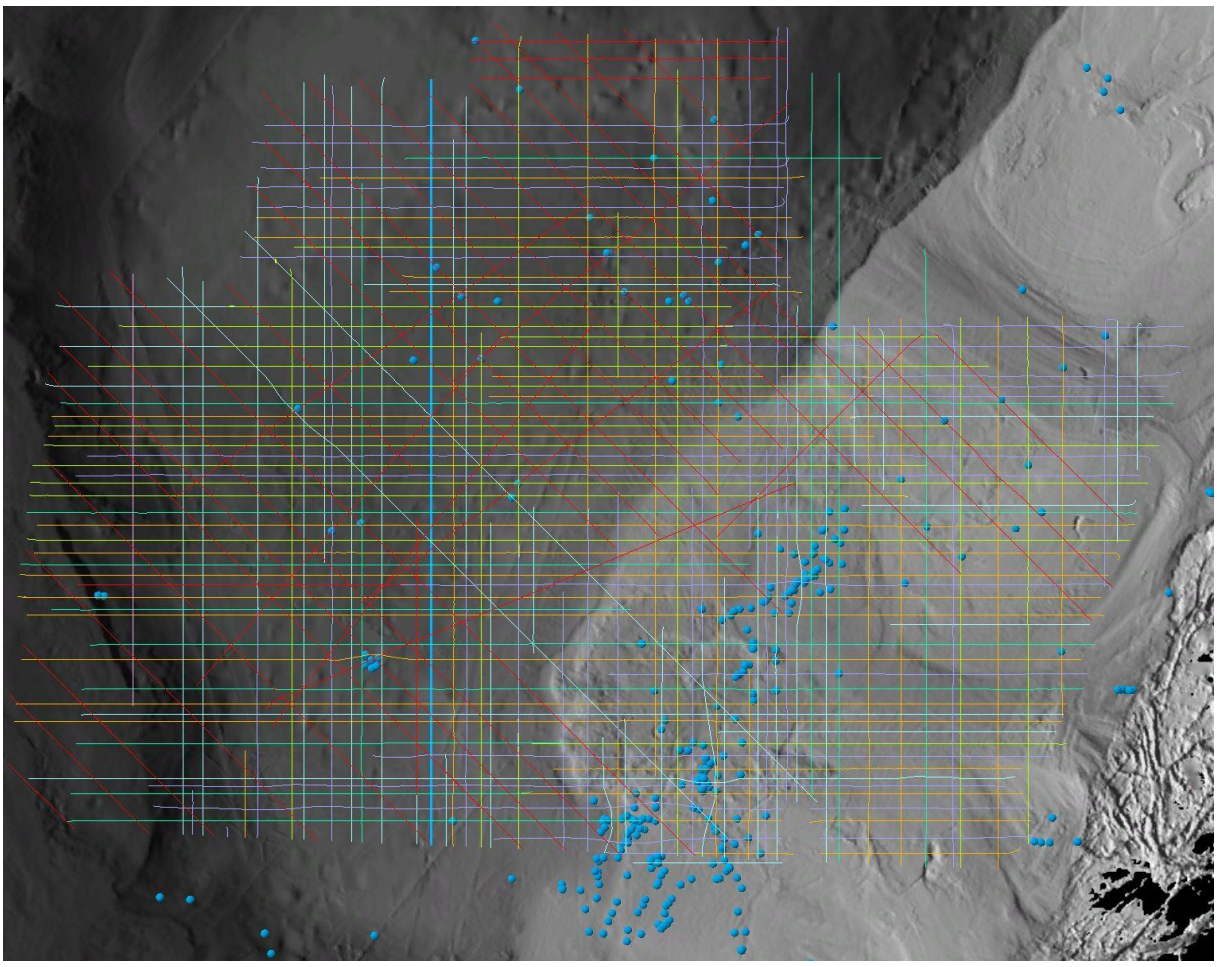

Figure 3-3-3: Location of the excessed well logs overlapping the seismic lines.

Finding the mean velocity (equation 5):

$$Velocity\ ft/\sec = \frac{1}{\Delta t \frac{\mu s}{ft} \times 10^{-6}} \times 0{,}3048$$

Where Δt is the slowness, and 0,3048 is the multiplication used to transform feet into meter. The found velocity is in m/s.

Finding the depth in TWTT (equation 6):

$$Depth\ TWTT = \frac{2 \times D}{V}$$

Where D is the depth in meter read of the composite log, and V is the calculated mean velocity.

4. Results

Chapter 4 presents the conducted results of this study. It includes the description and interpretation of the Kai formation in the study area, displayed by the different seismic surveys that were available. The overall stratigraphy of the formation will be presented. The area will thereafter be divided into subareas, based on stratigraphy and accumulation of sediments, and each area will be described and interpreted. This include the morphology of the base and the top of the Kai formation, as well as thickness variation throughout the formation. Internal seismic subunits will also be mapped to get a more detailed understanding of the paleo-environment of the formation and its controlling factors. The results will be discussed in Chapter 5.

4.1 Seismic stratigraphy, lithology and –age of the Kai formation

The seismic stratigraphy of the Kai formation were correlated to previous work including Rise et al., (2010), Chand et al., (2011) and Eidvin et al., (2014). This was done by using the depth of the base and top reflection of the formation from selected seismic lines. In addition, the established seismic stratigraphy was correlated to well logs. Multiple age estimates have been conducted in previous studies. Løseth & Henriksen, (2005) suggest a middle- to late Miocene age, while Eidvin et al., (2014) suggested that the oldest section of the Kai formation can be dated to mid Miocene – early Pliocene . This study is following the age estimate of Eidvin et al., (2014).

According to Eidvin et al. (2014) the Kai formation is overall clayey on the slope, with ooze in the basinal parts. This is in unity with Stoker et al., (2005) and Riis et al., (2005) who found that the Kai formation had deposits of fine-grained calcareous and siliceous oozes in the basin areas.

4.1.1 Seismic anomalies within the Kai formation

In the Vøring basin seismic anomalies occur at different depths. The strongest negative reflection in the Kai formation is a diagenetic reflector due to the Opal A to Opal CT conversion (DBSR) (Fig. 4-1-1), and occur along a wider area beyond the shelf edge. According to Chand et al. (2011) this is a bottom simulating reflector (BSR), which may be related to fluids flowing through pathways created by underlying polygonal fault systems in the Kai and Brygge formations. The DBSR may in some areas disturb the reflection pattern in the Kai formation, but since it is not a topic of this thesis it will not discussed further.

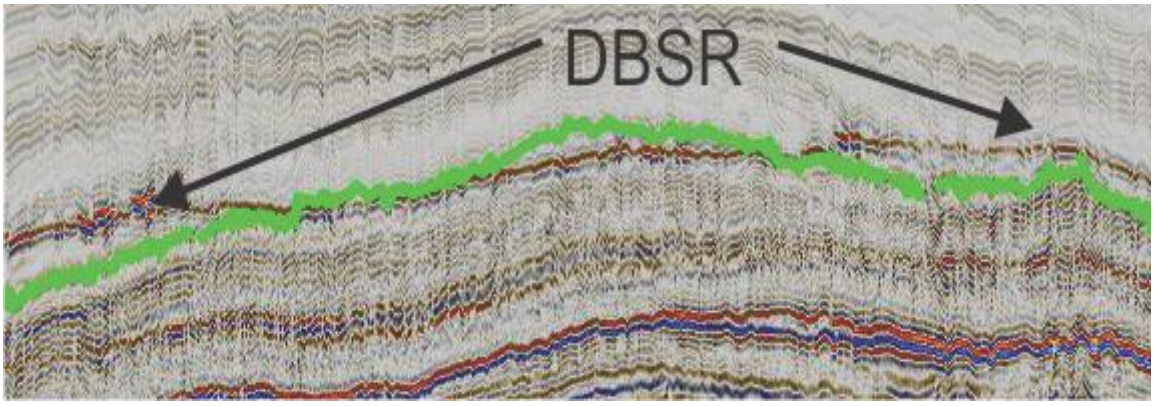

Figure 4-1-1: Outcrop of a seismic section displaying an example of The DBSR reflector, and how it may disturb the interpretation of horizons in the Kai formation. Green line: Base reflection of the Kai formation. The location of the image is shown in Figure 4-1-4.

4.1.2 Stratigraphy of the Kai formation

Multiple seismic profiles at different locations of the study area have been look upon (Fig. 4-1-2 and Fig. 4-1-6). This were done to create a better understanding of the prevalence of the Kai formation, as well as to what extent the formation is disturbed by the topography of anticlinal structures, like the Helland-Hansen Arch and Modgunn Arch. The thickest part of the Kai formation is found in the Vøring basin, while a thinner part of the formation is found further inland underlying the Naust formation (Fig.4-1-3). The seismic lines displays an interruption of the Kai formation between the basin and the shelf, due to the ascendance of the Helland-Hansen Arch (Fig. 4-1-3). The Kai formation is mostly absent here, as a result the Naust formation is directly overlying the Brygge formation. This interpretation is in accordance with Rise et al. (2010) (Fig. 2-5-2).

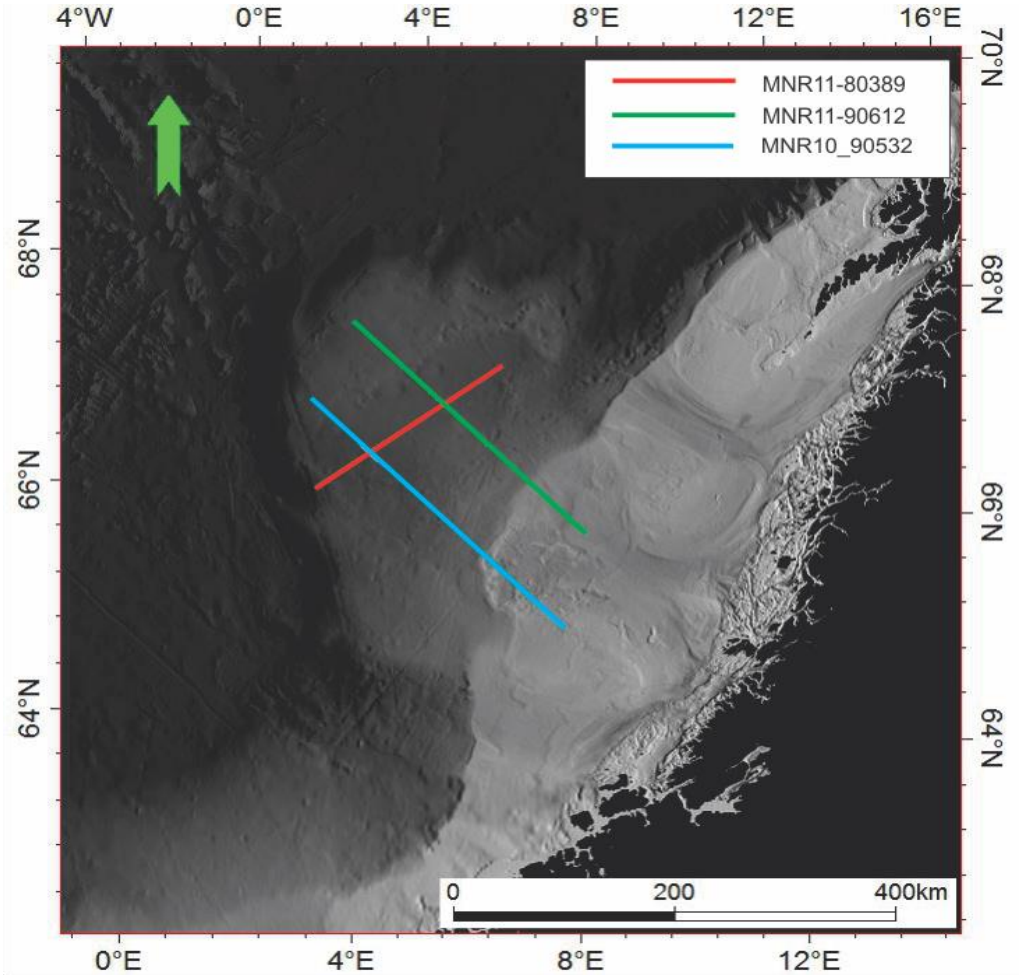

Figure 4-1-2: Bathymetry map of the mid-Norwegian margin with the location of seismic lines MNR11-80389, MNR11-90612 and MNR10_90532M, which makes up the first set of seismic lines used to describe the Kai formation.

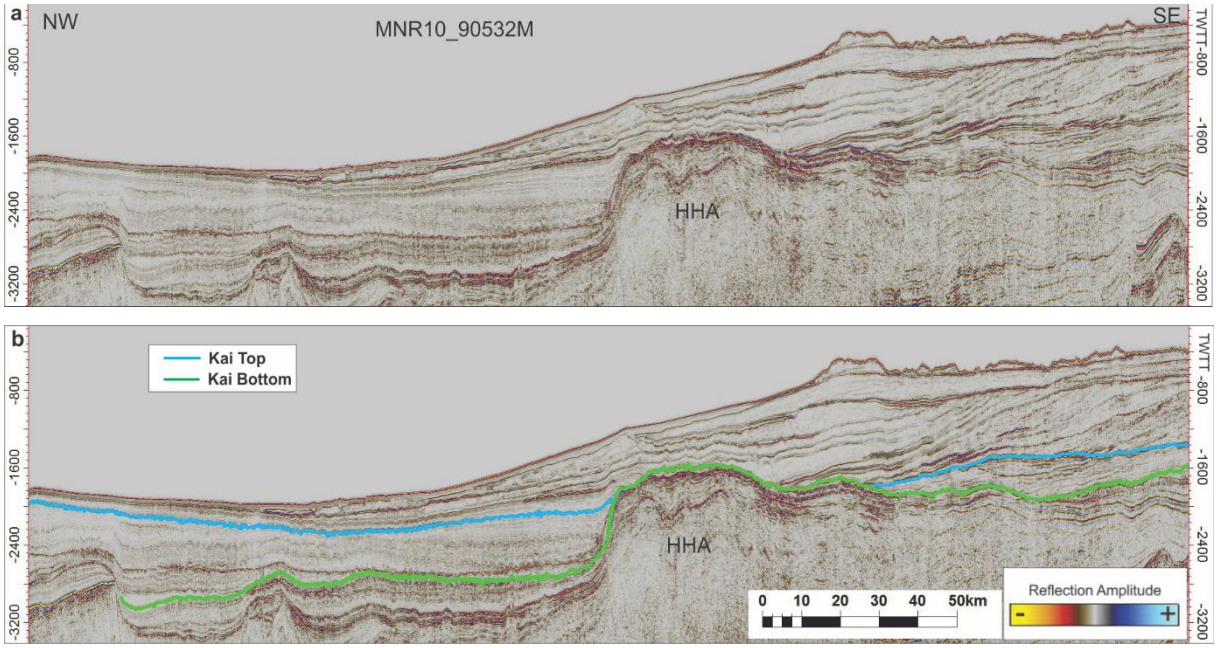

Figure 4-1-3: Seismic section of 2D-line MNR10_90532M displaying the top and base of the Kai formation. a) Line without interpretation. b) Line with interpretation of the top and base. HHA: Helland Hansen Arch. Scale on the sides are in m/s TWTT. Location of the seismic line is displayed in Fig. 4-1-2.

A distinct change in stratigraphy between the relatively flat-lying Kai formation and the propagating Naust formation is seen in the south-eastern part of the study area, which makes the boundary of the two formations relatively easily detectible. To the Northwest the distal part of the Naust formation is flattening, resulting in an internal seismic signature similar to the Kai formation. This made the interpretation of the formation problematic, and correlation to other studies were needed (Chand et al., 2011). The deepest part of the base Kai formation can be located in the northwestern part of Vøring basin (>3100 m/s TWTT) with a thickness up to ~1100 m/s TWTT.

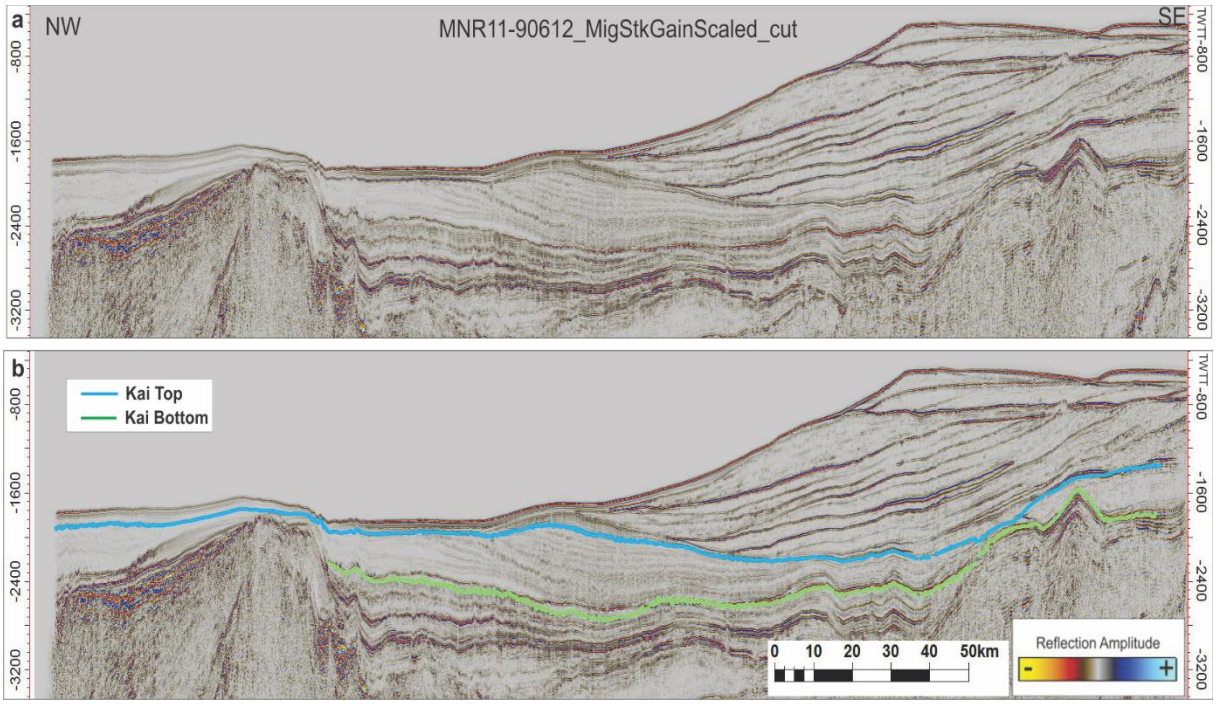

Figure 4-1-4: Seismic section of 2D-line MNR11-90612 displaying the top and base of the Kai formation. a) Line without interpretation. b) Line with interpretation of the top and base. Scale on the sides are in m/s TWTT. Location of the seismic line is displayed in Fig. 4-1-2.

Further north, seismic line MNR11-90612 (Fig. 4-1-4) shows the prevalence of the Kai formation without the influence of the Helland-Hansen Arch. This makes the interpretation of the top Kai formation easier in the northern part of the study area. Here, the Kai formation has a greater thickness in the basin (up to 1000 ms TWTT) while thinning landwards where the Naust formation is at its thickest. Contrary to the southeastern part of the study area, the depth of the base in the basin, is increasing southeastward, with its highest peak at the Vøring marginal high. The top reflection of the formation can be observed over the Vøring marginal high, while the base of the formation is ending on the northwestern flank of the marginal high, and its precise depth is difficult to locate further westward. Figure 4-1-4 displays the Kai

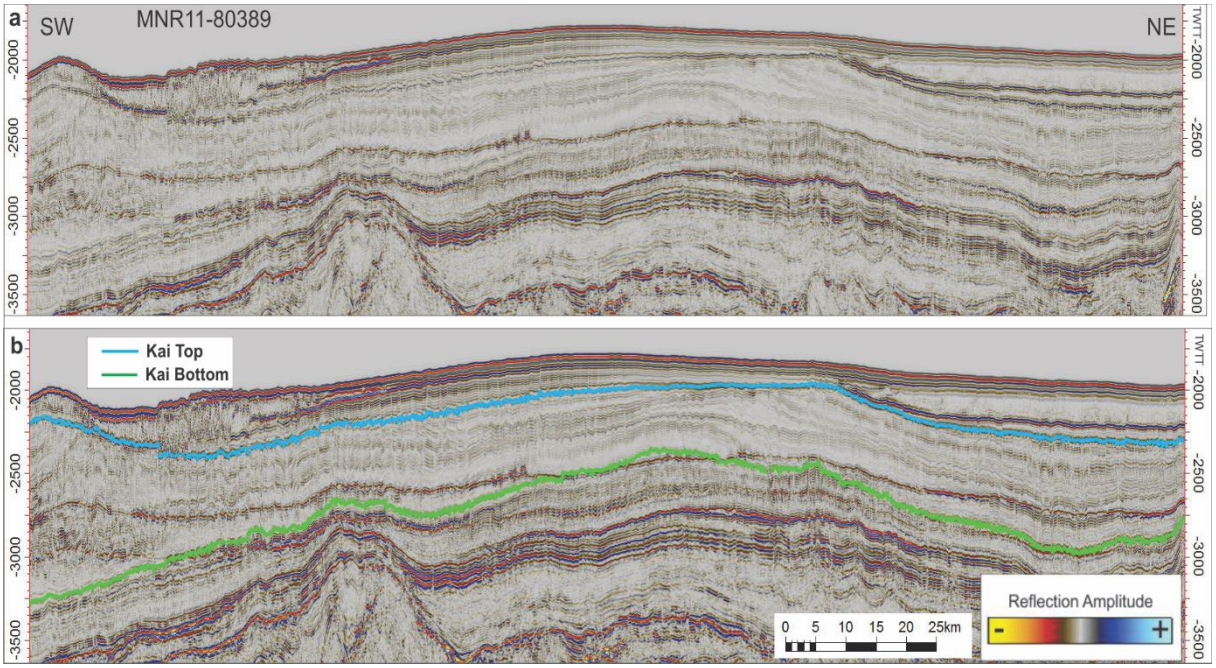

Figure 4-1-5: Seismic section of 2D-line MNR11-80389 displaying the top and base of the Kai formation. a) Line without interpretation. b) Line with interpretation of the top and base. Yellow outline displays the location of Figure 4-1-1. Scale on the sides are in m/s TWTT. Location of the seismic line is displayed in Fig. 4-1-2.

formation as a continuous formation, not following the trend of the formation being absent around the western basinal high of the Vøring basin.

Interpreting the top and base of the Kai formation in a southwest/northeast orientation is displaying how the Kai formation propagate from the earlier described northern and southern part of the study area. In the Vøring basin the Kai formation has a relatively uniform thickness throughout the section, with exception of the southwestern part (Fig. 4-1-5). Here the formation is ay its deepest (~3250 ms TWTT below the sea floor) and thickest (~1000 ms TWTT). The whole formation, as well as older sediment packages is experiencing an elevation of the formations in the middle of the Vøring Basin (Fig. 4-1-5).

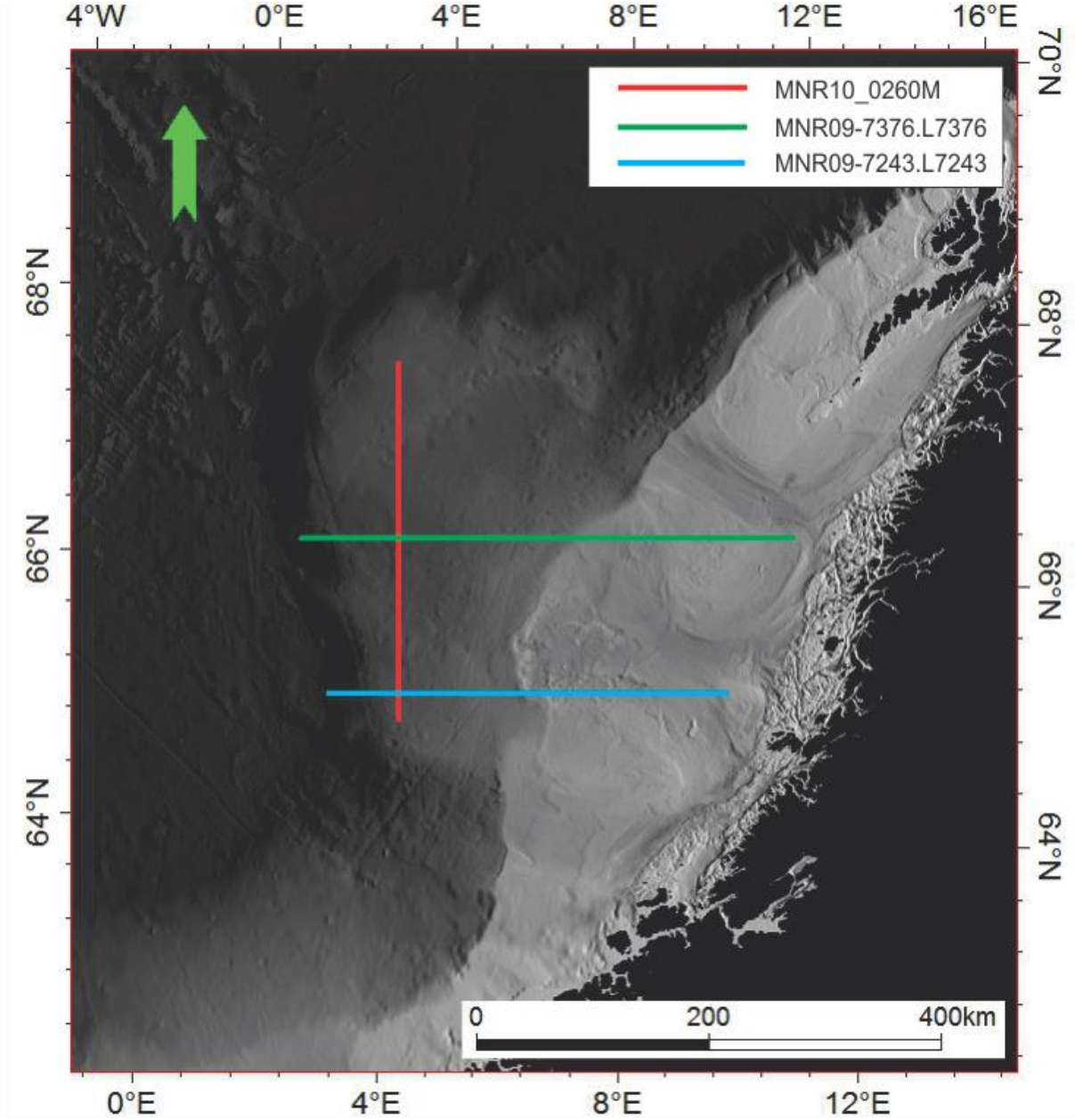

Figure 4-1-6: Bathymetry map of the mid-Norwegian margin with the location of seismic lines MNR10_0260M, MNR09-7376 and MNR09-7243, which makes up the second set of seismic lines used to describe the Kai formation.

To get a better understanding the study area, seismic profiles with different orientation are interpreted (Fig. 4-1-6). In the very southern part of the study area, the Helland-Hansen Arch plays a major part in the prevalence of the Kai formation, because of the great size (2-1-1) of the arch. Here the Vøring basin is rather narrow, resulting in a restricted distribution of the formation west of the Helland-Hansen arch. East of the Arch, the formation thickens up to approximately 400-500 ms TWTT, slowly thinning westwards. Figure 4-1-7 displays the Kai formation being continuous towards Molo formation in the east, which may indicate that Kai and Molo formation were deposited at fairly the same time-period. This will be interpreted and discussed later on.

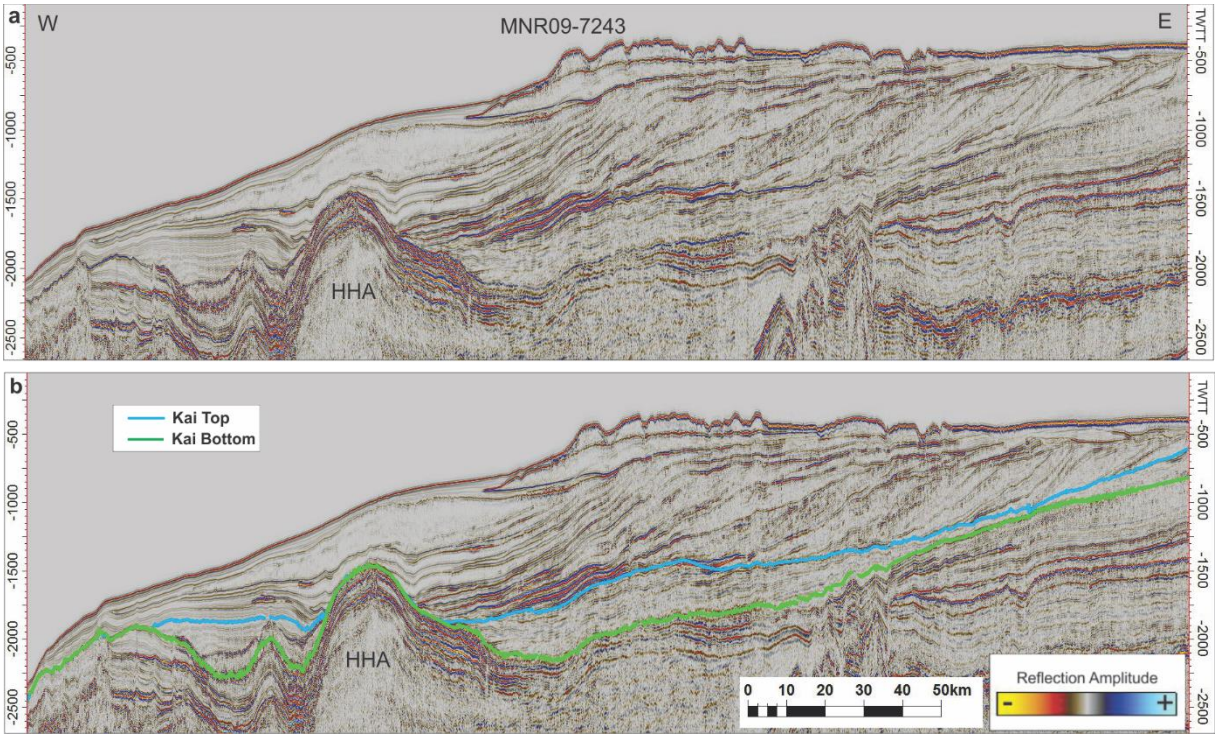

Figure 4-1-7: Seismic section of 2D-line MNR09-7243.L7243 displaying the top and base of the Kai formation. a) Line without interpretation. b) Line with interpretation of the top and base. HHA: Helland Hansen Arch. Scale on the sides are in m/s TWTT. Location of the seismic line is displayed in Fig. 4-1-6.

Further north the Kai formation is not as afflicted by the Helland-Hansen Arch, which results in a fairly uniform distribution of the formation in the basin, with the deepest part to the west (3200 ms TWTT) with a thickness of approximately 1000 ms TWTT (Fig. 4-1-8). Here, the distribution of sediments towards the eastern part of the section is fairly low and not as uniform as further south, with the Kai formation disappearing in some areas.

In a north/south orientation (Fig. 4-1-9) the Kai formation does not variate much in thickness (600-800 m/s TWTT). North of the Vøring basin, the Kai formation is hard to interpret, due to the marginal high. By interpreting the Kai formation in a north/south orientation, multiple structures and fault patterns have been found, that differs from structures observed in profiles orientated perpendicular to the shelf. There is an elevation of the base Kai formation in the mid-northern part of the section. This elevation is only affecting the base, and not the top of the Kai formation.

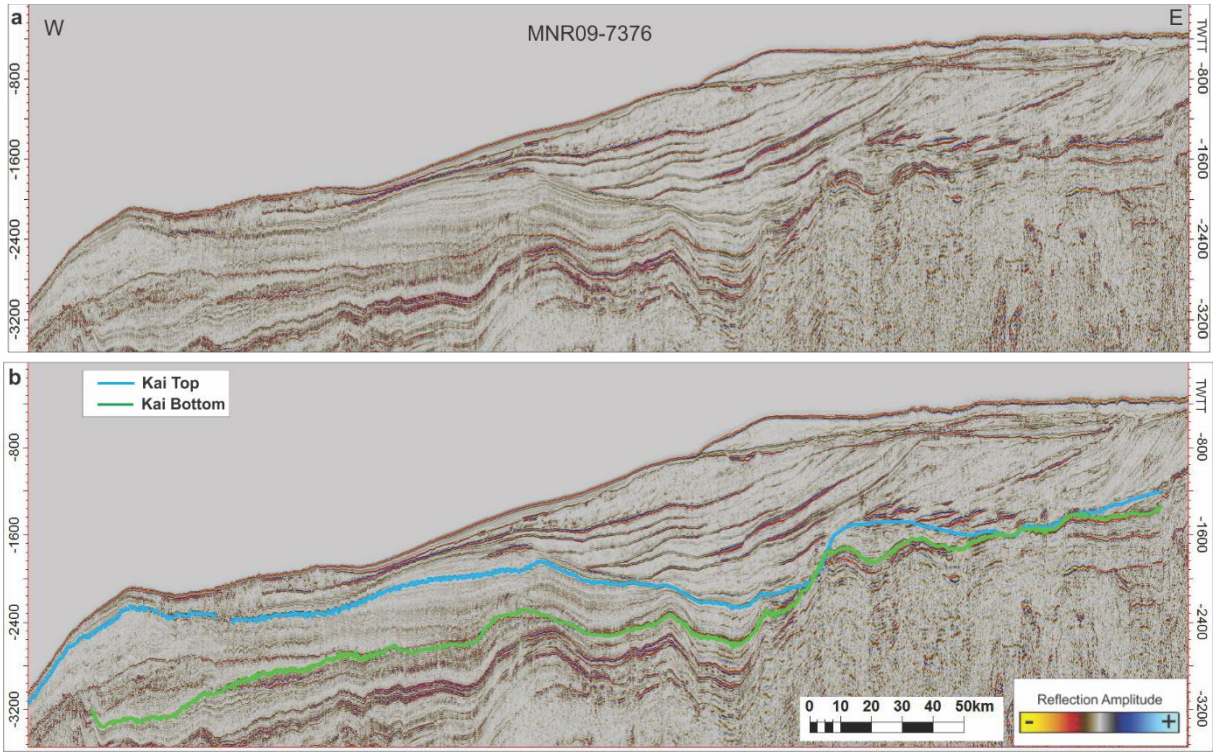

Figure 4-1-8: Seismic section of 2D-line MNR09-7376 displaying the top and base of the Kai formation. a) Line without interpretation. b) Line with interpretation of the top and base. Scale on the sides are in m/s TWTT. Location of the seismic line is displayed in Fig. 4-1-6.

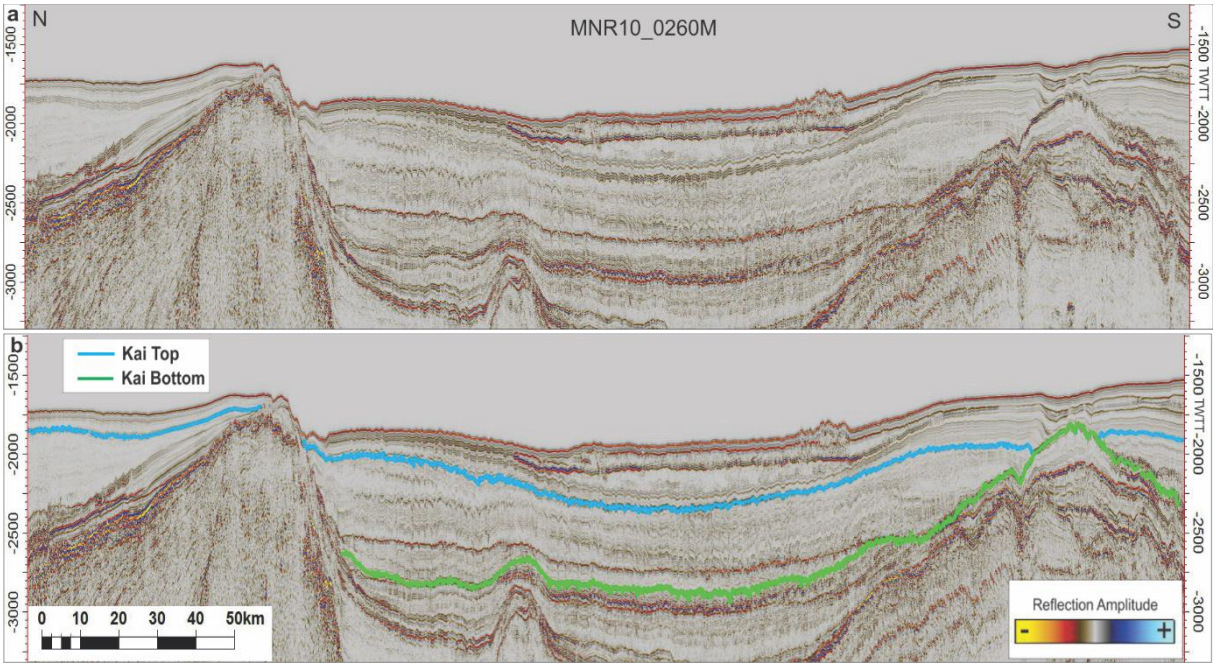

Figure 4-1-9: Seismic section of 2D-line MNR10_0260M displaying the top and base of the Kai formation. a) Line without interpretation. b) Line with interpretation of the top and base. Scale on the sides are in m/s TWTT. Location of the seismic line is displayed in Fig. 4-1-6.

4.2 Geometry of the Kai formation

To describe and interpret the Kai formation, isochrones of the top and base of the formation were generated, as well as an isopach map to display the thickness variation of the formation throughout the study area.

4.2.1 Bottom surface

Figure 4-2-1 shows how the paleo-relief of the studied part of the mid-Norwegian continental shelf and the Vøring margin before the Kai formation were deposited, at the end of the deposition of the Brygge formation. The base Kai isochrone map clearly shows how, in a

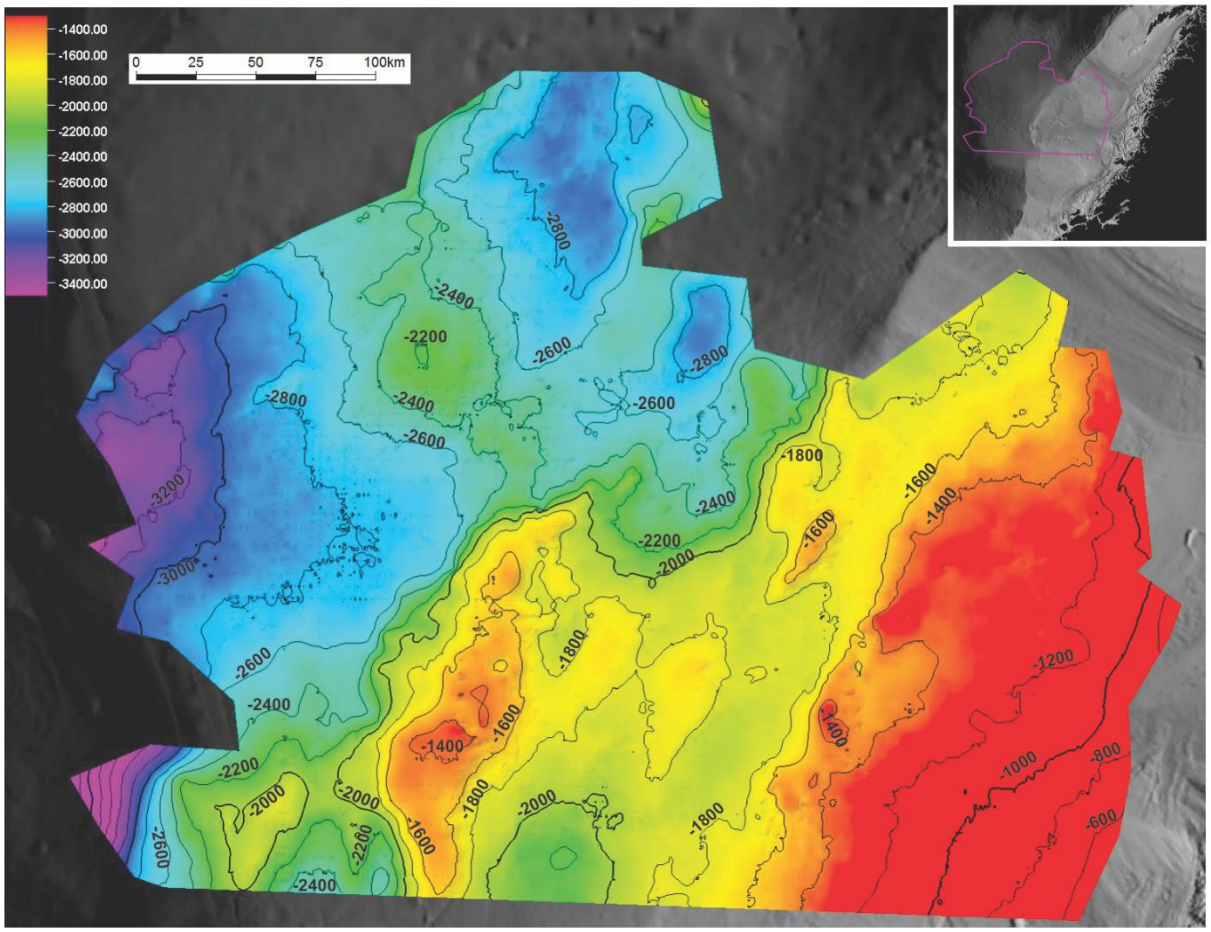

Figure 4-2-1: Seismic horizon of the base Kai formation surface, displaying the depth prevalence of the surface in the study area. Location of the generated surface is displayed as a polygon in the top right corner. The shown depth color table is in TWTT.

general trend, the base Kai formation is located at greater depth in the western part of the study area, in the Vøring basin as compared to the east. Since the Helland-Hansen Arch is located in the central part of the study area, there is a heightening of the base Kai paleo-surface. Here the Arch lies at a depth of up to approximately -1400ms (TWTT). The eastern part of the study area is found at a relatively uniform depth of about -1400 m/s. In the Vøring

basin, the base Kai formation is found at greater depths in the southwestern and northeastern part of the basin, while there is an NW/SW oriented elevation in the middle part of the basin.

4.2.2 Top surface

The top Kai paleo-surface displays how the mid-Norwegian continental margin looked like right before the deposition of the Naust formation began. The top surface have many similarities to the base surface (Fig. 4-2-2). The Helland-Hansen Arch is still a visible feature

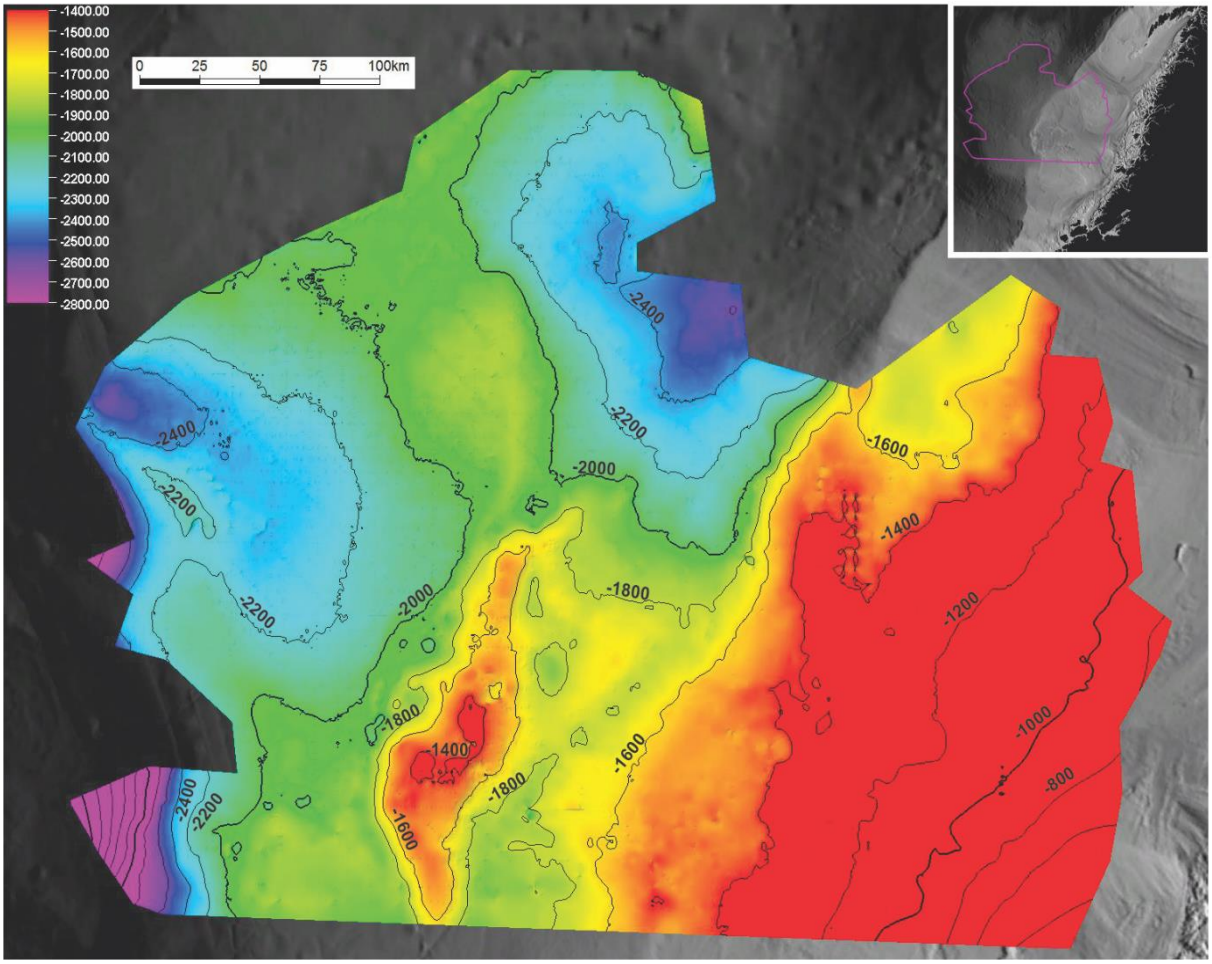

Figure 4-2-2: Seismic horizon of the top Kai formation surface, displaying the depth prevalence of the surface in the study area. Location of the generated surface is displayed as a polygon in the top right corner. The shown depth color table is in TWTT.

having an elevation of approximately the same depth as the base surface of the Kai formation which shows that the Kai formation is very thin or completely absent here. The deepest part of the top surface is located in the Vøring basin, in the southwestern and northeastern part of the basin, displaying the same trend as the bottom surface. Landwards the interpreted top reflection rises to a depth lower than 800 ms TWTT below the surface. In the southwestern part of the study area, an elevation is located. This may be the Modgunn Arch, as it fits with

the location displayed in Figure 2-1-1. The visibility of the two arches in the top surface of the Kai formation, suggest that they have had an influence on the deposition of the formation.

4.2.3 Thickness of the formation

By using the Kai formation base and top surface horizons, a thickness map was created to display the thickness of the formation in the study area. The thickness map (Fig. 4-2-3) shows the distribution of the sediments comprising the Kai formation in the study area. The thinnest

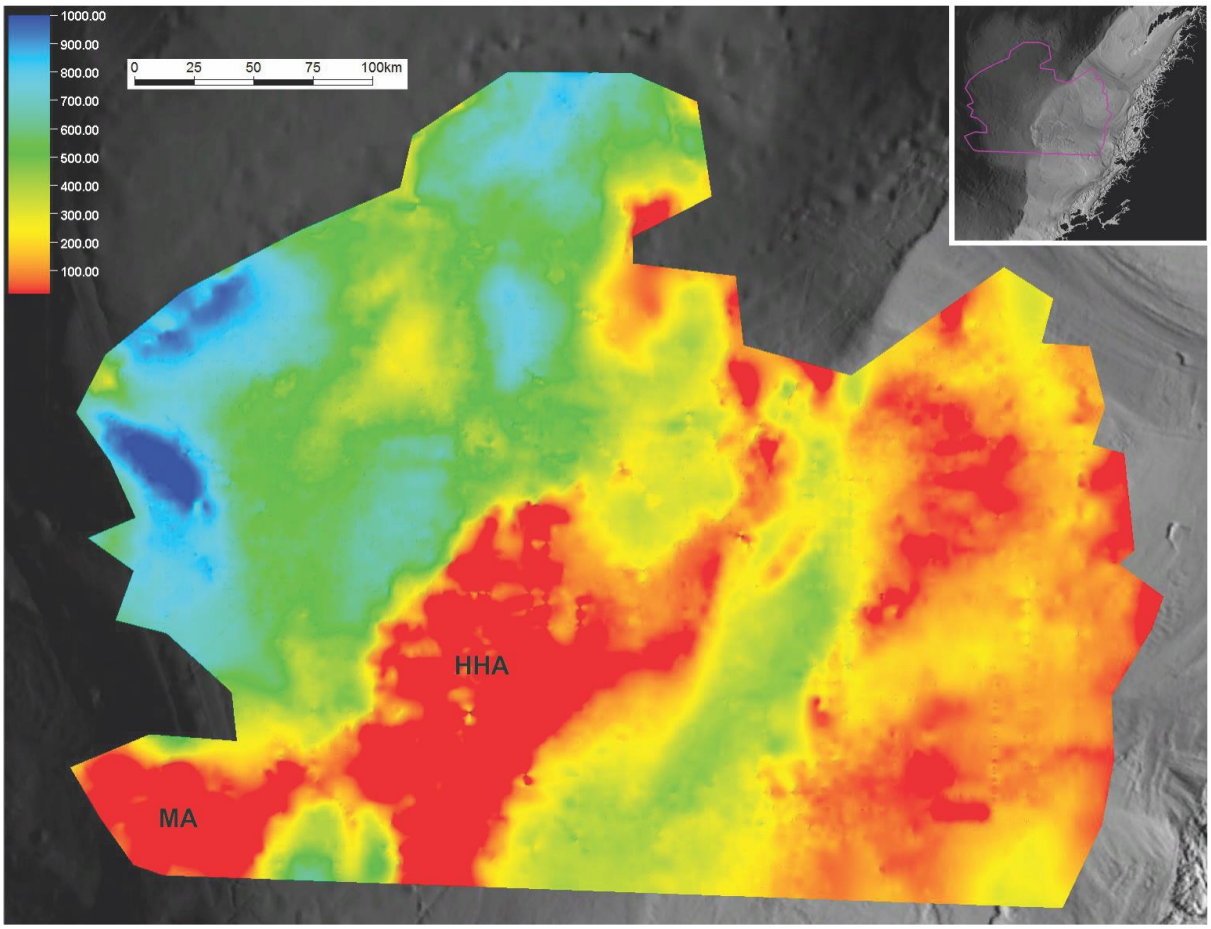

Figure 4-2-3: Thickness map of the Kai formation, displaying the prevalence of the sediments in the study area. Location of the generated map is displayed as a polygon in the top right corner. HHA: Helland-Hansen Arch, MA Modgunn Arch. The color table displays the thickness in TWTT.

part of the Kai formation is found in the area of the HHA and the Modgunn Arch, as well as in the easternmost part of the study area (towards the coast of mainland Norway). The greatest thickness is found in the Vøring basin, as well as on the shelf east of the HHA. Here the thickness is in excess of 1000 ms (TWTT).

According to Rise et al., (2010) the absence of the Kai formation above the HHA and the MA can indicate that the depositional environment was affected by bottom currents.

4.2.4 Subareas for further interpretation

By looking at the thickness map as well as some regional seismic lines, the study area can be easily be divided into different subareas based on sediment thickness, location and local sequence patterns throughout the formation. All northwest/southeast orientated seismic lines used to display the stratigraphy of the formation in chapter 4.1 has a similar trend of having two different areas of sediment deposition. These two areas are located at the inner shelf (Area 1) and at the outer shelf, in the Vøring basin (Area 2). The thickness map displayed in figure 4-2-3 confirms this, as there is a clear reduction in deposits at the HHA and further northeast (Fig. 4-2-4).

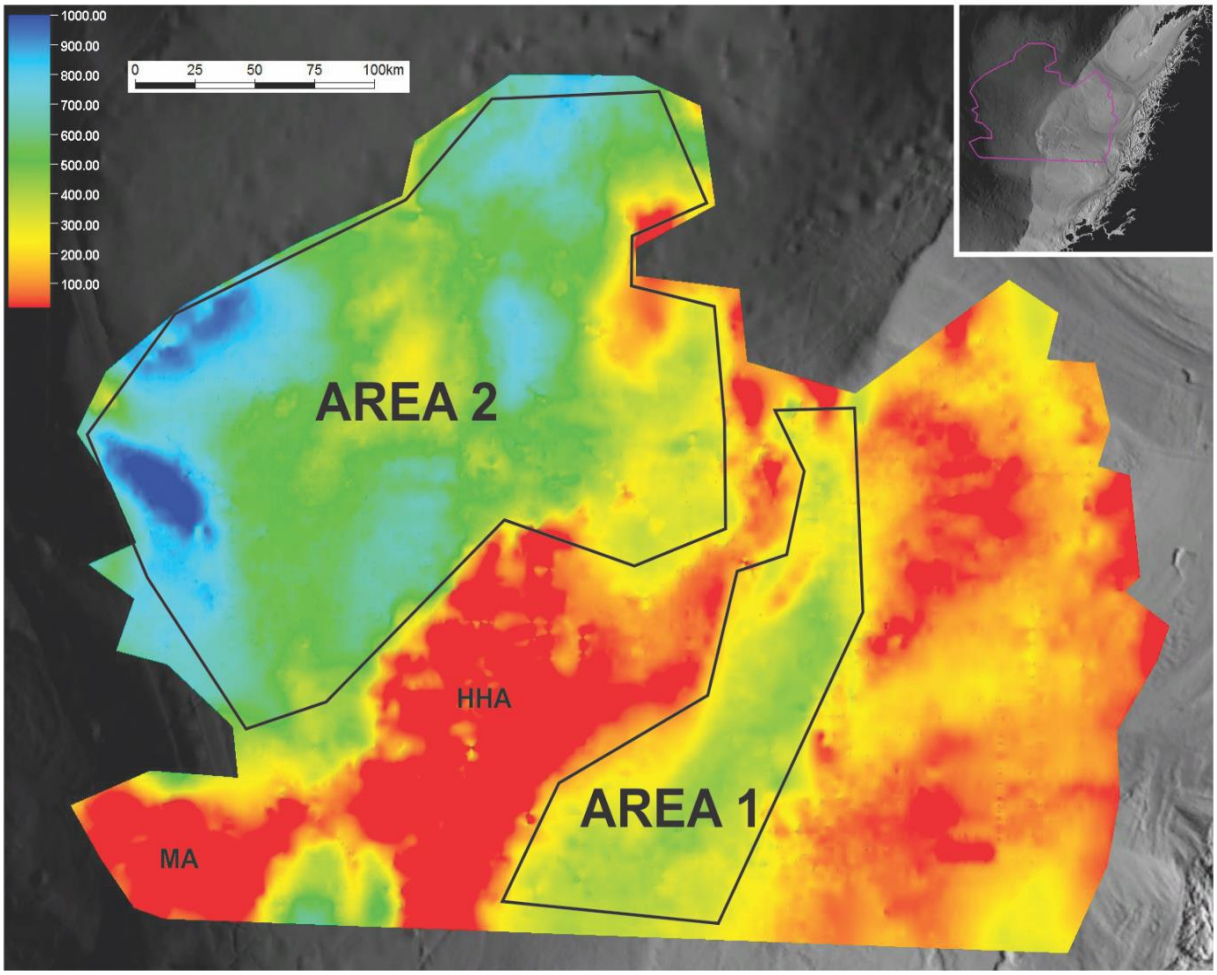

Figure 4-2-4: Location of area 1 and 2 in the study area, displayed in a thickness map. Location of the generated map is displayed as a polygon in the top right corner. HHA: Helland-Hansen Arch, MA Modgunn Arch. The color table displays the thickness in TWTT.

4.3 Geometry, sediment thickness and internal seismic reflection pattern

The geomorphology of the Kai formation will first be described and interpreted for the inner shelf (Area 1), and then the outer shelf (Area 2) will be presented. In addition to this, the relation between the Kai formation and the Molo formation towards the mainland will be addressed.

4.3.1 Area 1

In area 1 sediment thickness varies between 200 and 500 m/s TWTT. Here, the Kai formation has a northeast/southwestern orientation, following the orientation of the continental margin. The area is approximately 90 km wide in the south, decreasing to 30 km to the north (Fig 4-3-1). The thickness of the package is relative consistent throughout the area, with no major interruption or deviation of the sequence. The Kai formation in area 1 is confined by the HHA in the west, and by a thinning of the formation to the east, where the Naust formation is more dominant.

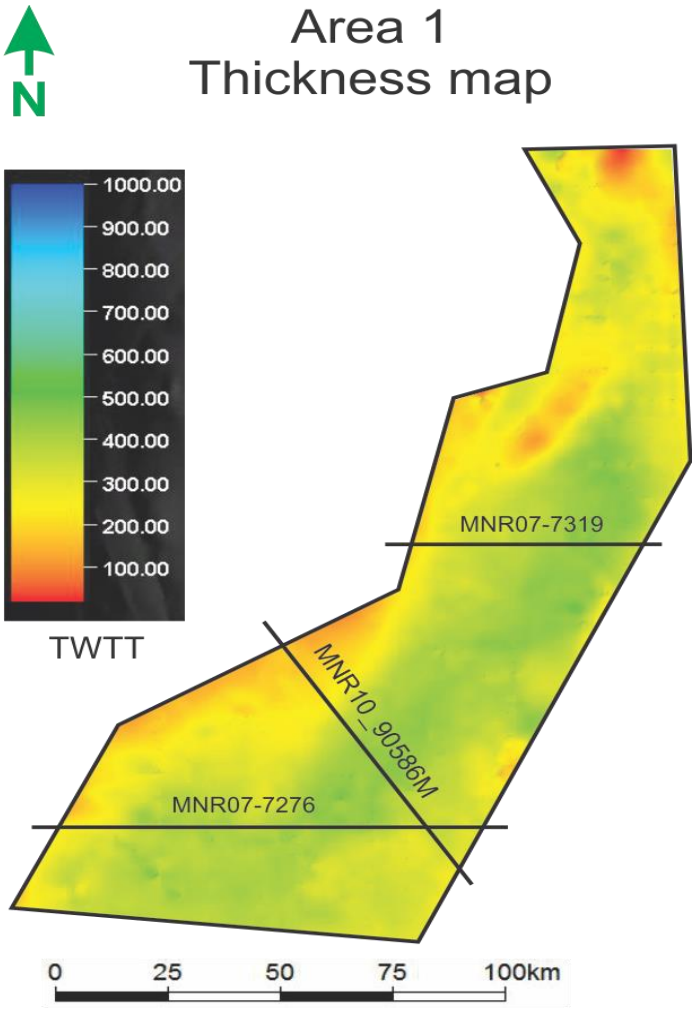

Figure 4-3-1: Thickness map of Area 1, showing the sediment thickness as well as parts of different seismic lines for further interpretation. Location of the area is displayed in Figure 4-2-4.

In the middle part of Area 1, the Kai formation reaches a thickness up to 400 ms (TWTT) (Fig. 4-3-2a). Seismic line MNR07-7319 is a W/E orientated line located in the middle part of area 1 (Fig. 4-3-1). The seismic section include mostly weak, parallel-sub-paralell reflectors throughout the formation. To the west, the reflectors are downlapping the basal reflection (Fig. 4-3-2b), while to the east, an onlapping pattern is present.

In conformity with Nielsen et al., (2008), this seismic signature is interpreted to represent a Mounded elongated drift system comprising contouritic sediments.

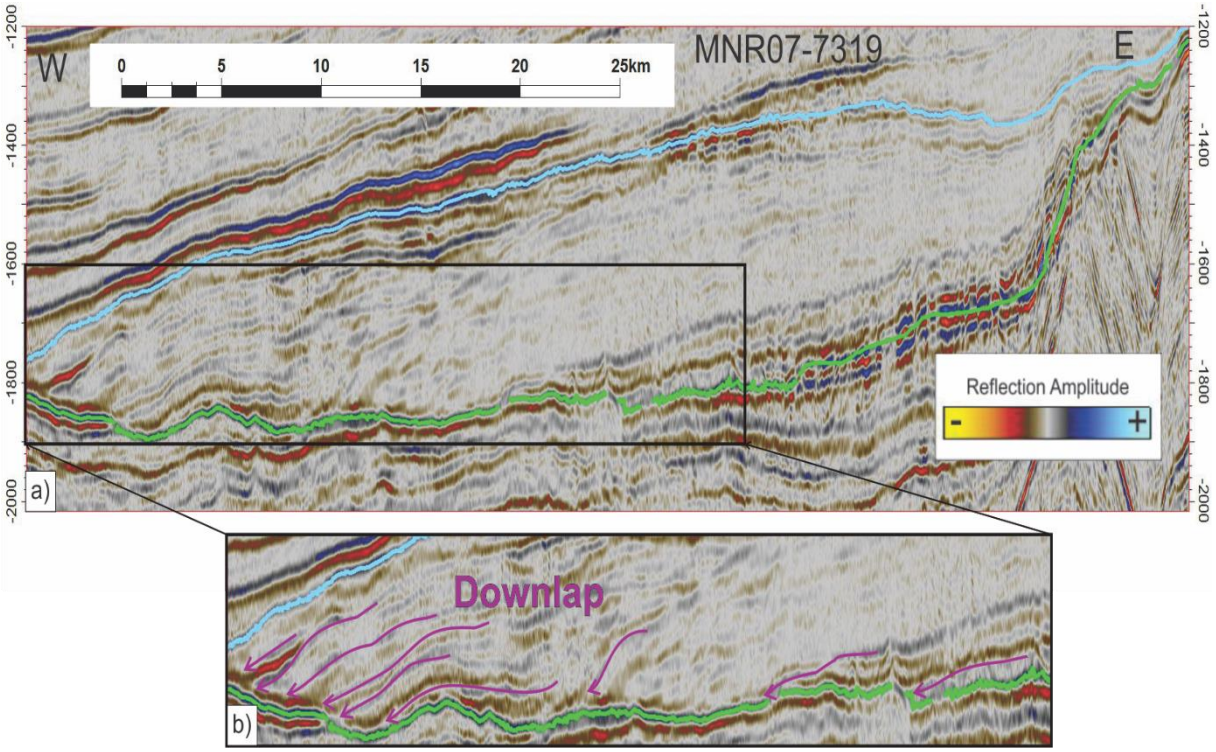

Figure 4-3-2: a) seismic section of line MNR07-7319. b) Framed section of a). Blue line: top Kai formation, green line: base Kai formation, purple arrows: orientation and extent of the reflectors interpreted as downlap. Scale on the side is ms TWTT.

In the southeastern part of area 1 (Fig. 4-3-3a) the Kai formation is thinning out towards the northwest and interrupted in the southeast by a dome-like structure. The thickness of the Kai formation reaches approximately 400 ms (TWTT) southeast of the dome-like structure. The seismic reflectors mostly follows the orientation of the underlying base of the Kai formation. In the northwest there is a similar seismic pattern further north (Fig. 4-3-2), with down-dipping weak reflectors creating downlap onto the underlying unconformity (Fig. 4-3-3b) towards the northwest. In the southeast seismic reflectors are divided at the interrupting dome. The two different path of reflectors are separated by a simulated black dotted line in the seismic profile in Figure 4-3-3a. The top local sequence follows the dome structure with upward inclining reflectors. The bottom local sequence on the other hand are dipping

downwards into the base unconformity of the Kai formation, creating an onlap seismic stratigraphic reflection (Fig. 4-3-3c) because of the strata being terminated progressively against an initial inclined surface of the dome structure. Where the two seismic paths separates, there is a moat due to the lack of sediments towards the dome. This may suggest that there is an elongated mounded drift there, comprising contouric sediments (Nielsen et al., 2008).

Laberg et al., (2001) and Bryn et al., (2005) identified the occurrence of mounded contouritic deposits and associated moats along the outer Vøring and Lofoten margins, as well as low-mounded sheeted drifts in the Møre basin.

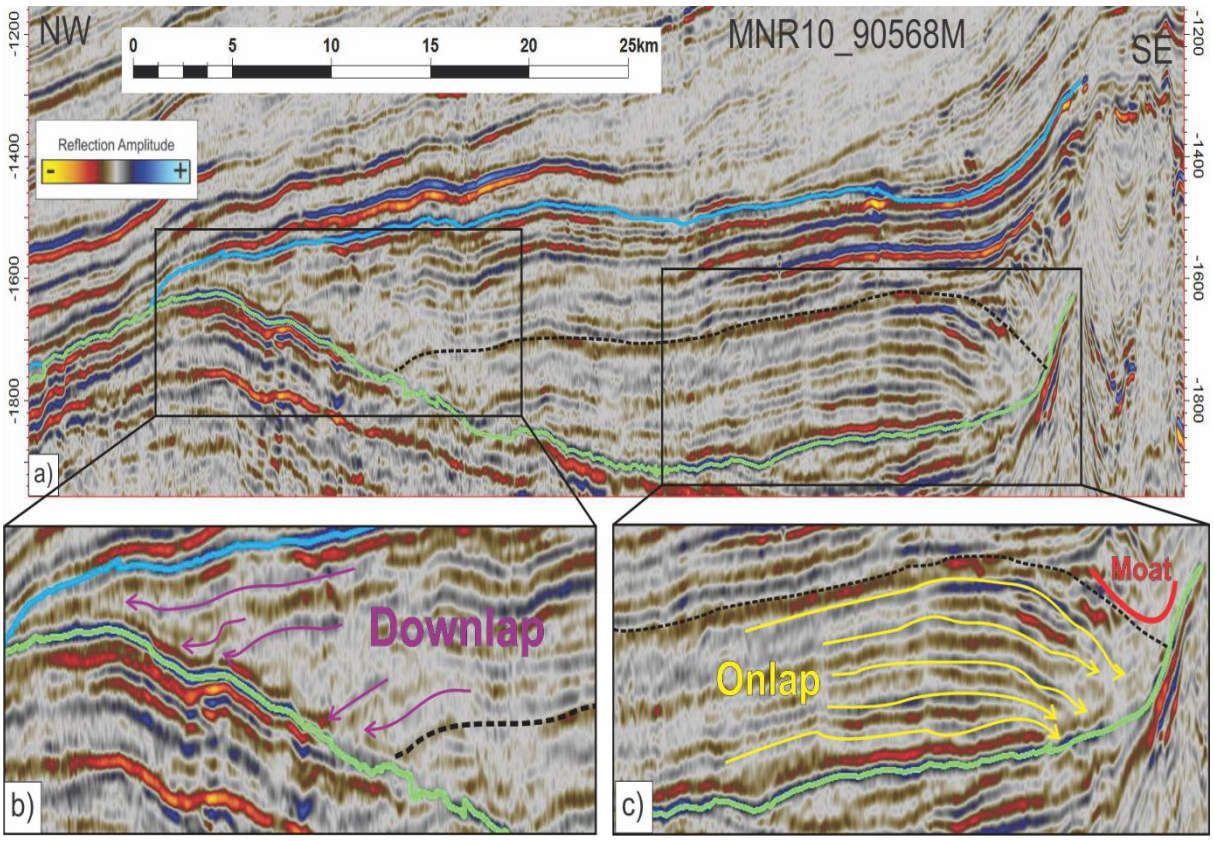

Figure 4-3-3: a) Seismic section of MNR10_90568M. b) Framed section displayed the northwestern part of the line. c) Framed section displaying the southeastern part of the line. Black dotted line: separation of local seismic sequences. Purple arrows: downlapping reflectors. Yellow arrows: Onlapping reflectors. Red line: Moat channel. The scale on the side of a) is in ms TWTT.

In the southern part of Area 1, the seismic section has a similar stratigraphy as the previous described section, with the Kai formation being absent in the west, and interrupted by a dome-like structure in the east (Fig. 4-3-4a). The formation gradually increases in thickness, from west to east, up to approximately 400 ms (TWTT) before the dome structure. The seismic reflectors mostly follows the orientation of the over- and underlying top and base of the Kai formation. The reflection strength varies throughout the section, with weak downlapping reflectors in the west (Fig. 4-3-4b). In the middle part of the section there is an abrupt change in reflection amplitude strength (Fig. 4-3-4c). This seems to be the result of an unconformity of similar disruption of the seismic reflection, because of discontinues reflections over the amplitude change. The bright amplitudes are following the eastern high, while the bottom (low amplitude) local sequence is dipping downwards into the unconformity of the base Kai formation, creating an onlap seismic stratigraphic reflection (Fig. 4-3-4d) because of the strata

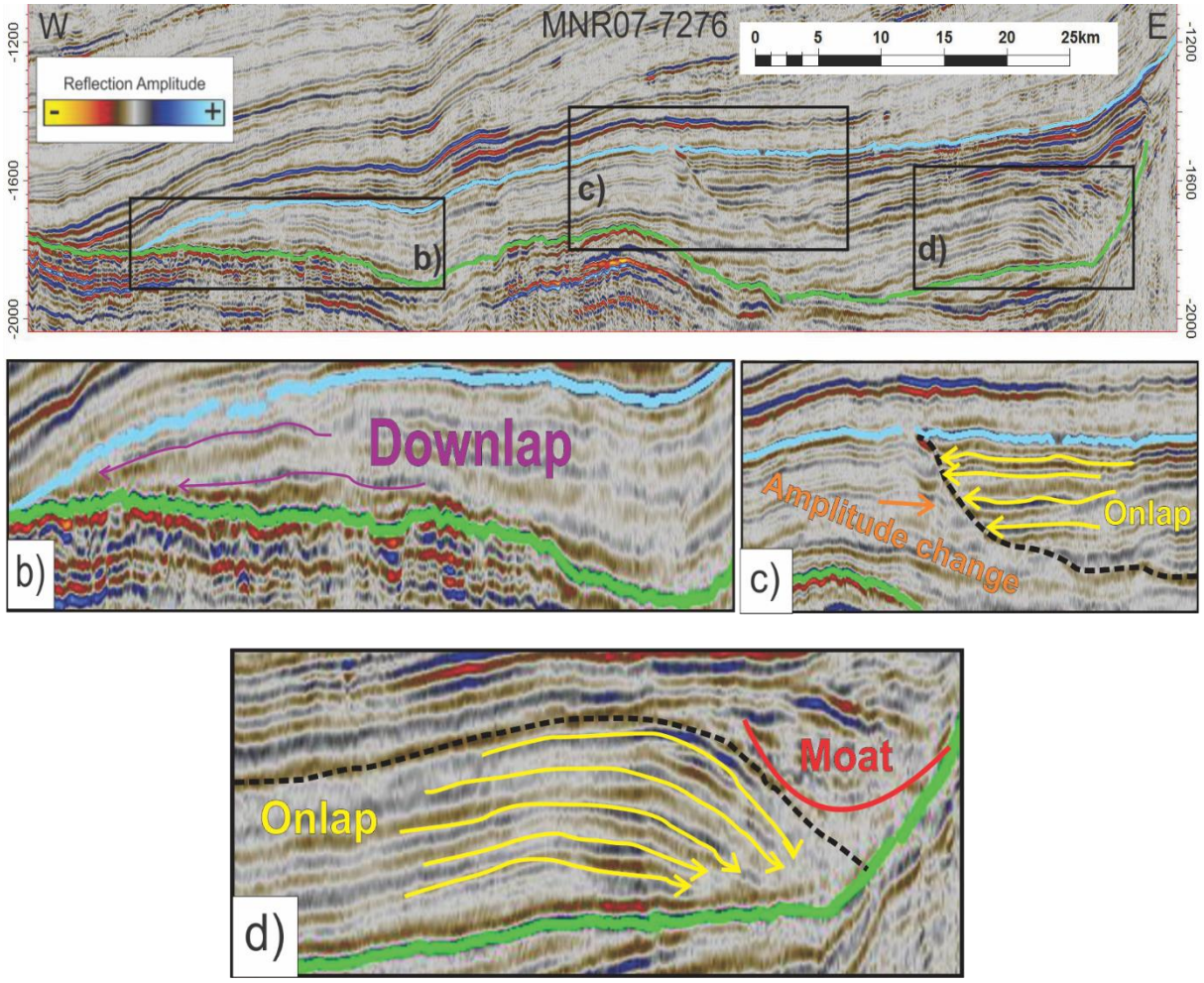

Figure 4-3-4: Seismic section of MNR07-7276. Blue line indicate the top Kai formation. Green line indivate the base of the Kai formation. b) Framed section displayed the western part of the line. c) Framed section displaying the amplitude change in the middle part of the line. d) Framed section displaying the eastern part of the line. Black dotted line: separation of local seismic sequences. Purple arrows: downlapping reflectors. Yellow arrows: Onlapping reflectors. Red line: Moat channel. Orange arrow: Abrupt amplitude change. The scale on the side of a) is in ms TWTT.

being terminated progressively against an initial inclined surface of the dome structure. Where the two seismic paths separates, there is a moat due to the lack of sediments towards the dome. The lack of sediments may be the result of bottom currents being too strong in this area to deposit sediments. On the western side of the moat, the current strength may have reduced, which resulted in the deposition of more sediments.

The orientation of the moat channel illustrated in Figure 4-3-4d, shows that there have been a north/south going oceanic current depositing the contourites. Bryn et al, (2005) have found similar moat channels in the further south in similar sequences which have been interpreted to have flowed in a north direction, due to the orientation of found current ripples.

4.3.2 Area 2

Area 2 has a sediment thickness between 200 and >1000 ms TWTT. The Kai formation is thinnest north of the Helland-Hansen Arch (Fig. 4-2-4), which marks the eastern confinement of the Vøring basin. The thickest part of the formation is found in the western part of the Vøring basin (Fig. 4-3-5). Area 2 does not have a clear orientation like area 1, with the exception of a decrease in sediment thickness in a north/south going direction in the Vøring basin. Bryn et al., (2005) also found that the thickness of the Kai formation in the Vøring basin get up to over 1000 ms (TWTT). Seismic lines displayed on Figure 4-3-5 shows the inner structure of the formation in the Vøring basin, as well as local sequences throughout the formation. Both north/south and west/east orientated lines will be described and interpreted to better illustrate the internal sequence signature.

Chand et al., (2011) suggested that the deeper part of the Vøring basin comprise shale-prone sediments of calcareous and siliceous oozes deposited in deeper water.

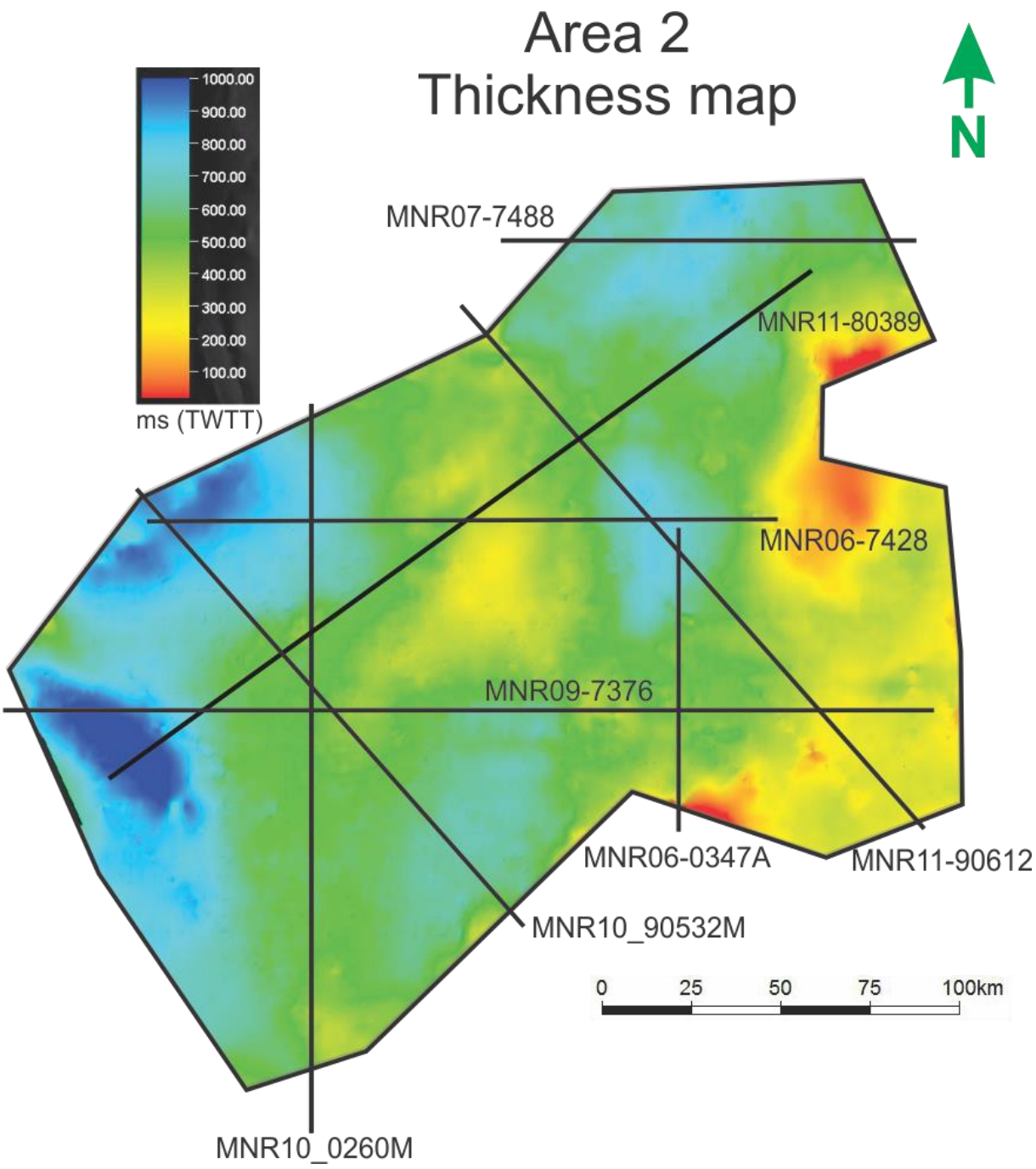

Figure 4-3-5: Thickness map of Area 2, showing the sediment thickness as well as parts of different seismic lines for further interpretation. Location of the area is displayed in Figure 4-2-4.

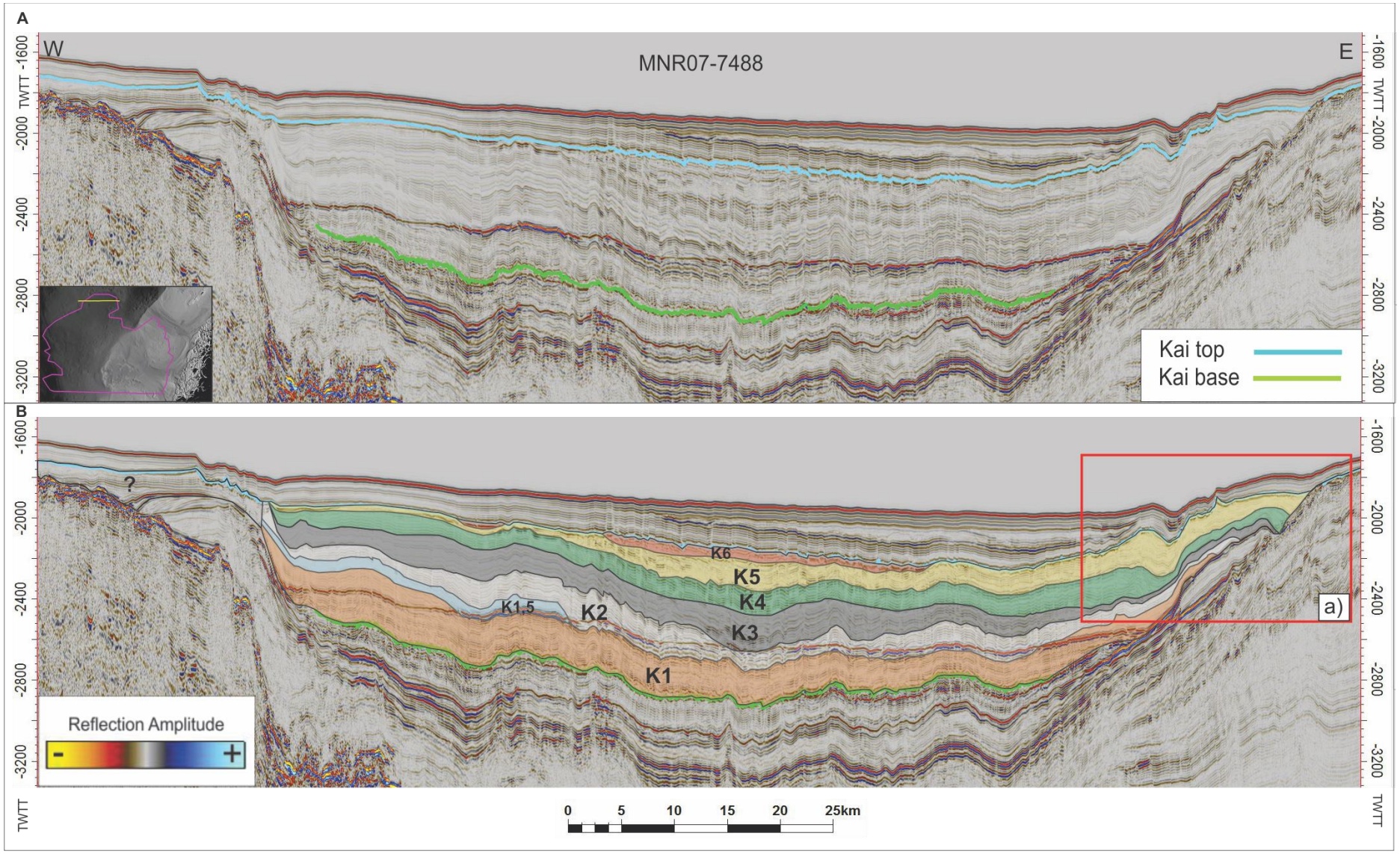

Figure 4-3-6: Outcrop of seismic line MNR07-7488 located in the northern part of Area 2.. A) Displaying the top and the base of the Kai formation, with no further interpretation. B) Seismic line with interpretation of the internal sub-units. K1-K6 shows the different sub-units, from oldest to youngest. Black dotted line shows area where unit borders are hard to determine. Red box (a)) shows the location of Figure 4-3-7. TWTT is in ms. Location of the line is displayed in Figure 4-3-5.

4.3.2.1 Northern part of Area 2

In the northern part of Area 2 (Fig. 4-3-5), the Vøring basin is confined by the Baserock of the Vøring Escarpment to the west and Naglfar Dome towards the east (Fig. 2-2-1). The Kai formation has been found between the unconformities of the underlying Brygge formation and overlying Naust formation. The top and base reflection of the unit share similar uniform reflection patterns resulting in a relative continuous sediment thickness at 600-800 ms (TWTT).

The internal seismic signature is characterized by parallel to sub-parallel reflectors with low to medium amplitude, including unconformities and correlative conformities. Based on the unconformities and correlative conformities, the Kai formation has been divided into six (K1-K6). The bottommost, oldest sub-unit (K1) has a continuous parallel reflection pattern throughout the formation, with weak onlapping concordance towards the dome. Subunit K1.5 can only be detected in the northwestern part of the basin (Fig. 4-3-6), although the extent and prevalence of the boundaries around of K1.5 can be uncertain, due to the strong negative amplitude of the DBSR, disturbing the boundary reflection, as well as a low internal amplitude within the sub-unit. The K1.5 sub-unit is found between K1 and K2 and is approximately 100ms TWTT thick and stretching out 30km from the Naglfar Dome into the basin. The local sub-unit is characterized by a low amplitude reflection within the unit. Sub-

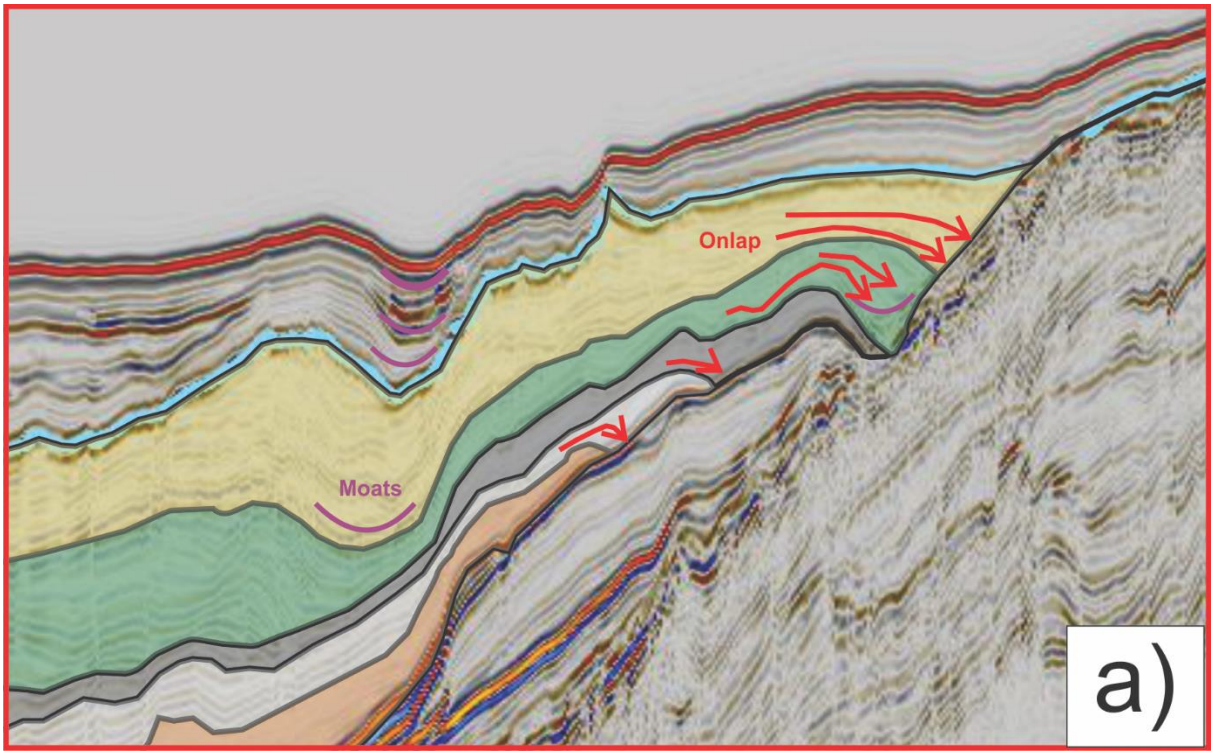

Figure 4-3-7: Outcrop from Fig. 4-3-6. Purple line displays moat-like structures. Red line display onlapping reflection termination towards the high.

units K2-K4 have similar reflection terminations as K1 (Fig. 4-3-6) towards the east, with onlap into moat structures. K2 and K3 is thinning out towards the eastern side of the seicmic section, whilst K4 and K5 is experiencing an increase in thickness. Seismic sub-unit K5 (Fig 4-3-6) have a similar onlapping reflection pattern as the older sub-units, but have been eroded by the overlying Naust formation creating erosional truncation, both in the western and eastern part of the unit. This truncation cannot be found in the middle (deepest) part of the basin, due to the K6 not being completely terminated in this area (Fig. 4-3-6). The reflectors in K6 are terminated in the western and eastern part, due to erosional truncation from the Naust formation. K4 and K5 has a U-shaped structure in the eastern part, at the flank of the Vema Dome (Fig. 4-3-7). The structure has a moat-like shape with reflections dipping down into the U-shape. This may be the result of a current flowing perpendicular to the seismic line. The structure is also found on the present d ay seafloor, which may indicate that the interpreted erosion from currents still are active.

4.3.2.2 Middle part of Area 2

The middle part of Area 2 (Fig. 4-3-8) is situated in the Vøring basin, confined by the Baserock of the Vøring Escarpment to the west and Vema Dome to the east (Fig. 4-3-5). The top reflection of the formation is relatively horizontal, at a depth of 2000 ms (TWTT), and dipping to the east down to approximately 2300 ms (TWTT) -under the build-up of the Naust formation at the towards the east (Fig. 4-3-8). The base reflection has a variable reflection pattern, with the deepest part found at 3000 ms (TWTT) in the west and 2800 ms TWTT in the east. There is observed an elevation in the middle of the basin, where the depth reduces to approximately 2400 ms (TWTT). This elevation is not noticeable in the top of the Kai formation. The same internal seismic sub-units found in the northern part of Area 2 has also been found to characterize K1-K6 here. The bottommost, oldest sub-unit (K1) has an onlapping concordance towards the escarpment to the west, with a termination of the sub-unit to the east. K2 have an almost constant thickness throughout the section, whilst the overlying K3 and K4 have a thinning of the sub-units in the middle of the basin, and thickening towards the west. The borders of K2 have been, interpreted with some uncertainties, due to a chaotic reflection pattern.

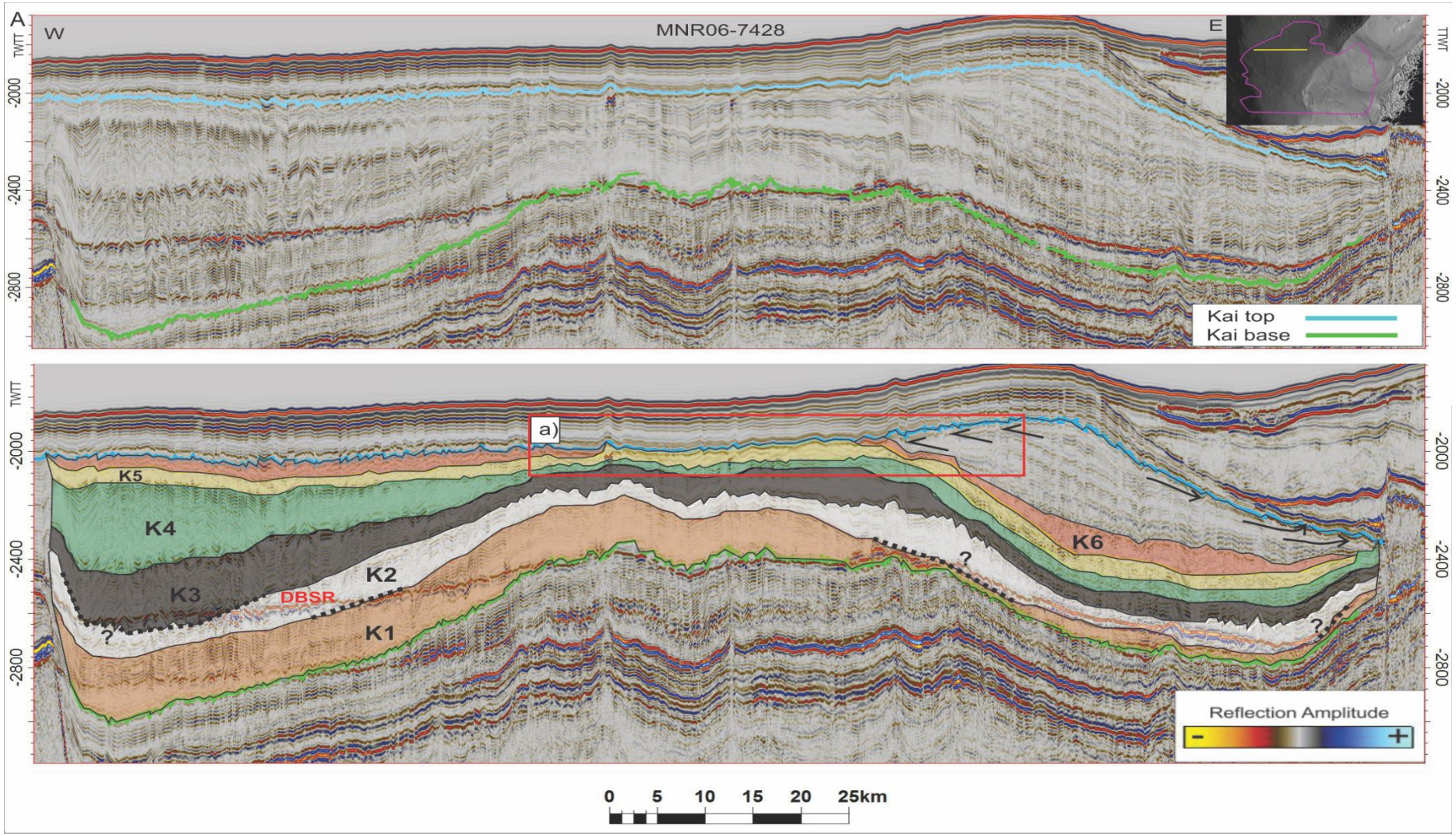

Figure 4-3-8: Outcrop of seismic line MNR06-7428, located in the middle part of Area 2.. A) Displaying the top and the base of the Kai formation, with no further interpretation. B) Seismic line with interpretation of the internal sub-units. K1-K6 shows the different sub-units, from oldest to youngest. Black dotted line shows area where unit borders are hard to determine. Red box (a)) shows the location of Figure 4-3-9. TWTT is in ms. Location of the line is displayed in Figure 4-3-5.

K5 is in some areas affected by erosion where K6 is absent. Unlike the northern part, the erosion of K5 is here limited to the middle part of the formation, with prevalence of K6 in the eastern and the western part. This is inverted from the northern part, which may indicate that the erosional truncation done in the top part of the unit is affected by the prevalence of the underlying deposits. In the northern part, there is no elevation of the base of the Kai formation, which results in the sub-units to have a dipping orientation into the basin, whereas here the sub-units are dipping upwards into the basin, resulting in erosional truncation of the youngest units. The thickest part of K6 is found towards the east, and can represent the area with lowest amount of erosion. The sub-unit thins out to termination towards the Vema dome, due to erosional.

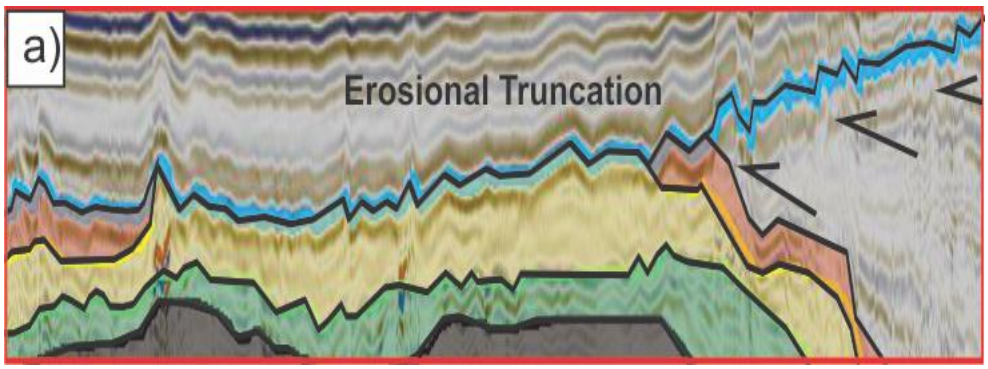

Figure 4-3-9: Outcrop from Fig. 4-3-8, displaying erosional truncation of K6 (red area).

Figure 4-3-9 displays examples of erosional truncation of K6 in the seismic section. The abrupt interruption of the reflector may indicate erosion from overlying sediment, which classify the stratigraphic reflection termination as truncation and not toplap. The separation of K5 and K6 can be difficult, due to a chaotic reflection pattern in the upper part of the Kai formation here. This may be the result of the thickness of the sub-units decreases to below the seismic resolution.

Erosional truncation of Miocene and Pliocene deposits around the Naglfar and Vema domes was also shown by Hjelstuen et al, (1999). Stoker et al, (2005) found that the thinning of sheeted drifts over intra basinal highs and erosional truncation of beds is an indication of contour-current activity.

4.3.2.3 Southern part of Area 2

In the southern part of Area 2, the formation is just thinning out eastward (Fig. 4-3-10), with the western part of the basin being confined by the Vøring Escarpment. The base of the Kai formation has its greatest depth towards the western escarpment, reducing its depth towards the middle of the basin. In this area the top of the formation seems to have been greatly affected by the sediments over, locally resulting in a sag, downward bending geometry. In the eastern part of the section, the top and base of the formation share a similar pattern of parallel to subparallel intra units. As further north in the study area, The Kai formation have been divided into six internal units (K1-K6) in the southern part.

K1 is located in the western part of Area 2, down into the Vøring basin. The sub-unit is terminated towards the east, although the boundaries of K1 are somewhat unclear due to a chaotic reflection pattern, as well as disturbance from the strong DBSR negative reflector. (Fig. 4-3-10). Sub-units K2-K5 mostly have a similar depositional pattern as the top and base Kai, with thickest accumulation of sediments in the western part of the Vøring basin. Internal units K4-K6 all have onlap stratigraphic reflection on the border of the Vøring escarpment. Related moat-like structures can be found here. These structures is also located below the base Kai formation, which may indicate that the structures are just the recreation of the underlying topography.

Overlying K6 there are locally found several units with erosional terminations both in the west and the east, which are terminated due to internal convergence stratigraphic reflections. Due to the local extent of the units, a proper interpretation of the amplitudes is found to be difficult.

According to Larberg et al, (2005a) internal reflections in the area show progressive upslope migration and onlap of internal units at the eastern part of the Vøring Marginal High, as well as indications of paleo-moats.

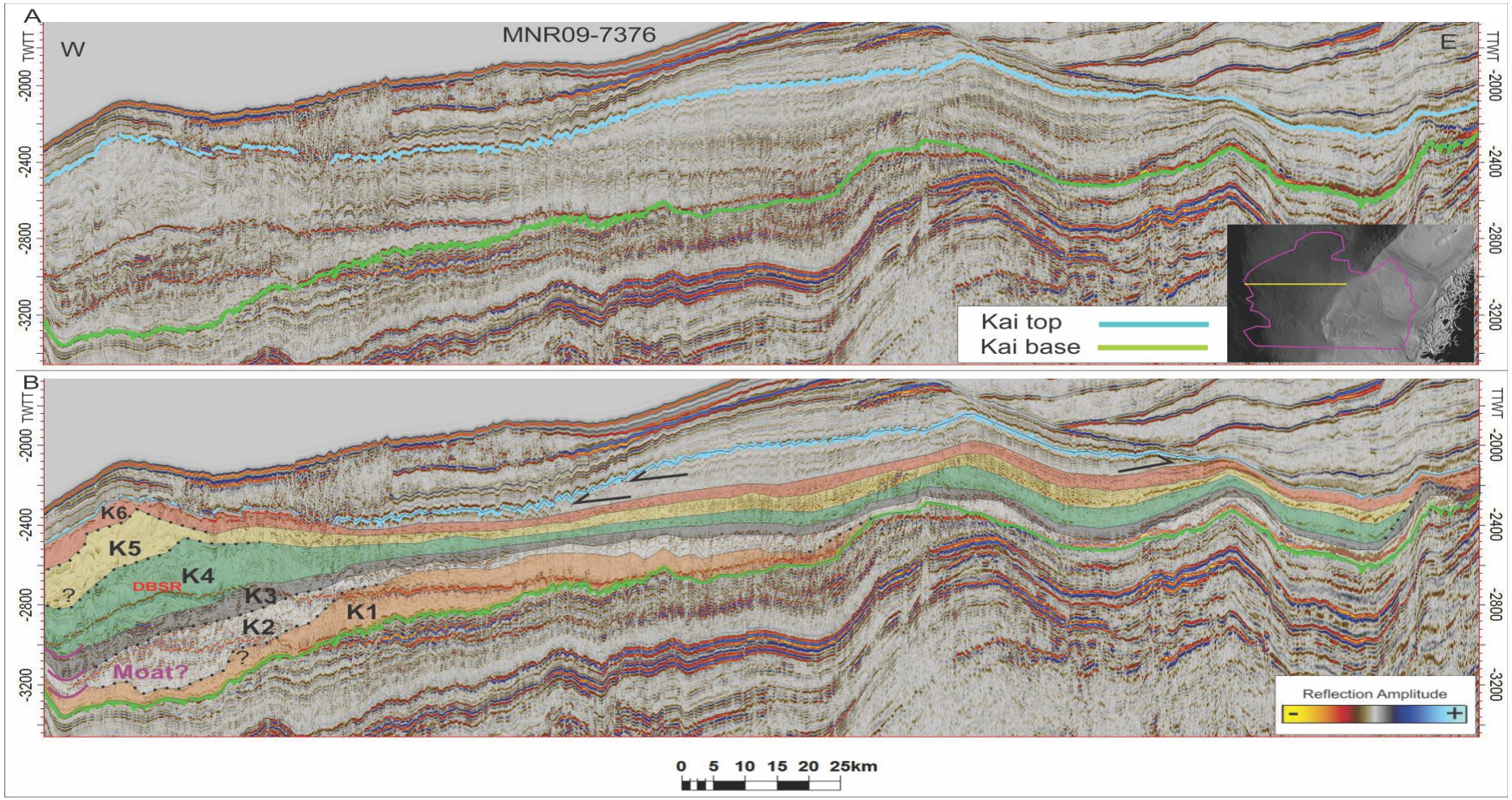

Figure 4-3-10: Outcrop of seismic line MNR09-7376, located in the southern part of area 2. A) Displaying the top and the base of the Kai formation, with no further interpretation. B) Seismic line with interpretation of the internal sub-units. K1-K6 shows the different sub-units, from oldest to youngest. Black dotted line shows area where unit borders are hard to determine. TWTT is in ms. Location of the line is displayed in Figure 4-3-5.

4.3.2.4 The deeper parts of the Vøring basin.

To get a better understanding of the prevalence of the sub-units in Area 2, seismic sections orientated perpendicular to the Norwegian shelf is looked upon (Fig. 4-3-5). In the middle-north-eastern part of Area 2, the base of the formation follows a similar pattern as the

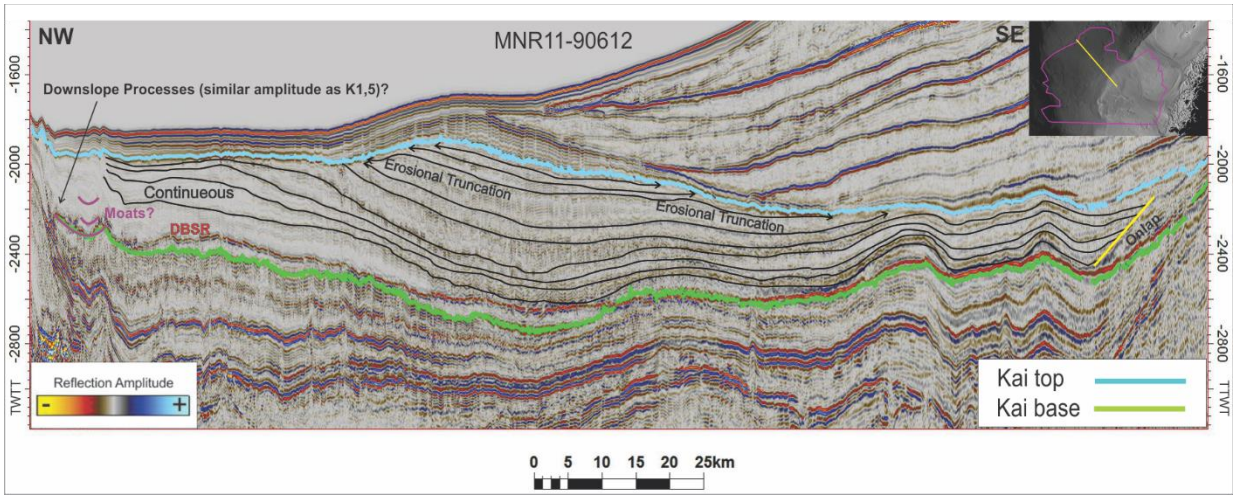

Figure 4-3-11: Outcrop of seismic line MNR11-90612, displaying the deeper parts of Area 2. Displaying Seismic section with interpretation of the internal patterns, as well as stratigraphic reflection terminations Yellow line display an onlapping reflection. Red box (a) and b)) shows the location of Figure 4-3-12 and 4-3-13. TWTT is in ms. Location of the line is displayed in Figure 4-3-5.

underlying sediments, while the top formation is greatly influenced by erosional truncation (Fig 4-3-11). The base seismic reflection is greatly disturbed by the DBSR negative reflector, especially to the southeast, making the interpretation of the base Kai formation difficult. The formation has its greatest thickness in the middle of the seismic section, with thinning out towards the northwest, and termination of the formation to the southeast. Here the top and base of the formation are sharing a wavy pattern suggesting that both have been affected by the same processes of folding as the deeper, older sediments. The upper sub-units of the formation can only be located where the formation is thickest, being eroded further into the basin, as well as landwards. All subunits share a parallel reflection pattern similar to the base formation reflection, with no sub-unit exclusively located to an area, aside from the eroded upper units only found in the middle part of the section. Landwards the reflections are terminated towards a strong reflector (marked as a yellow line in Fig. 4-3-11), creating an onlap reflection termination. The onlap unto an older sub-unit within the Kai formation might suggest sliding mechanisms. At the northwestern termination the Kai formation top reflection is dipping downwards, resulting in a frequent truncation of the sub-units. At the southeastern termination, the formation top reflection is bending the other way, making the sub-units terminate less frequently. The termination of the upper units are interpreted as erosional

truncation, due to the abrupt cutting of the reflections, as well as the location of the termination in relation to the top reflection of the Kai formation.

In the northwestern part of Area 2, moat-like structures have been found. These are found near the Vøring escarpment and have similar geometry and prevalence as moat-like structures found on the E/W orientated lines. This strengthen the interpretation that there may have been paloe-moat-channels in the area near the western/northwestern part of the Vøring basin. The moat-structures seems to be migrating northwest as they are deposited upwards in the unit with the same angle as the Vøring escarpment. Laberg et al, (2005a) found indications of paleo-moats on the same side of the Vøring escarpment on lines with similar orientation.

Further south, in the middle southwestern part of Area 2, the Kai formation is found in a more basin-like topography, with clear confinements to the Helland-Hansen Arch towards the southeast and the Vøring escarpment at the northwestern part of the basin. Sub-units K1-K6 have been identified within the Kai formation. Here, in the deepest part of the Vøring basin, K1 is locally only found towards the northwest (Fig. 3-4-12). K2-K3 share a similar topographic pattern as the base of the Kai formation, suggesting low-energy deposition. K4 is less affected by the topographical changes, and have onlap with associating moat-structures toward the confinements of the Vøring basin. These structures are more apparent in K5 and

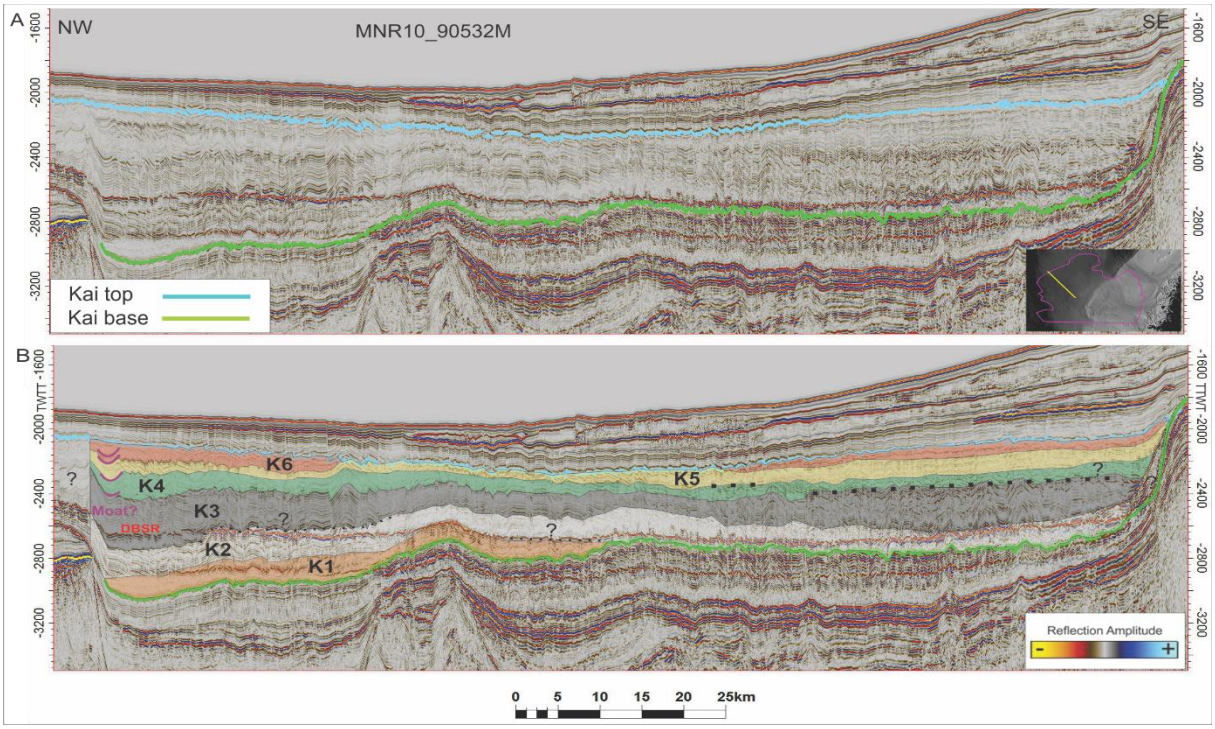

Figure 4-3-12: Outcrop of seismic line MNR10_90532M. A) The seismic section with the interpretation of the top and base Kai formation, with no further interpretation. B) Seismic line with interpretation of the internal sub-units (K1-K6). Black dotted line shows area where unit borders are difficult to determine. TWTT is in ms. Location of the line is displayed in Figure 4-3-5.

K6, suggesting a gradual change in depositional environment. The two top sub-units have suffered from some erosional truncation towards the top of the Kai formation. K6 is absent in the middle part of the basin, suggesting that the erosion were most prominent here.

In a northeast/southwest orientation the thickness of the Kai formation is observed to have a thickness between 400 and 600 ms TWTT in the northeast and middle part of the Vørin Basin, with an increase up to approximately 1000 ms TWTT in the southwestern part of the basin (4-3-13). In the northeastern part of the middle area, the top and base of the formation share a similar pattern of parallel to subparallel intra units, with some deviation from the norm when the thickness increases. The change in reflection pattern occurs before the increase in thickness due a dome structure creating a basement high affecting the base Kai formation. The pre-Kai sediments are greatly affected in the middle part of the section by an elevation of the reflectors, creating another basement high. This elevation is also recognizable in the Kai formation as well as in the overlying Naust formation.

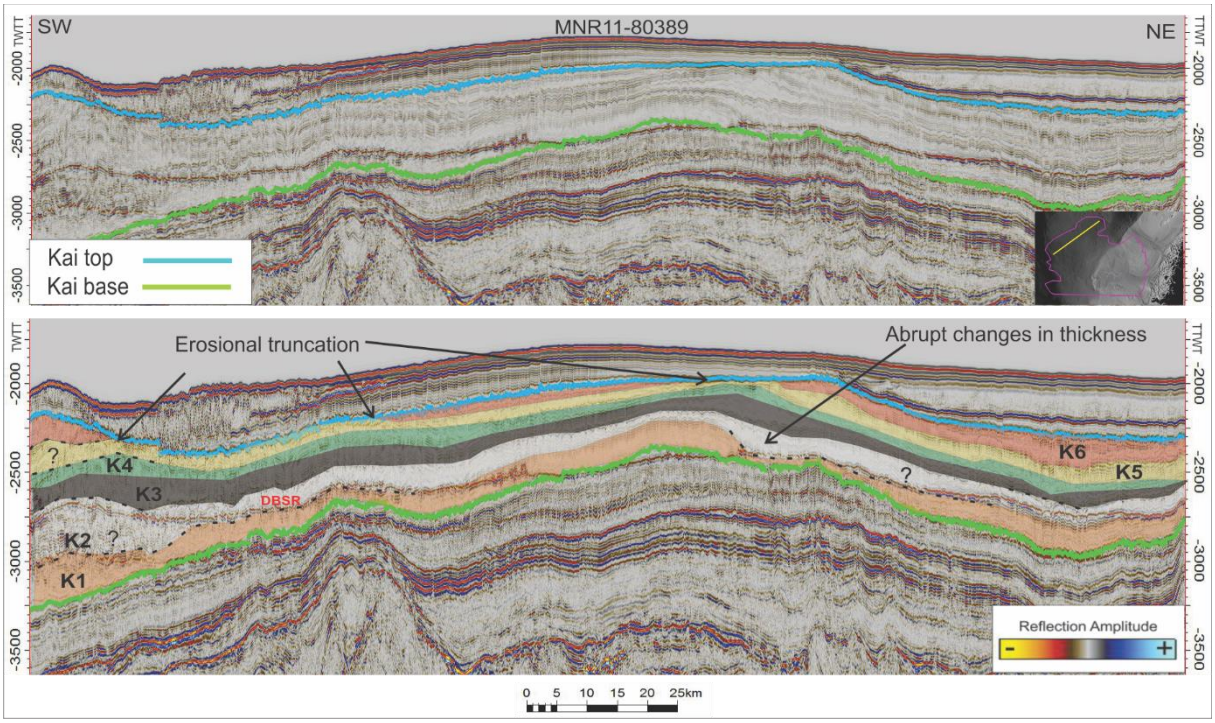

Figure 4-3-13: Outcrop of seismic line MNR11-80389. A) Displaying the top and the base of the Kai formation, with no further interpretation. B) Seismic line with interpretation of the internal sub-units. K1-K6 shows the different sub-units, from oldest to youngest. Black dotted line show areas where the borders have been interpreted with some uncertainties. TWTT is in ms. Location of the line is displayed in Figure 4-3-5.

The internal seismic signature of the seismic section (Fig. 4-3-13) is characterized by low to medium reflection amplitudes, and can be divided into the similar K1-K6 pattern (Fig. 4-3-13). Subunit K1 is characterized by a parallel to sub-parallel pattern with non-uniform thickness throughout the section. K1 has a thickness between 50 and 300 ms TWTT. K1 have

been interpreted with some uncertainties, partly due to chaotic reflections, and partly due to the disturbance of the DBSR (Fig. 4-3-13). In the middle part of the section, K1 is experiencing an abrupt change in thickness (Fig. 4-3-13). The reflectors seems to be dipping towards the base of the formation, but because of the low-medium amplitude reflections and the DBSR reflector, it is difficult to interpret whether K1 is being terminated or is continuous throughout the section. K2-k5 share a similar, relative parallel reflection pattern, with exception of K2 in the southwest and at the abrupt change in thickness of K1. In the southwest K2 has an increase in thickness, up to approximately 400 ms TWTT. Subunits K3-K5 as well as rest of K2 has a continuous thickness of 50-150 ms TWTT throughout the profile. Subunit K6 is multiple locations in the section experiencing a termination of the reflections. This termination has been interpreted to be erosional truncation from the overlying Naust formation. K6 has its greatest thickness in the northeast, where the Naust formation is dipping downwards into a concave pattern. This may suggest that the erosion of the Kai formation have been the lowest here. The downward dipping of the base Kai formation, and the upwards dipping of the top reflections, mixed with an internal chaotic reflection pattern in the southwestern part of the section, makes the internal sub-units difficult to map. The interpretation shows that K2 marks a change in whether the reflections are following the top or bottom pattern of the formation.

In the western part of Area 2, the top and base reflection of the Kai formation share similar topographic patterns resulting in a relative continuous sediment thickness at 600 ms TWTT in the middle of the basin. The thickness deviate from the continuous pattern in the southern and northern part of the basin. The south confinement experience a gentle sloping of the base towards the escarpment, and northwards the base formation is affected by underlying structures ascending into the reflection pattern (Fig. 4-3-14), as well as an increase in thickness before the base is affected by a steep confinement at the northern Vøring escarpment. Several moat-like structure have been observed in the northern and southern (Modgunn Arch) confinement of the Vøring basin. In the south these structures can be located from above the Kai formation, down vertically into the pre-Brygge basement. Figure 4-3-16a displays the largest structure found, as well as smaller moat-structures further inwards into the basin. The overlying reflectors clearly shows a dipping pattern into the northern wall of the moat,creating an onlap seismic stratigraphic reflection termination, because of the strata being terminated progressively against an initial inclined surface of a terminating structure. On the northern confinement of the basin, there are found similar but smaller structures. As Figure 4-

3-15c illustrates, there can be found onlapping reflections here as well. These structures can be an indication of alongslope sedimentary processes, which can be related to current erosion, transport and deposition.

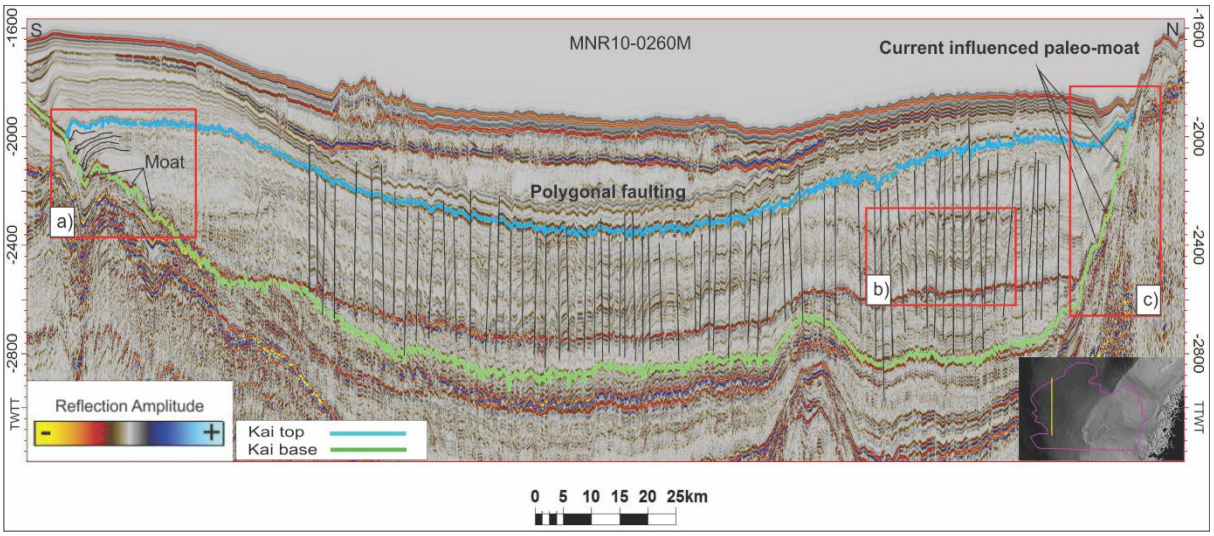

Figure 4-3-14: Outcrop of seismic line MNR10-0260 displaying the distribution of polygonal faults in a north/south orientation of the study area. a) displays moat structures at the southern part of the basin. b) shows an outcrop of the effect the polygonal faults have on the internal units. c) displays current influenced paleo-moat structures in the northern part of the basin. TWTT is in ms. Location of the line is displayed in Figure 4-3-5.

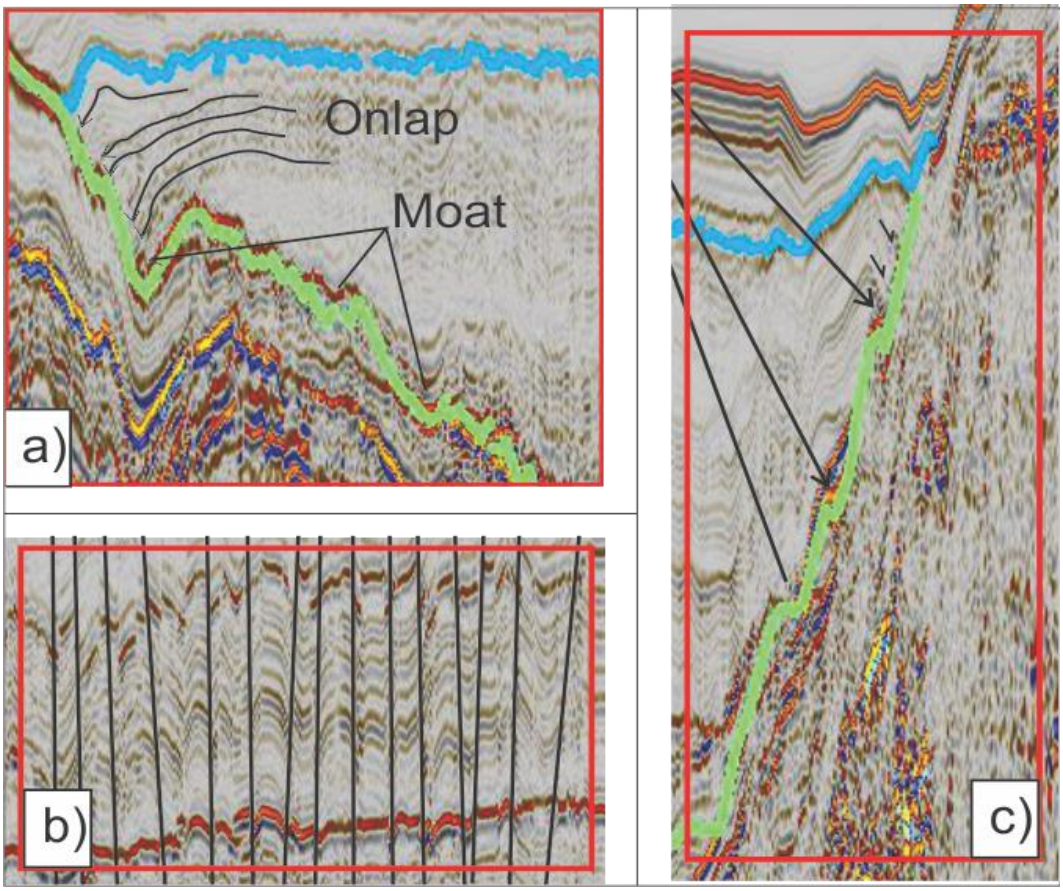

Figure 4-3-15: Outcrop a), b) and c) from Figure 4-3-14. a) displaying moat structures in the southern part of study area 2, with overlying onlap reflections. b) showing the extent of how polygonal faults are disrupting the internal seismic pattern in the Kai formation. c) displaying moat structures in the northern part of study area 2, with overlying some onlaping reflection patterns.

4.3.2.5 Post-depositional polygonal faulting of the Kai formation

The uppermost Brygge and Kai formations are heavily disrupted by polygonal faulting throughout Area 2 (Fig. 4-3-14; 4-3-15b; 4-3-16). The polygonal faulting pattern is most evident in the Kai formation and is in some areas found in the bottommost part of the Naust formation as well. The polygonal faults have a different orientation within a seismic section, which indicate a lack in dominant strike direction. Figure 4-3-14 displays that the extent of the polygonal faults differs throughout the formation, with some faults limited to the Kai formation, and some faults stretching through multiple stratigraphic levels. The fault frequency is also clearly reduced where the host formation thins out. In the seismic section displayed on Figure 4-3-15 this applies to the southern part as well as the dome structure affecting the base of the formation. Berndt et al, (2003) has found that the frequency of polygonal faults in the area increases downwards, due to the fact that the polygonal faults start to grow in the lower part and advances upwards until they are terminated by an upper boundary or another fault. The polygonal faults observed in the study are exclusively found in Area 2. This will be further discussed in chapter 5.

Figure 4-3-15b show to what extent the polygonal faulting are disrupting the internal sub-unit pattern in the Kai formation. The faults have no distinct dipping orientation, but rather a chaotic random pattern of zero-low angel dipping. The internal reflectors are clearly affected by the faulting, making the sub-units difficult to map properly. The displayed red line indicates the DBSR reflector. This negative reflector is less affected by the faulting, due to the diagenetic conversion happing after the deposition of the Kai formation. According to Berndt et al, (2003) the polygonal fault systems located at the mid-Norwegian continental margin may be a fluid source, as well as pathways for fluid migration from deeper stratigraphic levels.

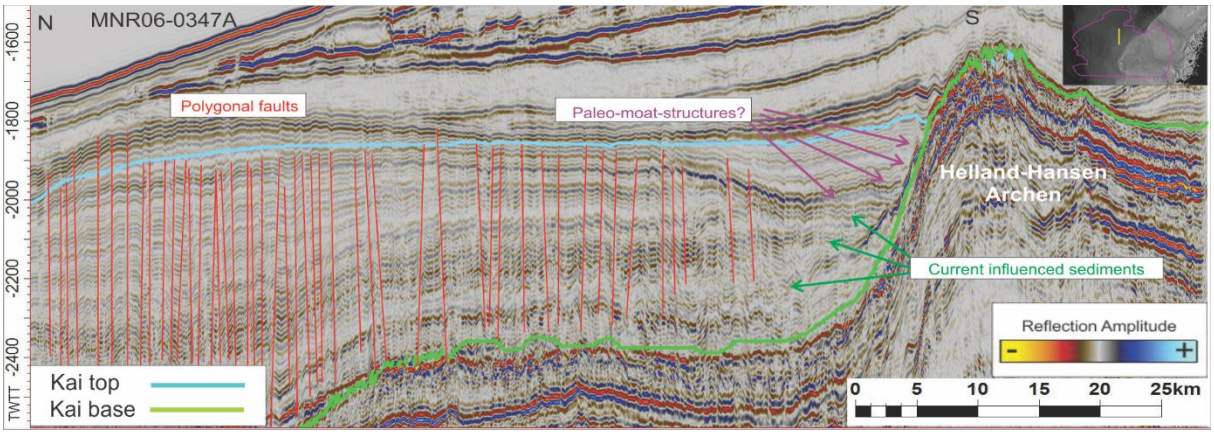

Figure 4-3-16: Southern part of seismic line MNR06-0347A displaying current related structures and polygonal faults near the Helland-Hansen Arch. The TWTT is in ms Location of the seismic section is displayed in Figure 4-3-5.

North of the Helland-Hansen-Arch, there is also found a similar polygonal fault system as in the deeper parts of the Vøring basin. Here the polygonal fault system is found with a more frequent occurrence of faults in the deeper part of the basin, and less frequent in the shallower areas towards the Helland-Hansen Arch. The polygonal faulting have a mostly vertical orientation with some random dipping in both directions throughout the seismic profile.

4.3.3 Areas of interest, not covered by Area 1 and 2.

Some of the anticlinal highs (Vema Dome, Nyk High, Utgard High and Modgunn Arch) may be of interest to this study, because bottom currents may have had a flow pattern affected by these highs. Some of these anticlinal structures are located at the edge of the study area and cannot be observed in any of the surface maps or the generated thickness map, because of a chaotic reflection pattern and a lack of seismic data in these areas.

South of Area 2 there is a sediment package between the Helland-Hansen Arch and the Modgunn Arch. As the present day ocean circulation have a general northeastern flow pattern, this area is of interest since it may represent the entrance of the ocean current circulation pattern, into the study area from the south. This southwestern area is characterized by moat structures with onlapping reflection termination towards both the Modgunn Arch (MA) and the Helland-Hansen Arch (HHA) (Fig. 4.3.17). The outer part of the Modgunn Arch have not been studied, due to the lack of seismic data here. Hjelstuen et al., (2004) found similar mounded reflectors with aggradating onlap pattern at the flanks of the Modgunn Arch.

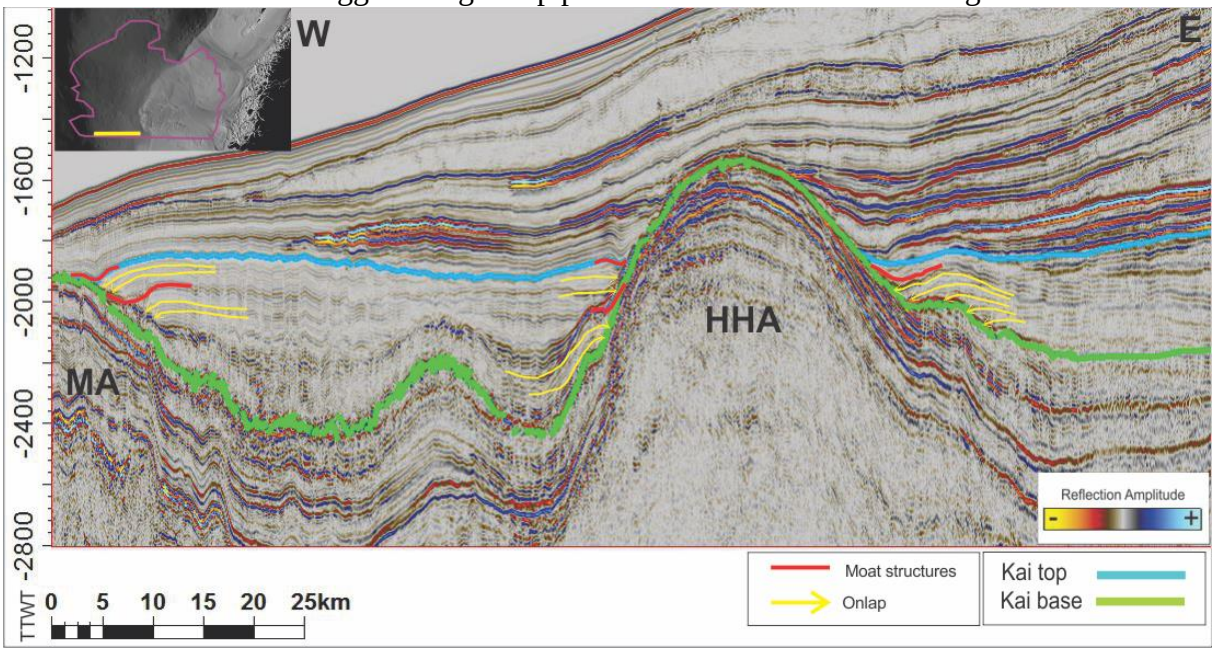

Figure 4-3-17: Seismic profile of the southwestern part of the study area, which is located between the Helland Hansen Arch and the Modgunn Arch. Interpreted reflections are showing moat structures (red) with associating onlap termination (yellow) toward the arches. HHA: Helland Hansen Arch, MA: Modgunn Arch.

Northeast in the study area, around the Vema Dome and the Utgard High, contouritic deposits, as well as current related moat structures have been observed (Fig. 4-3-18). This strongly suggest that a bottom current passed through here during the deposition of the Kai formation. It further strengthen the hypothesis that the bottom currents were affected by local anticlinal structures, and may be an indication that these troughs were passageways for ocean currents exiting the study area in the northeast.

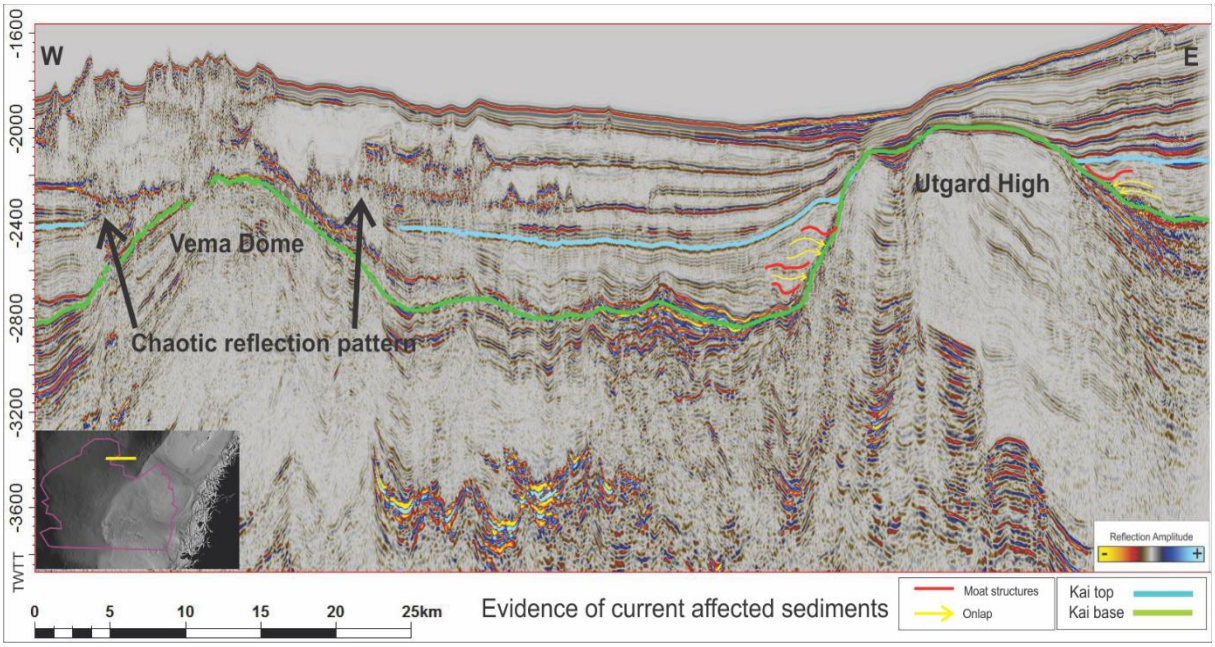

Figure 4-3-18: Seismic profile of the northwestern part of the study area. The Kai formation between the Vema Dome and the Utgard High shows evidence of contouritic origin, suggesting that the area were affected by currents during the deposition of the Kai formation.

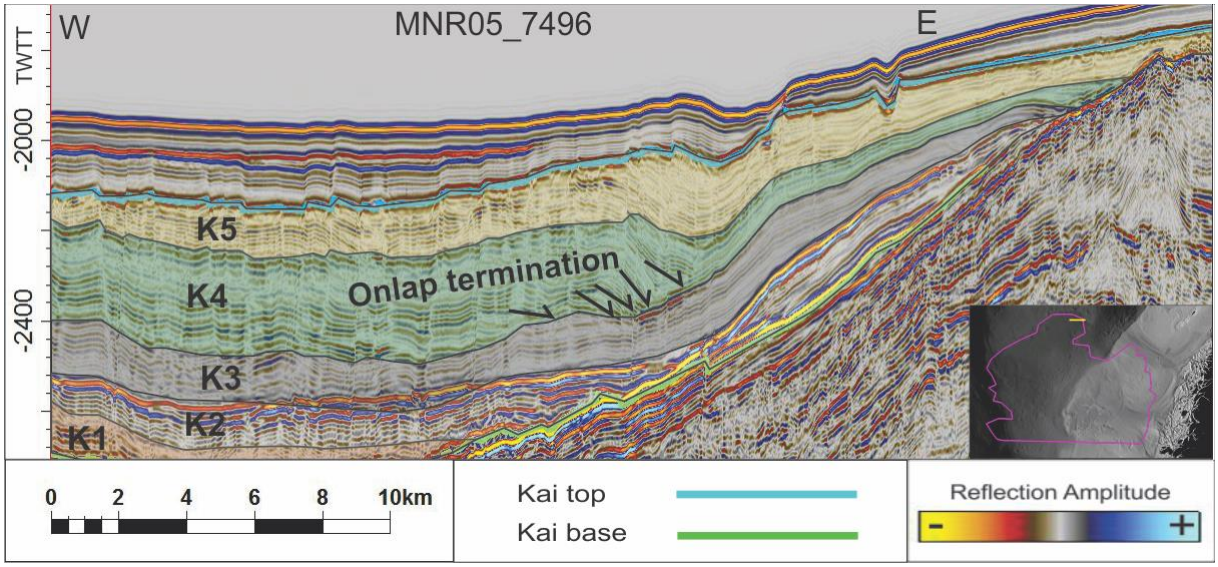

Figure 4-3-19: Seismic profile of the western confinement of the Vøring Basin in the northern part of the study area. Sub-units K1-K5 is observed here. K4 is experiencing from a onlapping reflection pattern within the sub-unit, down onto the underlying K3 sub-unit.

Just northeast of area 2 on the outer shelf, there is observed a change in reflection pattern within the Kai formation. Sub-units K1-K5 can be identified here, with K6 being absent. The seismic reflections comprising the K4 sub-unit is observed to create an onlapping reflection termination within the sub-unit, down on the underlying K3 sub-unit (Fig. 4-3-19). This suggest a change in either ocean pattern, or a change in sea-level during the deposition of sub-unit K4. These onlapping reflectors within K4 have only been observed in the northeastern part of the study area, over the boundary of Area 2.

4.3.4 Summary

The depositional pattern in the Vøring basin indicate that at the onset of the deposition of the Kai formation the deep-sea basins on the mid-Norwegian continental shelf were characterized by elevated anticlinal structures like the Helland-Hansen Arch. Both the inner- (Area 1) and outer shelf (Area 2) are characterized by a parallel-laminated internal seismic signature. Area 1 is consists mainly of mounded elongated contourite drift deposits. Within Area 2 the internal reflection can be divided into sub-units, which generally creates an onlapping pattern onto the local structural highs. This includes the HHA and the Vøring Marginal High. The whole Kai formation share the trend of have a sheet-form geometry, with variable thickness throughout the formation. The thickest part can be found in the Vøring basin, while the thinnest part is located on the Trøndelag Platform, as well as the eastern, eroded part of the Vøring basin. The reflection terminations, as well as internal structures is evidence of alongslope processes, related to erosion, transport and deposition from ocean currents. The Kai formation is found to be little affected by mass wasting processes. The deposits in the Vøring basin is characterized by continuity disruption of the reflections, due to polygonal faulting in the Vøring basin

Hjelstuen et al, (2004) have inferred that currents followed the flanks of these elevated structures, causing the observed (Fig. 4-3-19) Miocene non-deposition above the Helland-Hansen Arch, as well as current-related mounded structures along the Arch.

4.4 The relation between the Kai formation and the Molo formation

The age of the Molo formation, and the stratigraphic relationship with the Kai and Brygge formations is debated. This study have found that the relation between the Kai formation and the Molo formation changes with latitude. The Kai formation may be the downslope continuation of the Molo formation, or an older sediment package, deposited before, and under the Molo formation. In the mid-eastern part of the study area, there is not found any clear reflector representing a change between the interpreted Kai- and the Molo formations, although a change in reflection lithology suggest an approximate boundary between the two (Fig. 4-4-1). Here, the interpreted Molo formation can be characterized as a relative small package of sediments with downwards dipping reflectors that differs from the Naust formation in terms of dipping angle. Due to a chaotic reflection pattern near the interpreted base of the Kai formation, it is uncertain whether the Kai formation ends at the Molo transition, or is located below the Molo formation. Previous studies have described Molo as a sandy sediment package (Eidvin et al., 2014), which may be the reason to why the reflection pattern changes from the Kai formation to the Molo formation. Further north, the boundaries between the Kai formation and the Molo formation are easily interpreted.

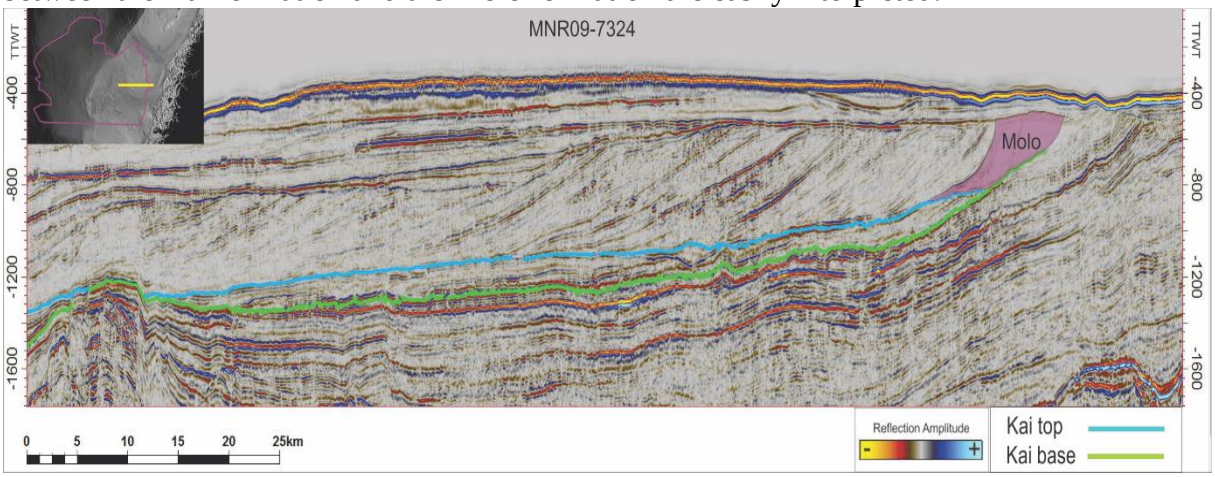

Figure 4-4-1: Seismic profile of MNR09-7324 displaying the possible relation between the Molo and the Kai formations in the mid-western part of the study area. The location of the line is shown in the top left corner.

This study suggest two different interpretation of the Kai/Molo relation (1 and 2 in Figure 4-4-2) in the northern part of the study area. Interpretation 1 suggest that the interpreted Molo formation and the interpreted Kai/Molo sediment package constitutes off the same formation. In this interpretation, the Kai formation is absent in this area, and can only be located further west in the study area. Previous studies (Eidvin et al., 2007; Eidvin et al., 2014) of the Molo formation have not found evidence of the Kai formation this far east, which strengthen interpretation 1.

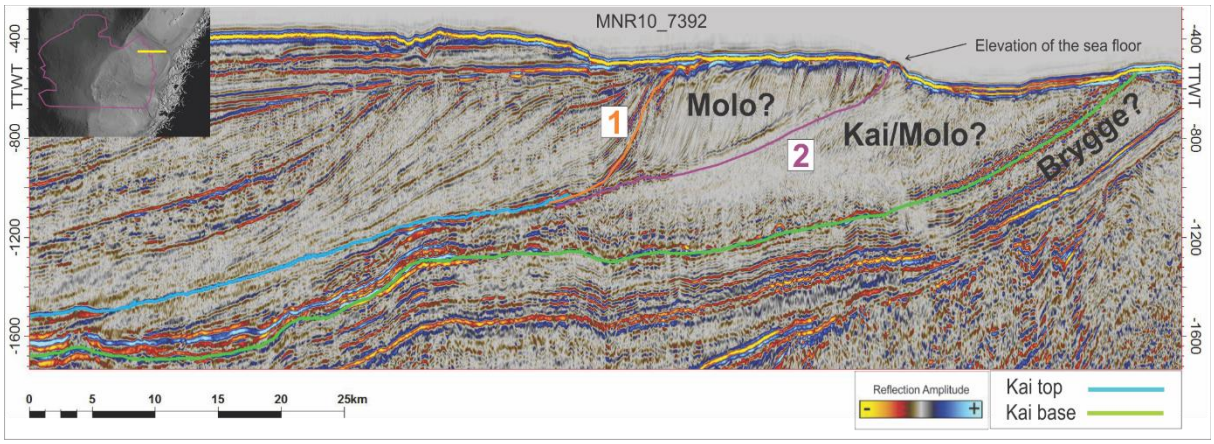

Figure 4-4-2: Seismic section of MNR10_7392 with the interpretation of the top and base Kai formation, and two interpretations of the Molo formation boundaries. 1 and 2 shows the two interpretations, the location of the seismic line is displayed as the yellow line in the top left corner.

Interpretation 2 suggest that the Molo formation and the Kai/Molo sediment package are two different formations, which suggest that the Molo formation were deposited on top of the Kai formation and are therefore younger. This interpretation opens up the possibility that the Kai formation, and even the Brygge formation can be found at the seafloor-level on the inner part of the Vøring Margin (Fig. 4-4-2). A bright thick reflection package located beneath the Brygge formation throughout the formation, also stretches up towards the seafloor, which implies that the overlying formations (Brygge and Kai) also can be found within this area. The boundary between the interpreted Molo and Kai formations separate two different reflection patterns. The Molo formation has a fairly steep clinoform pattern, while the Kai formation has a more chaotic reflection pattern mostly following the underlying topography. This change in lithostratigraphy suggest a change in depositional environment. There is also found an elevation of the seafloor at the boundary of the two formations, which may suggest a change in the sediment structure here. The relation between the Kai and Molo formations will be further discussed in chapter 5.

4.5 Well correlation

The established seismic stratigraphy was correlated to selected commercial wells in the area, this to increase the reliability and interpretation control of the interpreted top and base of the Kai formation from seismic data, as well as for precise estimates of the thickness of the formation. All wells used were located on seismic lines used in the interpretation of the Kai formation. This secured the quality of the correlation. Six wells were used in the correlation process, distributed in different parts of the study area, including both Area 1 and Area 2, as well as at the Helland-Hansen Arch (Fig 4-4-1). Due to the fact that most of the available wells did not include acoustic logs, or had outdated logs not covering the Naust and Kai formations, no more than six wells were used in the correlation.

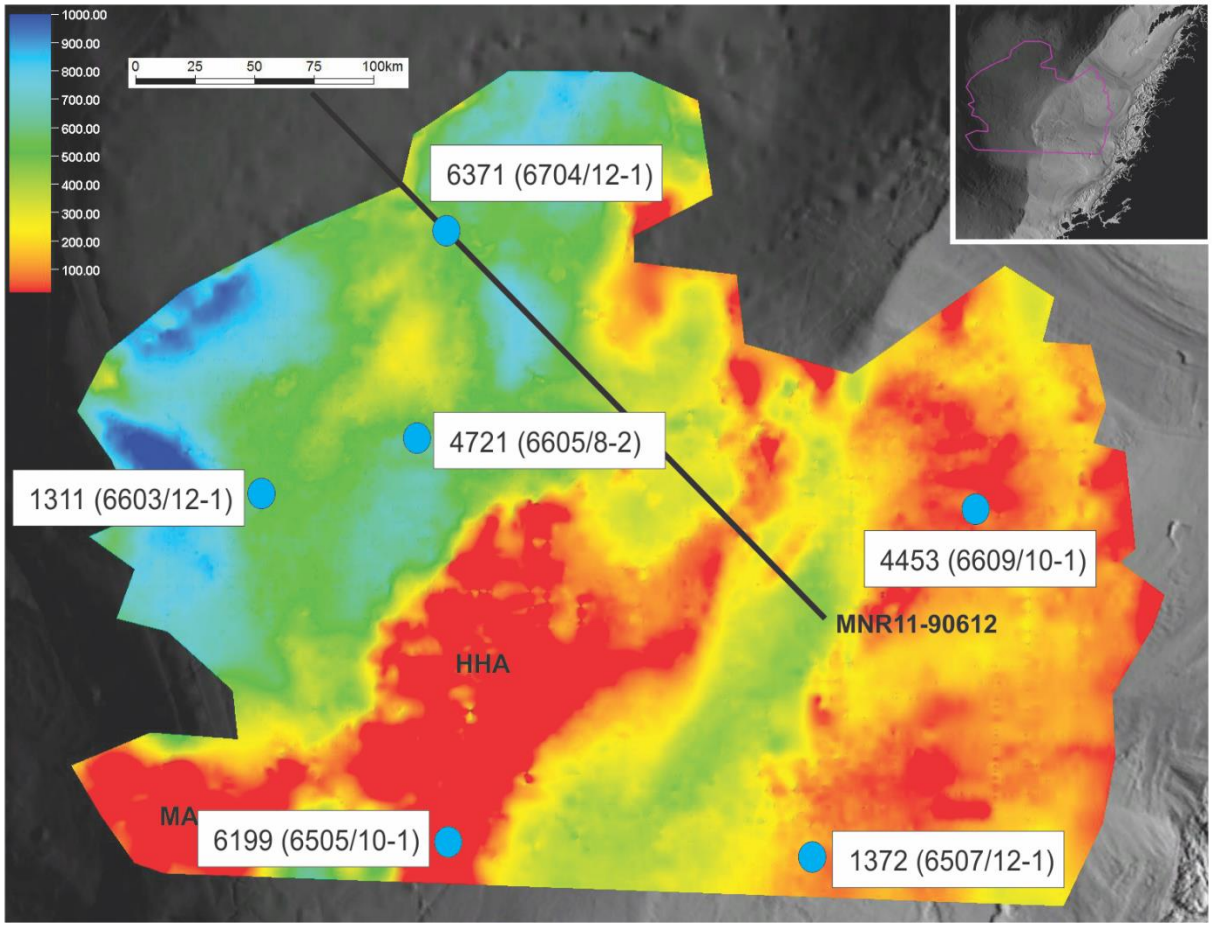

Figure 4-4-1: Thickness map of the Kai formation including the location of the wells used as a control of the seismic interpretation. Black line: Seismic line MNR11-90612 (displayed in Figure 4-4-2). HHA: Helland-Hansen Arch, MA: Modgunn Arch. Location of the map is displayed in the top right corner of the figure.

The depth in TWTT was calculated for three different levels, due to difference in velocity of the formation; the sea water column, the Naust formation and the Kai formation. Equations 5 and 6 have been used in the calculation (see Chapter 3.3.4). The first depth calculated is the depth of the top Naust formation (seafloor). This depth is not directly relevant to this study,

but is a necessity because it has to be added to the underlying depths (thickness of the underlying formations) to find the correct depths of the top and base of the Kai formation. Table 4-1 (a) displays the calculated depth of the top Naust formation given that the mean velocity of seawater is 1500 m/s. The table then shows the depth estimated from the seismic data. Due to the relatively accurate velocity in seawater, the calculated difference is minimal. The calculated depth is denoted D1, and represent the thickness of the sea water column.

Table 4-2 (b) shows the calculated depth of the top Kai formation based on well logs, and the interpreted depth from the seismic data. The depth and the mean slowness of the Naust

a) Naust top (seafloor)

Well Log	Depth (m)	Mean slowness (µs/ft)	Mean Velocity Seawater (m/s)	Calculated depth (D1) (ms TWTT)	Observed depth (ms TWTT)
6371 (6704/12-1)	1377	-	1500	1836	1850
4721 (6605/8-2)	841	-	1500	1121	1121
6199 (6505/10-1)	710	-	1500	947	925
1372 (6507/12-1)	250	-	1500	333	310
1311 (6603/12-1)	1400	-	1500	1866	1860
4453 (6609/10-1)	288	-	1500	384	370

Table 4-1: Table displaying the factors used to calculate the TWTT depth of the top Naust formation. Depth and mean slowness values have been conducted from NPD. D1 is the thickness of the seawater over the Naust formation.

b) Naust base (Kai top)

Well Log	Depth (m)	Mean slowness Naust Fm (µs/ft)	Mean Velocity Naust Fm (m/s)	Calculated depth (D1 + D2) (ms TWTT)	Observed depth (ms TWTT)
6371 (6704/12-1)	1459	210	1451	1949	1948
4721 (6605/8-2)	1688	160 *	1905	2010	1990
6199 (6505/10-1)	-	-	-	-	-
1372 (6507/12-1)	1342	140	2177	1336	1280
1311 (6603/12-1)	1673	160 **	1905	2152	2200
4453 (6609/10-1)	1312	140 **	2177	1324	1260

*Table 4-2: Displaying the factors used to calculate the TWTT depth of the base Naust formation (top Kai formation). Depth and mean slowness values have been conducted from NPD. Well 6199 (6505/10-1) is located over the Helland-Hansen Arch, and shows that the Kai formation is absent here. D2 is the thickness of the Naust formation. The true depth is then D1 + D2. * The acoustic log used to determine the mean slowness is conducted from another well, approximately 6 km northeast of the original well. ** Uncertain values due to the acoustic logs not displaying the upper part of the well.*

formation is conducted from the NPD web page (see chapter 3.3.4). The slowness is taken from the acoustic composite logs of the wells, and converted to velocity (m/s). The thickness of the Naust formation is denoted D2, and together with D1 makes up the total depth in TWTT. Well 6199 (6505/10-1) is located at the HHA (Fig. 4-4-1) and confirms the interpretation that Kai formation is absent in this area. The calculated depth (D2) of the Kai top (Table 4-2 (b)) has greater sources of error than the calculated depth of the water column (D1). This may be the result of the mean slowness being an approximate value conducted from the well's composite log. Because the calculated depth of D2 is partly based the depth of the top Naust formation (D1), the small source errors from D1 (Table 4-1 (a)) may also be present here. The calculated depth of the top Kai formation is used to correlate and strengthen the interpreted top of the Kai formation.

c)		Kai base			
Well Log	Depth (m)	Mean slowness Kai Fm (µs/ft)	Mean Velocity Kai fm (m/s)	Calculated depth (D1 + D2 + D3) (ms TWTT)	Observed depth (ms TWTT)
6371 (6704/12-1)	1920	170	1793	2463	2420
4721 (6605/8-2)	2010	160 *	1905	2348	2320
6199 (6505/10-1)	1354	160 **	1905	1623	1615
1372 (6507/12-1)	1495	130	2344	1466	1400
1311 (6603/12-1)	2100	160	2905	2600	2616
4453 (6609/10-1)	1367	150	2032	1378	1310

*Table 4-3: Table of the values used to calculate the TWTT depth of the base Kai formation. Values for depth and slowness have been conducted from NPD. D3 is the thickness of the Kai formation. The actual depth is then D1 + D2 + D3. * The acoustic log used to determine the mean slowness of the Kai formation is conducted from another well, located approximately 6 km northeast of the original well. ** Uncertain values due to the acoustic log not showing the values of the upper part of the well.*

The calculated depth of the base Kai formation is displayed in Table 4-3 (c). The relation to the interpreted depth used in the seismic data is also included. The depth and the mean slowness of the Naust formation is estimated from data available through the NPD webpage. The slowness is taken from the acoustic composite logs of the wells, and converted to velocity (m/s). The thickness of the Kai formation is called D3, and together with D1 and D2 makes

up the depth in TWTT. The largest difference between the calculated depth (TWTT) and the interpreted observed depth is found to be 66 ms (TWTT), which is considered an acceptable value in the correlation process. The calculated depth is used for a control on the interpreted base of the Kai formation in the seismic data.

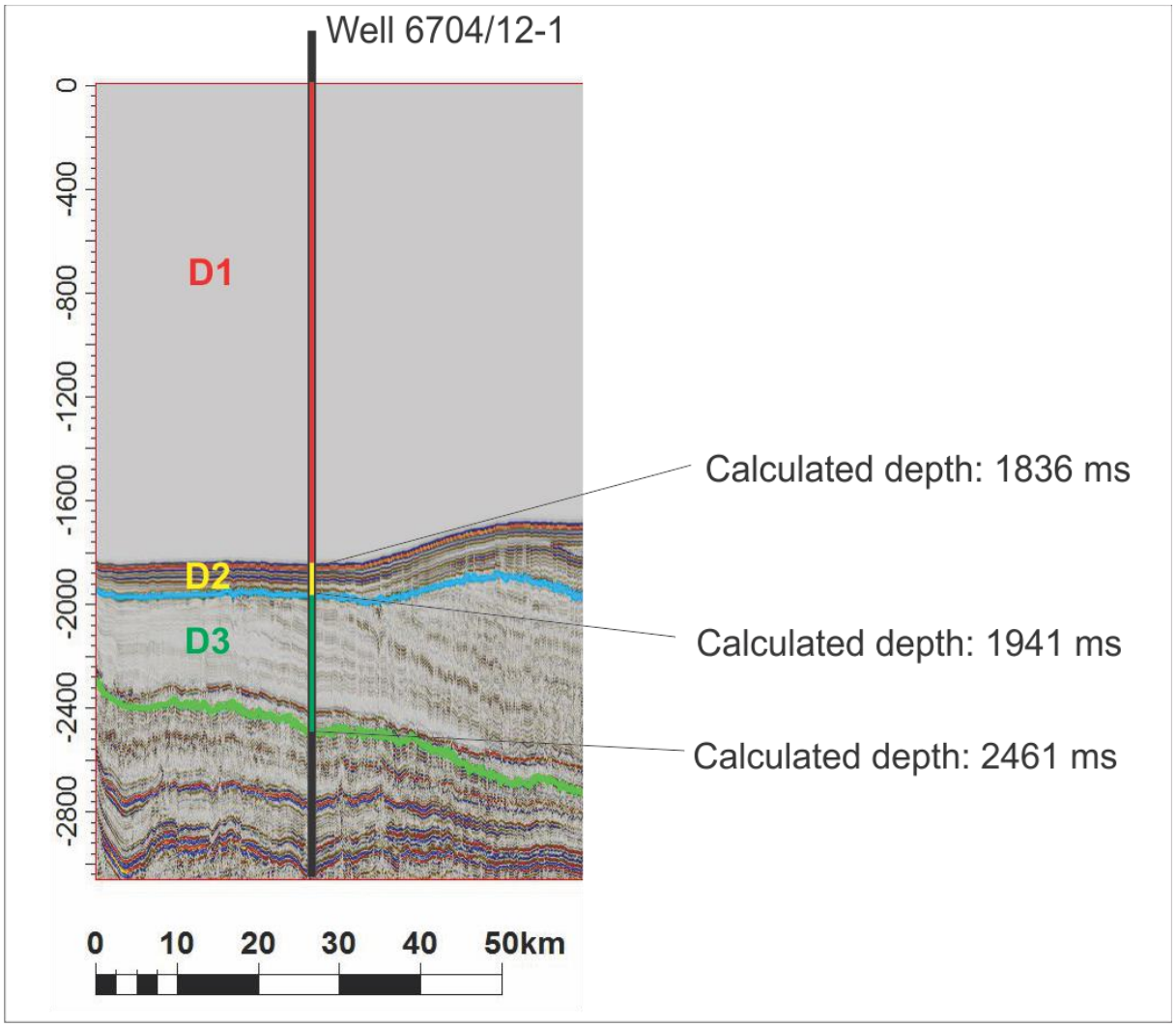

Figure 4-4-2: Example of a seismic section where a well is used to verify the interpretation of the base and top Kai formation. D1 is the seawater-sequence, D2 is the Naust formation and D3 is the Kai formation. The calculated values are conducted from table 4-1, 4-2 and 4-3. Location of the well and seismic line is displayed in Fig. 4-4-1.

5. Discussion

In this chapter, the conducted results will be discussed in relation to the depositional environment during the deposition of the Kai formation. The inner shelf (Area 1 and landwards) will be addressed first, discussing the origin of the reflection pattern within the Kai formation here. The depositional environment, in relation to the extent of ocean currents during Miocene-Pliocene will also be included in the discussion. The outer shelf (Area 2 / Vøring basin) will then be discussed in relation to the development of the interpreted sub-units K1-K6. The deposits will be discussed in relation to ocean currents affecting the area. Different structures and alongslope processes will be addressed, as well as similarities to areas further north and south. Finally, the relationship between the two areas, with suggested current flow patterns will be presented and discussed.

5.1 Sedimentary processes

The sedimentary processes of the study area, related to the deposition of the Kai formation can mainly be classified as alongslope processes, due to the interpreted indications of ocean bottom currents affecting the sediments. Non- to little evidence of downslope processes have been accounted for within the Kai formation.

5.1.1 Alongslope processes

In chapter 4.3 it was established that the deposits comprising the Kai formation is the result of alongslope processes, related to erosion, transport and deposition from slope-parallel ocean currents. The deposits were morphologically classified as mounded elongated contourite drifts. These contourite drift sediments were developed mostly free from the interaction of downslope processes. The elongated mounded contourite drifts are associated with moat structures and infilling drifts (Bryn et al., 2005). Studies show that the first indication of ocean bottom-current circulation along the Norwegian continental margin dates back to late Eocene time (Laberg et al., 2005b). The pronounced influence of downslope processes in the area did not start before the late Pliocene, when there was an increase in sediment supply from onshore uplift and glaciation. How much this change in sediment style affected the underlying contourites varies on the shelf, and had non- to little affect in the Vøring basin (Bryn et al., 2005).

The data shows a clear increase in the development of alongslope deposited sediments during Miocene, which can be due to changes in the oceanic circulation pattern. This may be the result of large-scale tectonic changes affecting the sea-floor morphology controlling the

distribution of the ocean currents. This is in conformity with Laberg et al., (2005b) who suggested that tectonic events created synclinal inverted domes, as well as established deep-water passages, resulting in an early Neogene expansion of deep-water circulation.

5.1.1.1 Local anticlinal highs

The continental shelf and the Vøring Basin were, during the deposition of the Kai formation, characterized by elevated anticlinal structures like the Helland-Hansen Arch and the Modgunn Arch, as well as marginal highs in the Vøring basin. The seismic reflection displays mound

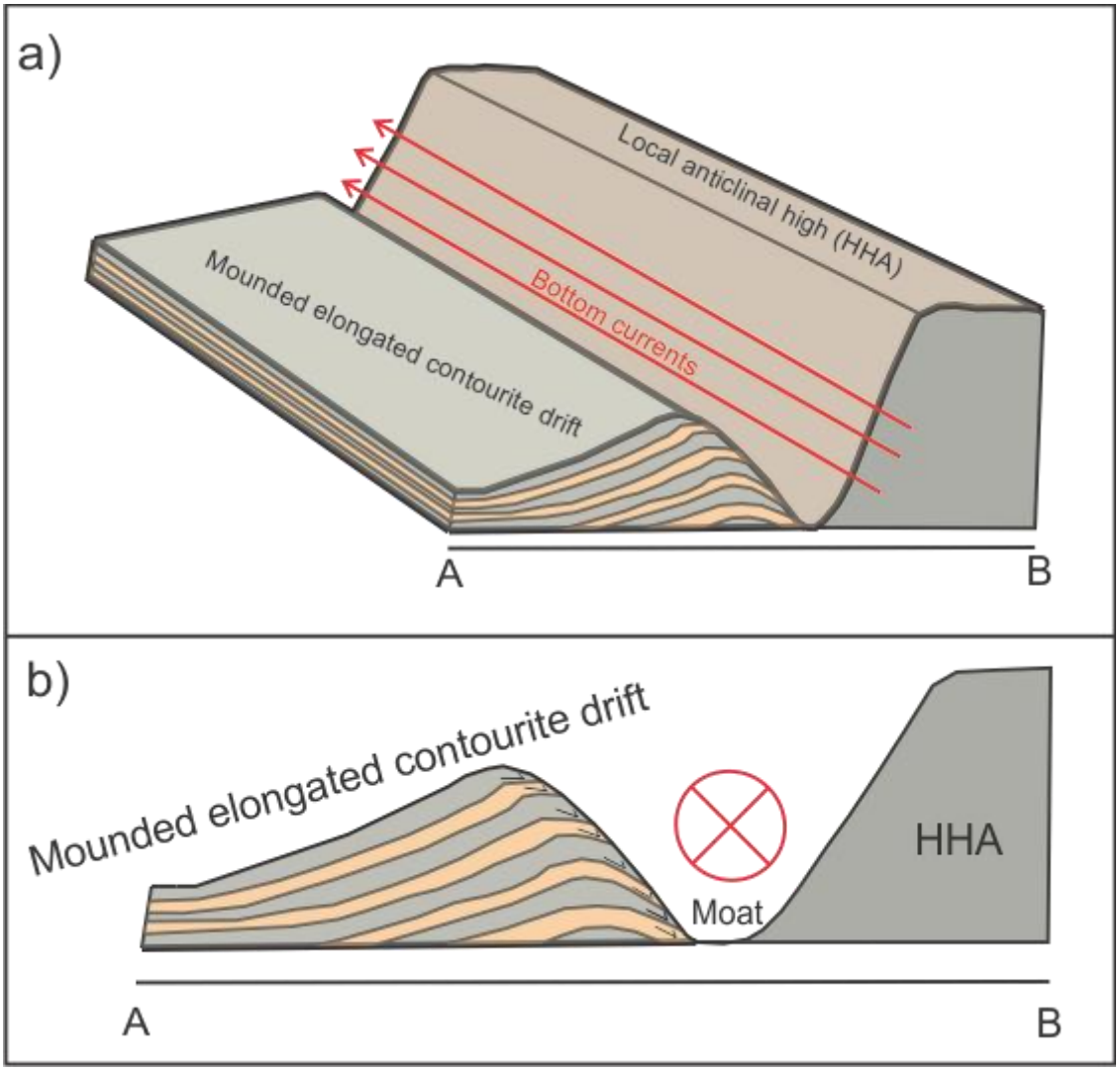

Figure 5-1-1: Illustration of how mounded elongated contourite drifts are deposited around local anticlinal highs, like the Helland-Hansen Arch (HHA). a) 3D model displaying the current pattern near the HHA. The model is based on a model from Rebesco (2005). b) Profile of the mounded elongated contourite drift system near the HHA, with associating onlaps and moat structure.

and moat structures towards these local highs. This is an indication that the deposits are off contour-current-controlled origin. There is observed non-deposition at the anticlinal structures. According to Brekke et al., (2000), the absence of the Kai formation on the highs is

the result of tectonic uplift in the area. Figure 5-1-1 displays an example of deposition on the flank of a local high, with moat structures where the bottom current is the most powerful. This is due to the current being too strong to deposit any sediments here. Where the current has a lower flow velocity, there was deposition of contourites.

The geometry of the Kai formation around the local highs and arches has many similarities to the equivalent structures of the Lofoten Contourite Drift, located north of the study area (Laberg et al. 2001). Here the sediments are characteristics of contour-current-controlled sediments. This strengthen the interpretation that the Kai formation has a contouritic origin. The interpretation is also in conformity with Bruns et al., (1998), who suggested, based on core data, that the mid- to late Miocene deposits in the Vøring basin originate from contour currents.

5.1.2 Downslope processes

No larger indications of downslope processes were found in this study. Local occurrence of sub-marine sliding/sloping may still be present, and cannot be ruled out. Sub-unit K1,5, which can locally be found in the northwestern part of the Vøring basin, is characterized by a distinct change in reflection pattern, with a chaotic, weak amplitudes. This amplitude pattern differs from the rest of the Kai formation in this area, and is found near the Vøring Escarpment confinement. Both these factors can be indications of downslope processes. In the west/northwestern part of the Vøring basin, the same change in reflection pattern is located within the bottommost K1 and K2 sub-units (Fig. 4-3-10). This change is found in a chaotic reflection pattern, around uncertain interpretations of the sub-unit, near the Vøring Escarpment. Since there are no clearer indications of sliding/sloping in the Vøring Basin, downslope processes will not have any larger affection on the interpretation of the depositional environment in the study area.

5.1.3 Possible input from land areas

In the eastern part of the study area, the sediments deviates from the contouritic sediment reflection pattern found within the Kai formation further west in the study area, as well as the reflection pattern within the interpreted Molo formation. This may suggest that even if the sediment package is consistent with the Kai formation time-period, it was deposited from a different sedimentary process. Therefore the sediment package may be the depositional product land-originating sediments. The observation of the sediment package reaching the seafloor can be a strengthening factor in this interpretation. There is also observed an increase

in thickness of the sediment package towards the mainland. If the package were the depositional product of alongslope processes, the thickness would most likely be increasing in the opposite direction. There is not observed any reflection terminations that indicate contouritic origin of the sediments. It is unclear to what extent the area have been afflicted by erosion, which makes it difficult to determine if there were located contouritic indications further up in the sediment package, before the deposition of the Naust formation. It is therefore hard to determine whether the found sediment package is the result of land-originating sediments or not.

5.2 Depositional environment

5.2.1 Inner shelf

The inner shelf covers Study Area 1 and the easternmost part of the main study area. It is characterized by a steady low-dipping slope, with some interactions from local high structures (Fig. 5-2-1). The general (Kai formation) relation between Area 1 and the easternmost part of the study area consists of a gentle buildup of contourites in Area 1 towards the east, with some interruption by local anticlinal highs. The thickest part of the Kai formation in Area 1 is located near the local anticlinal highs (Fig. 5-2-1), with a thinning of the formation eastward after the interruption. The thinning out of the Kai formation east of Study area 1 is interpreted to be the result of reduced current strength from the local high and eastwards, before the formation thins out. On the easternmost part of the study area, near the occurrence of the Molo formation, a new sediment packages is present. This sediment package has a gentle buildup eastward, below the Molo formation. This area will be further discussed in chapter 5.2.1.2.

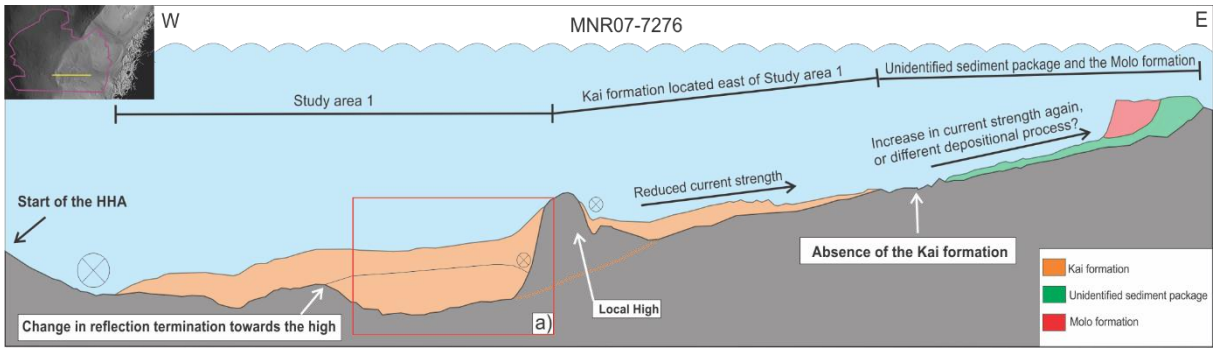

Figure 5-2-1: Sketch of the general prevalence of the Kai formation in Area 1 and eastward. The occurrence of an unknown sediment package is documented in the easternmost part of the sketch. The Kai formation is displayed with the interruption of a local high, with suggested base pattern for areas unaffected by local highs (orange dotted line). Red line (a)) marks the outcrop of Figure 5-2-3.

5.2.1.1 Area 1

The reflection pattern, as well as the reflection terminations found on the inner shelf suggest contouritic sedimentation, part of a mounded elongated drift system. This is evidence for ocean current affecting the sediments during Miocene and Pliocene time. The geometry of the contourites are affected by confinements toward both the west and the eastern part of Area 1. This, together with the direction of the identified moat structures in the area suggest a north-flowing bottom current system, during the deposition of the Kai formation in Area 1. The reflections clearly shows downlapping terminations towards the west, and onlapping terminations towards local highs in the east. The difference in termination in the west/east is interpreted to be the result of the ocean current being too strong to deposit sediments towards the Helland-Hansen Arch. The current decreases in strength towards the east, resulting in a low gradually buildup of contourites from the west to the east (Fig. 5-2-2), strengthen this hypothesis. There is also not found any clear unconformity from erosional truncation in the upper part of the Kai formation here, which indicate that the lack in sediment deposition towards the west are not the result of erosion from the massive overlying Naust formation, but rather from deposition-related events.

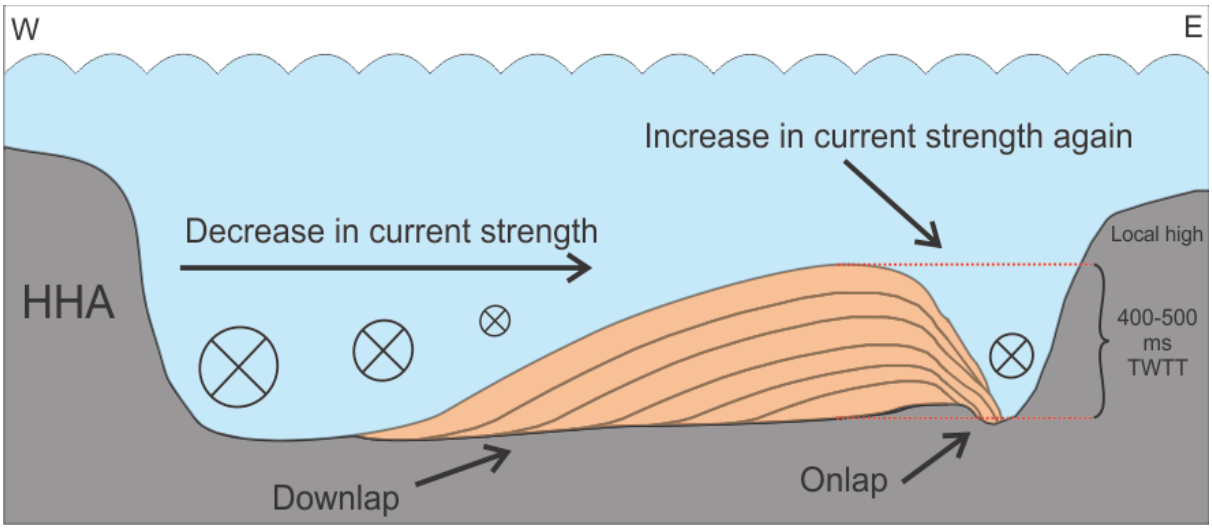

Figure 5-2-2: Drawing displaying the general low gradual build-up of mounded contourites towards the east in Area 1, as well as non-deposition along the HHA due to the north going current being too strong to deposit sediments here. The current increases again into a moat structure towards local high in the east. The orange layers are representing the contouritic Kai formation east of the HHA. HHA: Helland-Hansen Arch.

Similar contouritic systems with associated moat structures have been identified in the study area by Laberg et al., (2001); Bryn et al., (2005); Laberg et al., (2005a); Laberg et al., (2005b). There is found a notable change from reflection termination toward the east (Fig. 5-2-3), with onlapping terminations on the oldest part, and reflections following the structure of the local high on the youngest part. This may be an indication of alternating periods of

increased/decreased surface water circulation, possibly related to sea-level oscillation or change in current strength. There was also found an amplitude change in the middle of a section, which probably is related to the change in reflection termination (Fig. 5-2-3), suggesting a change in the current system. On the western part of the Helland-Hansen Arch, Hjelstuen et al., (2004) found multiple generations of current-influenced sediment packages, reflecting a Miocene change in the current system. Although these similarities were found on the western part of the Helland-Hansen Arch, there is reason to believe that these changes in the oceanography during Miocene-Pliocene affected the contourite deposits similarly, on both sides of the arch. Both the change in amplitude strength and reflection termination clearly indicates a change in sea-level, or current strength at the time. The oldest section of the

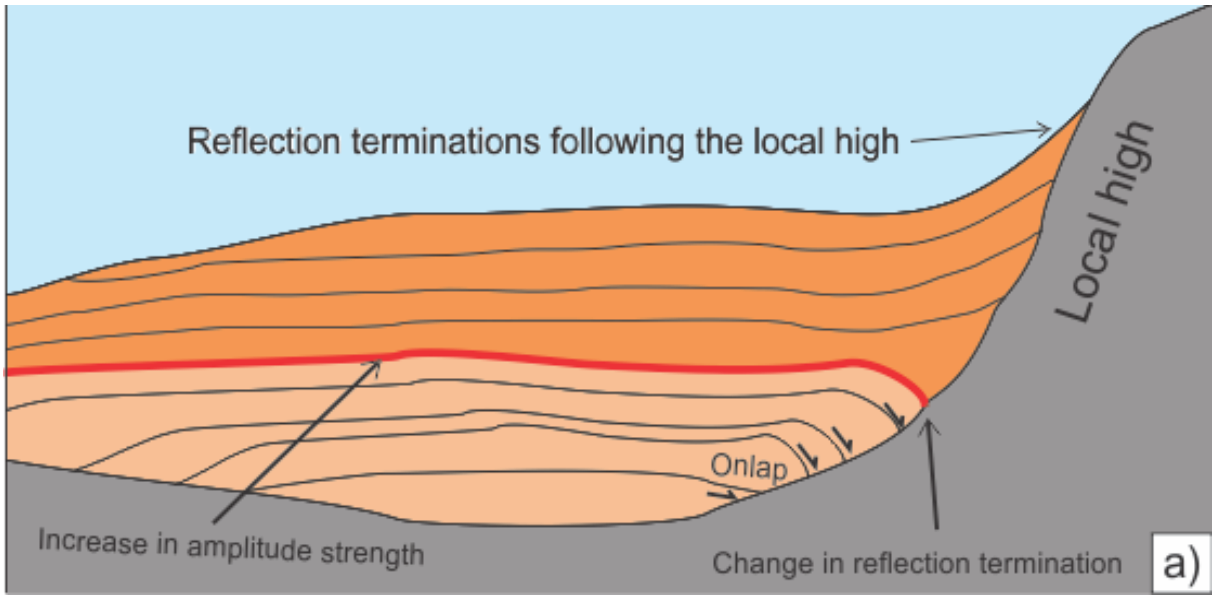

Figure 5-2-3: Image displaying multiple generations of current-influenced sediments, with change in both amplitude strength, and reflection termination at the local high towards the east. The bottommost contouritic sediments have an onlap reflection termination, while the upper contouritic sediments have a termination following the local high. Grey sediments: Older Brygge formation. Orange sediments: Contourites from Kai formation.

contourites displayed in Figure 5-2-3, displaying onlap is probably the result of a current near the flanks of the local high. Therefore the change in reflection termination suggests a change in this current pattern, with a more uniform deposition throughout the section.

It is difficult to determine whether Area 1 includes the same six sub-units as found in Area 2. This is because of the variation in reflection amplitude within the Kai formation in Area 1, as well as a locally chaotic reflection pattern. The two areas are locally separated by local anticlinal highs, which makes the interpretation of sub-units even harder. The Naust formation is at its thickest over Area 1, which makes it impossible to determine exactly how much the sediment package have been affected by erosion.

5.2.1.2 The occurrence of the Kai formation in the easternmost part of the study area

Although the prevalence of the interpreted Molo formation vary throughout the study area, a general model of the thickest northeastern part of the area is created (Fig. 5-2-4). The two suggested interpretation of the relation between the Kai formation and the Molo formation is discussed, based on this model. The interpretation of the base Naust and the top Brygge formations are established, and can be concluded that are the same in both interpretation 1 and 2. The extent of the sediment package is uncertain, and in this study it have only been located in the northwestern part of the study area.

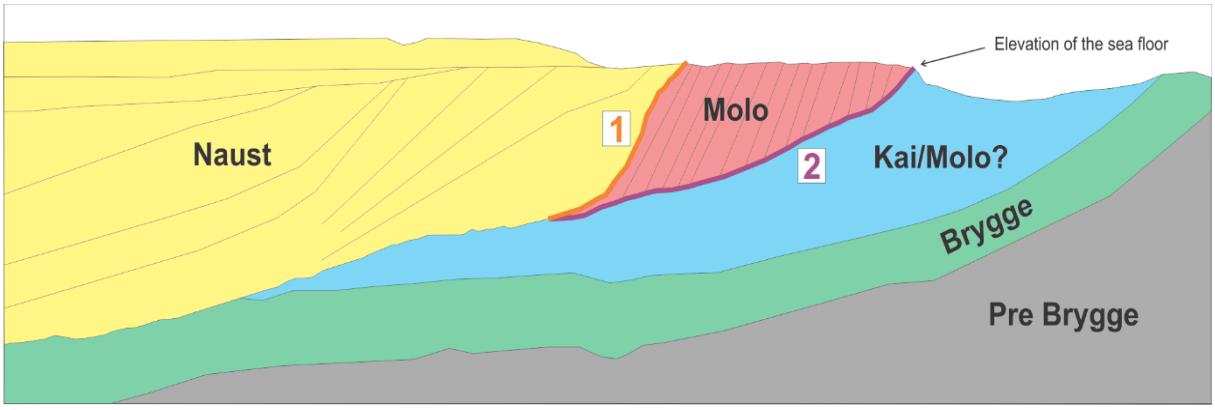

Figure 5-2-4: Illustration of the northwestern part of the study area, with the interpretation of the sediment packages found in the area. Orange (1) and purple (2) displays the two suggested interpretation of the Kai/Molo relation.

Interpretation 1 suggest that the Kai formation is not located this far east, and that the undecided sediment package is in fact an older part of the interpreted Molo formation.

Interpretation 2 suggest that the undecided sediment package found in the area is the reappearance of the Kai formation this far landwards. Both the internal sediment structure and the elevation of the seafloor at the exact point where the pattern changes, suggests two different formations is present, and that the border of interpretation 2 (Fig. 5-3-1) marks the boundary of the Kai and Molo formation. This interpretation suggest that the Kai formation can be located this far east, and up to the seafloor level. The interpreted Brygge formation and the Kai formation share the same depositional pattern here, which means that the Brygge formation also can be found up to the seafloor here.

Since the sedimentary system on the Vøring Margin is a prograding system with no greater folding present, there is reason to believe that the bottommost sediment package is the oldest one. Earlier studies (Eidvin et al., 2007; Rise et al., 2010; Eidvin et al., 2014) has found that the stratigraphic position strongly suggests that the sand-dominated and coast-parallel Molo formation is a proximal equivalent to the deeper marine-dominated Kai formation, and that

they were both deposited in roughly the same time period (Middle Miocene and younger). This is consistent with interpretation 1 in this study. Interpretation 2 suggests that the overlying Molo formation is younger than the found Kai sediment package in the area. Løseth & Henriksen (2005) assigned, in their study, a late Middle to Late Miocene age to the Kai formation and an Early Pliocene age to the Molo formation. This confirms that the two formations were deposited at approximately the same time, but with the oldest sediments of Kai formation being slightly older than the oldest part of the Molo formation, which may be an indication that the two formations are in fact not proximal equivalent, and that they were deposited under different depositional environments. There is not found any similar sediment packages in previous studies from the same area. It is difficult to determine which one of the two interpretations that is the most probable, due to the lack of well logs and age estimates in the area. The inner seismic pattern, as well as the interpretation of the top and base of the Kai formation, suggest a change in sediment structure between the two packages, but whether this change is related to a change in depositional environment is uncertain. My understanding is that the Kai formation have not been observed this far east before. No relevant well log is available to confirm either of the interpretations. The sediments deviates from the contouritic sedimentation pattern found within the Kai formation further west in the study area, which suggest that even if the sediment package is consistent with the Kai formation time-period, it has a different lithology than the Kai formation. Therefore the sediment package may be the depositional product land-originating sediments. The observation of the sediment package reaching the seafloor can be a strengthening factor in this interpretation.

5.2.2 Outer shelf (Area 2)

On the outer shelf (west of the HHA), the sediments comprising the Kai formation were divided into multiple sub-units (K1 – K6). These sub-units will be interpreted and discussed, based on reflection pattern, -termination and distribution. Multiple models for the origin of the different sub-units have been made. Although the sub-units vary both in distribution and thickness throughout the study area, an illustration of the general W/E and S/N seismic profile is presented. The western located (north/south orientated) illustration is correlated from seismic line MNR06-7428 and MNR09-7376 (displayed in chapter 4.3.2). The northern located (west/east orientated) illustration is modified from seismic line MNR07-7488 (displayed in chapter 4.3.2), and is included to better display the local sub-unit K1,5.

K1

In the northern part of the study area, sub-unit K1 has a relative uniform thickness (Fig. 5-2-3a), following the underlying base of the formation. The sub-unit have few evidence of contouritic deposition, only located by a thinning out of the sub-unit into an onlapping reflection termination towards the northeast. Therefore it is reasonable to believe that the deposits comprising the K1 sub-unit is the result of suspension with some affliction from bottom currents. The relative uniform thickness of the sub-unit strengthen the suggestion that the K1 were less affected by ocean currents, but rather were the result of suspension from a more hemipelagic environment. Some onlapping terminations towards the eastern confinement in the north may suggest, even if K1 were mostly a product of suspension, bottom currents have played a minor role as well. This show a different pattern from the bottommost part of the Kai formation on the inner shelf. The difference between the inner and outer shelf will be further discussed in chapter 5.2.3.

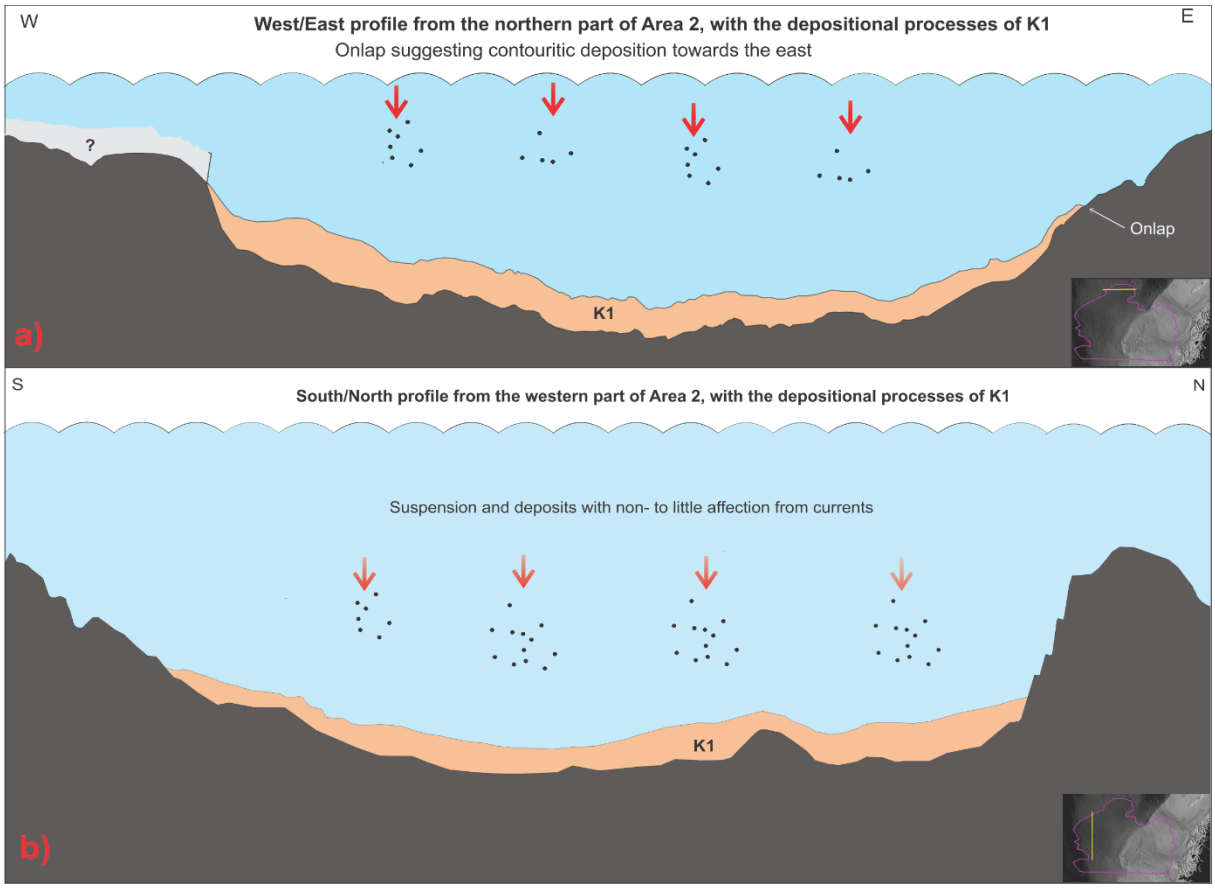

Figure 5-2-3: Illustration of the depositional processes during the deposition of K1. a) Deposition in the north of Area 2 (W/E). b) Deposition in the western part of Area 2 (S/N).

The results showed that K1 were absent in the southerneastern part of Area 2, which may be an indication of stronger erosion of K1 here. The lack of contouritic evidence, and the fact that the absent area covers a relatively huge part of the basin, strengthen the suggestion that the K1 were eroded in the southeast. Due to a chaotic reflection pattern near the base Kai formation here, there is difficult to confirm this theory.

There were found a gradual reduction in thickness of the sub-unit southwards (Fig. 5-2-3), which may indicate that the sediments deposited had a gradually increase in erosion towards the south. In the southwestern part of Area 2, there is found that K1 have large moat-like structures. The vastness of the structure suggest that this is the result of the sub-unit following the topography of the underlying Brygge formation. The moat-like structure can, in this area, be found below the base Kai formation, which enhances this interpretation.

K1,5

In the northern part of the study area a local sub-unit is located, close to the confinement towards the west (Fig. 5-2-4). The extent of this local unit is uncertain, but it is clear that the unit is only locally found in the north. This may be an indication that the unit are not deposited from ocean currents, but rather from downslope processes like submarine sliding/slumping from the nearby highs. Sub-unit 1,5 might also be the result of a current eroding the surrounding areas, although because of a chaotic reflection pattern, there is not possible to determine whether the top K1,5 is an erosional truncation, or a change in reflection amplitude due to the change in the paleo-oceanography. This hypothesis of a change in paleo-oceanography may be unlikely due to K1 not being affected by erosion where K1,5 is absent. If K1,5 were eroded away completely, it is likely that K1 had been affected too.

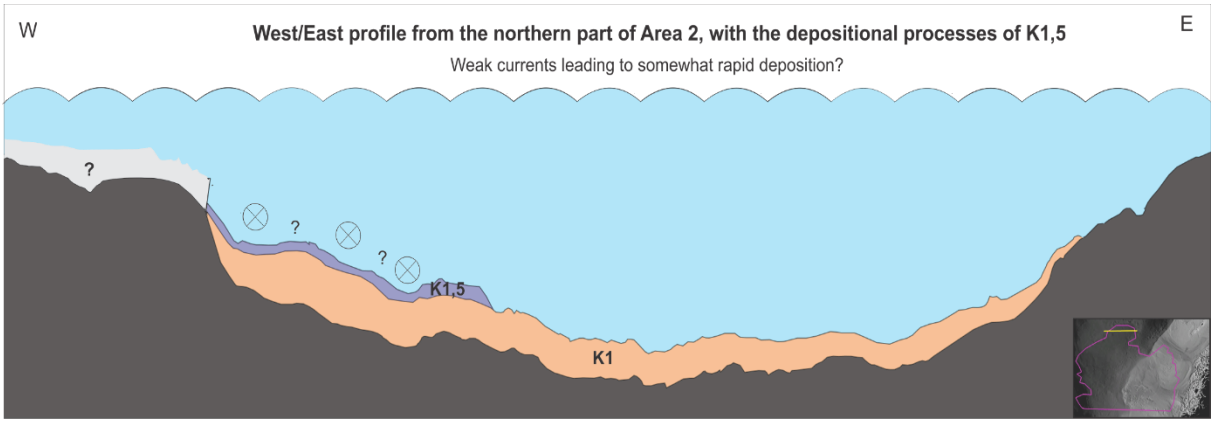

Figure 5-2-4: Illustration of the depositional processes active during the deposition of K1,5 in the northern part of Area 2.

Since K1,5 only can be locally found in the northern part of study area 2, it may have been the result of a current following the flanks of the confinement here, although there is not found any onalpping reflection termination in the K1,5. The lack of local sub-units at different elevation levels suggests that the creation of local units due to the elevated highs are rather unlikely.

K2 and K3

Sub-units K2 and K3 are generally following the same structural pattern as the underlying sediments, but clearer moat structures as well as onlap suggest that K2 and K3 were more affected by bottom currents than the underlying K1. In the northern part of the area,

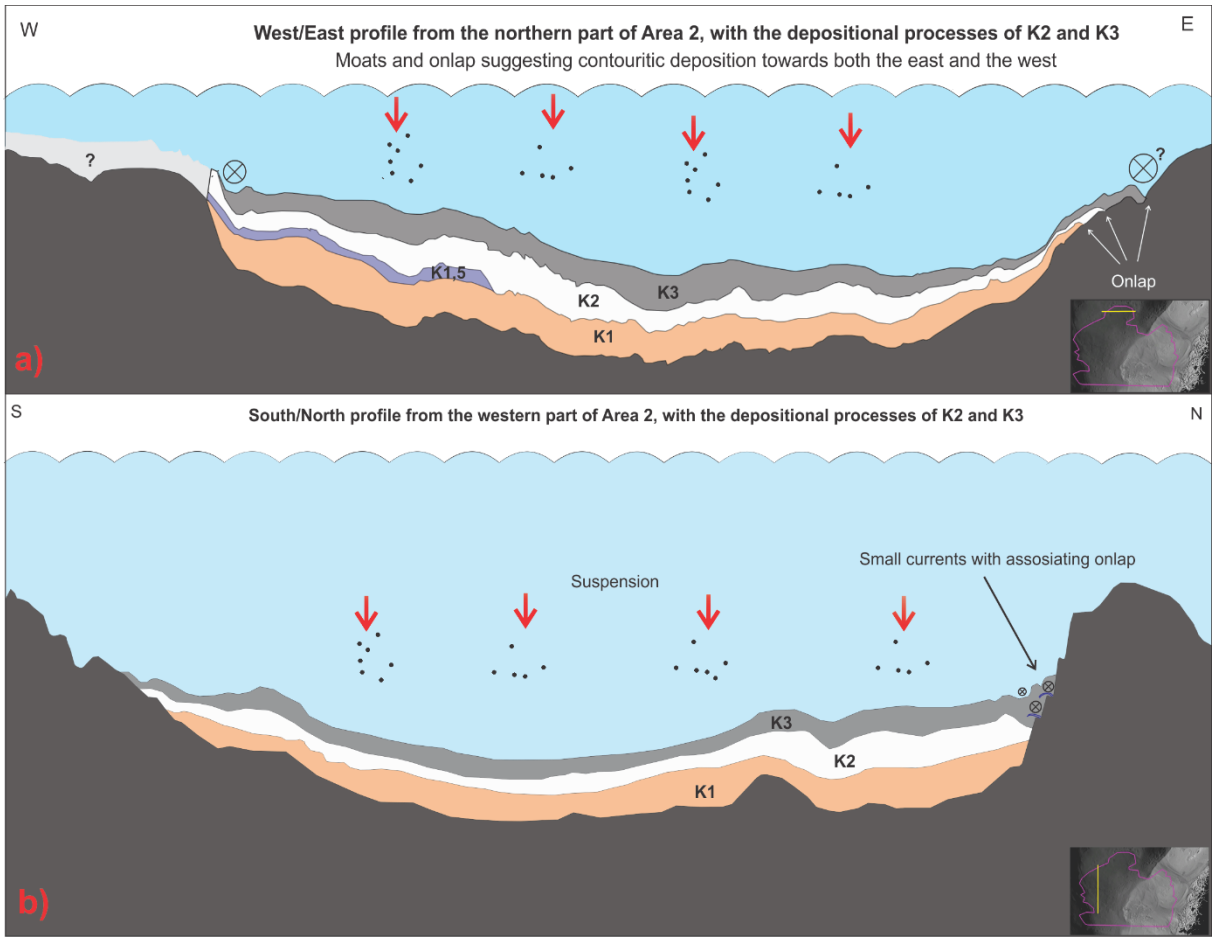

Figure 5-2-5: Illustration of the depositional processes during the deposition of K2 and K3. a) Deposition in the north of Area 2 (W/E). b) Deposition in the western part of Area 2 (S/N).

contouritic sediment structures have been observed in both the western and eastern part of the area. Here K2 and K3 is thinning out towards the elevated eastern confinements of the basin, which may suggest that the sediments here were more affected by current erosion. The increase in contouritic evidence in K2 and K3 suggest that these sub-units marks the change in depositional environment to a more bottom-current related system.

K4

In the middle of the Vøring basin, K4 is found to have a relative uniform thickness, and reflecting the same structural geometry as the deeper units. This may indicate that K4 have not been heavily affected by bottom current deposition here. The boundary between K3 and K4 displays an abrupt change in amplitude. This change is interpreted to be the result of a change in sediment composition, rather than any large change in the ocean circulation pattern. Geochemical evidence from previous studies (Bohrmann et al., 1990) have located shifts between carbonate- and opal-dominated sediments on the Vøring Marginal High, strengthening this interpretation. Alternatively the amplitude change may be the result of a change in current velocity, altering the grain-size of the contourite deposits. Some IRD (Ice Rafted Debris) deposits have also been found in the area during the deposition of the Kai formation (Jansen et al., 1991; Eidvin et al., 2007), which may have created the change in amplitude.

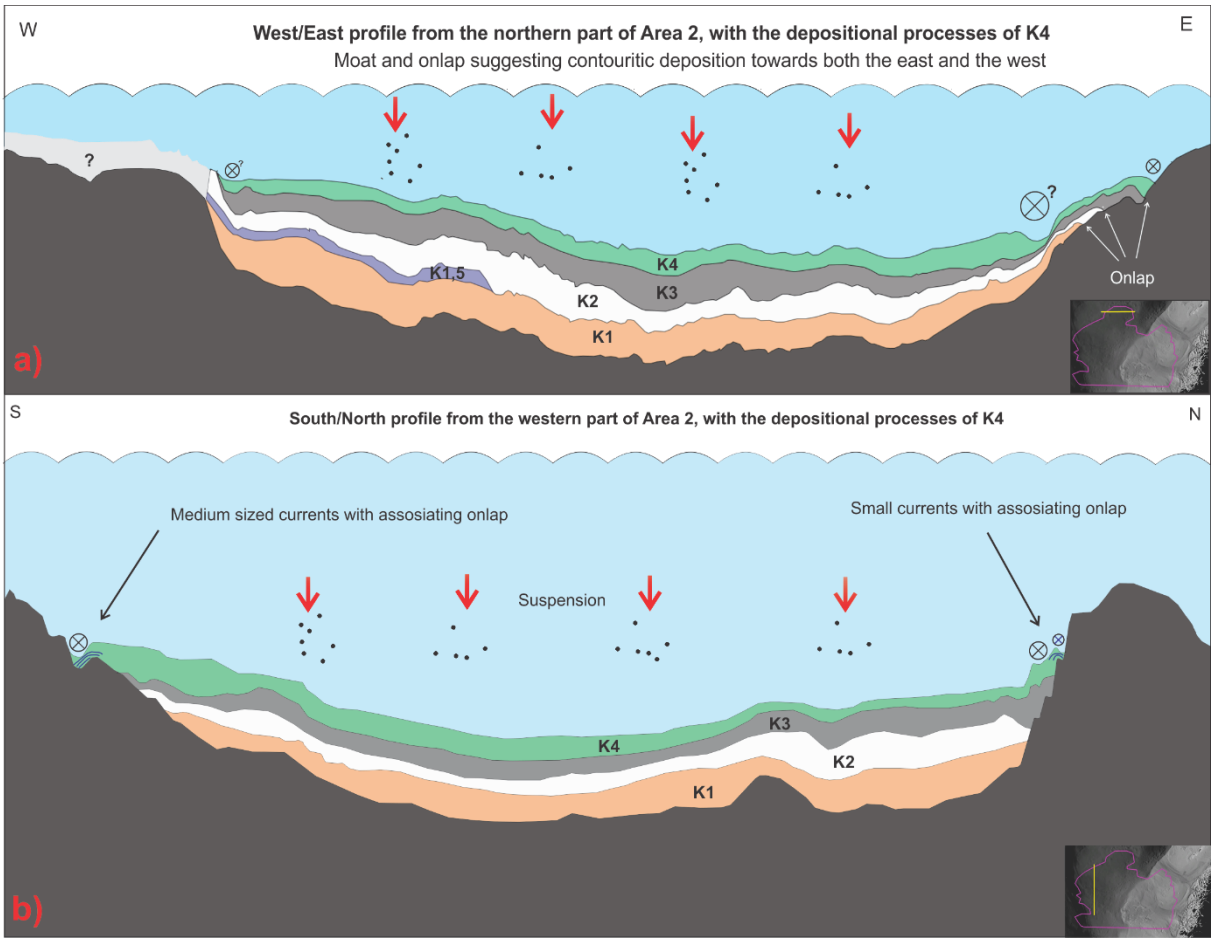

Figure 4-2-6: General illustration of the K4 sub-unit in the northern and western part of Area 2, and depositional processes associated with the sub-unit. a) Deposition in the northern part of Area 2. b) Deposition in the western part of Area 2.

In the western part of the study area, moat structures were found within sub-unit K4 (Fig. 5-2-6), which are for the most part, not consistent with the underlying sub-units. This indicates a change in current pattern or strength. The moats are related to onlapping reflections towards the elevated western escarpment of the Vøring basin. Moat structures with associating onlap pattern is also located in the northern and southern confinement. The oceanic current pattern is therefore interpreted to locally have a westward orientation in the southern part of Area 2, and a more eastern orientation in the north confinement. This will be further discussed in chapter 5.4.

In the northern part of the study area, multiple sets of moat structures have been observed towards the eastern confinement. Whether this is the result of separate bottom currents or tectonic changes (all sub-units are experiencing a thinning of the sediment package, as well as a steeper angle in the area, see Fig. 4-2-6a), it is not possible to determine from the seismic data.

K5

Sub-unit K5 is the oldest unit to clearly be affected by erosional truncation from the overlying Naust formation, since it is the oldest sub-unit which in some areas have a direct boundary to the base Naust formation. K5 have evidence of oceanic currents in the north-, east- and southern confinement of the Vøring basin. In the north, K5 is thinning out westwards, suggesting an increase in erosion. The erosion may be related to high current velocity in the area, but erosion related to the enormous thickness of the overlying Naust formation cannot be excluded.

At the northern, western and southeastern restriction of the Vøring basin, the base Kai formation has a steep slope pattern, because of the occurrence of the local highs. The current-related structures found is therefore located almost vertically to each other (Fig. 4-2-7b), suggesting that the current pattern in the area has not changed much. At the southern (Fig. 4-2-7b) and northeastern (Fig.4-2-7a) confinement of the Vøring basin, the base Kai formation has a gentler slope pattern, which results in that the current pattern are moved upslope during the deposition of the different sub-units (Fig.4-2-7). K5 is therefore located further south than K4, which is located further south than K3 etc. This indicate that the sub-units in the Vøring basin may have been greatly affected by changes in current- pattern and strength, as well as sea-level oscillation. K5 is thinnest in the parts of Area 2 where the Naust formation is largest, and in the middle of the Vøring basin. This is interpreted to be related to the increase in

erosion underneath the Naust formation. This pattern is easiest detected in the upper sub-units in the Kai formation, since it is connected to the visible erosion patterns only found in K5 and K6.

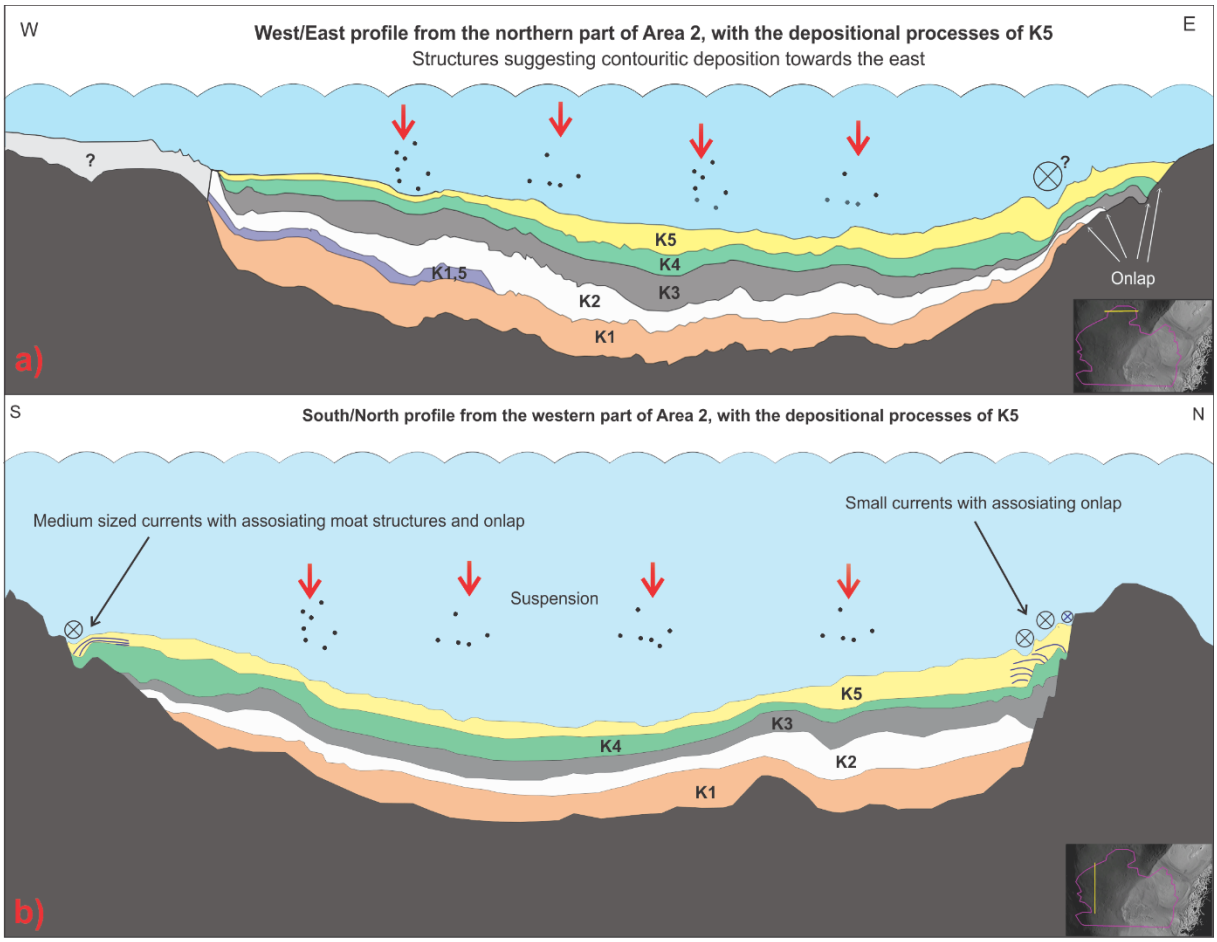

Figure 4-2-7: General illustration of the K4 sub-unit in the northern and western part of Area 2, including the depositional processes associated with the sub-unit. a) Deposition in the northern part of Area 2. b) Deposition in the western part of Area 2.

K6

K6 is the youngest sub-unit which have been located in all parts of Area 2. There have been located some older units in the middle and southern part of the area, which is greatly eroded in the basin as well as underneath the buildup of the Naust formation, but these only have a local extent. The K6 is mostly absent in the middle part of the Vøring basin, as well as near the thickest part of the Naust formation. Whether the sub-unit were deposited by suspension or in a bottom current system, is difficult to determine since the largest part of the sub-unit is affected by erosional truncation. The original thickness of the sub-unit is also uncertain. This applies to all the sub-units, but especially for K6, since it have been eroded directly by the overlying glacial deposits.

Sub-unit K6 were probably following the same depositional pattern as K5 during deposition. This may be a logical option because of the sub-unit being deposited at roughly the same time and, at less eroded areas, are seen to follow the same topographic patterns as K5. This interpretation suggest that K5 and K6 were affected by the same current regime, with some deviation only in the southern escarpment, where the slope pattern had a gentler dip, and the K6-current were forced further south toward the escarpment. In the middle part of the Vøring basin, K6 were probably deposited from suspension. This is interpreted with high confidence since K1-K5 have all been interpreted to have suspension-related deposits here.

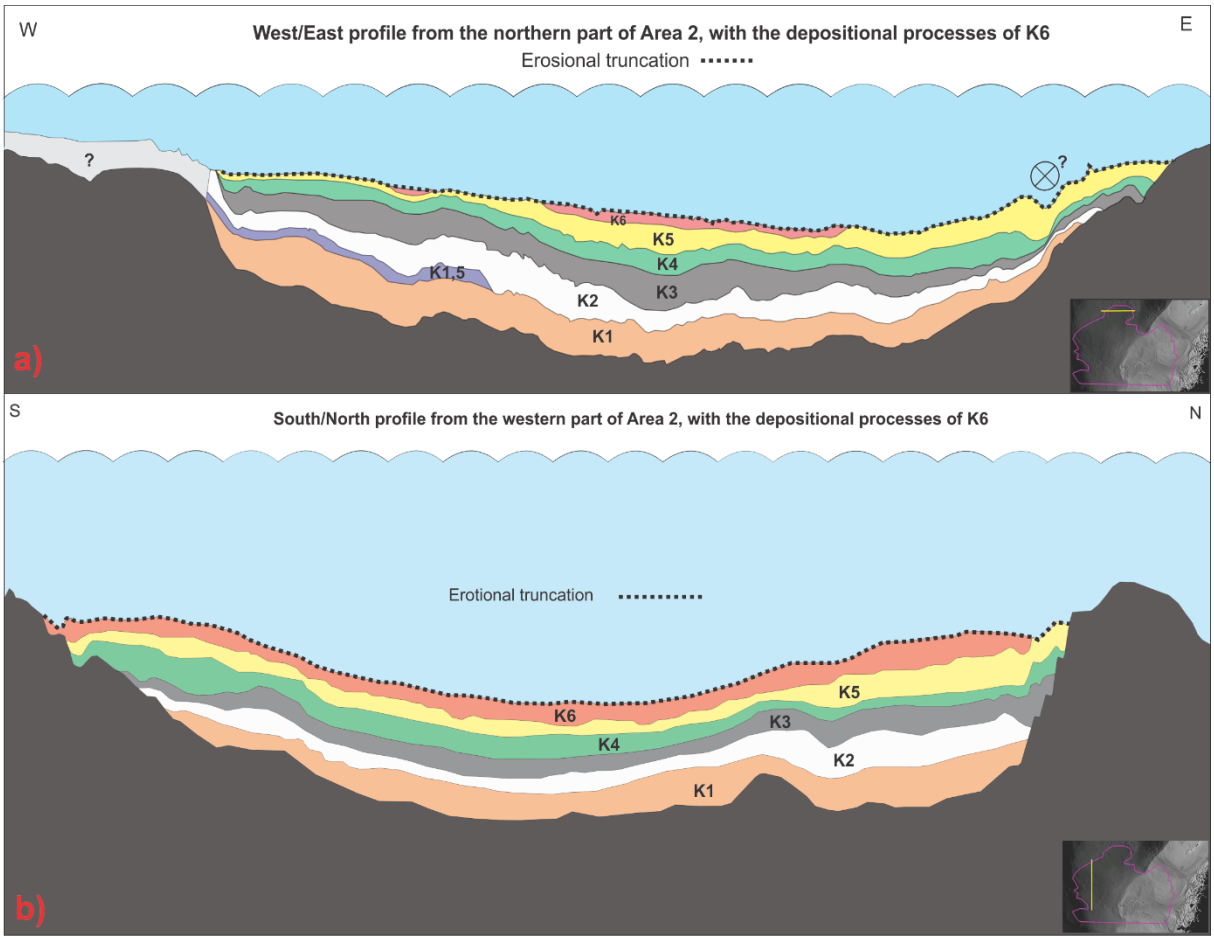

Figure 5-2-8: Illustration of the prevalence of sub-unit K6 in the northern and western part of Area 2, with the displaying of the erosional truncation in the area. a) Deposition in the north of Area 2 (W/E). b) Deposition in the western part of Area 2 (S/N). The thickness of the overlying Naust formation varies throughout Area 2.

5.2.3 Connection between the inner and outer shelf (Area 1 and 2)

It can be difficult to determine the stratigraphic connection between the two interpreted areas, because of the anticlinal structures separating them, as well as the general change in both topography and accumulation of younger, overlying sediments. There is found less heightening structures between the two areas in the middle part of the study area. This leads to a reduction in the topographical control on the ocean circulation system here. The connection between inner and outer shelf is still hard to determine, due to the erosional effect of the rapidly deposited Naust formation. The same sub-units found in Area 2 on the outer shelf can therefore not be observed with certain on the inner shelf in Area 1. Similar reflection pattern and sediment structures have been observed within the Kai formation in the two areas. Both Area 1 and 2 consists mostly of elongated mounded contourite drifts, with some indications of hemipelagic depositional environment in the bottommost sub-units in the Vøring Basin. No such suspension-based environment have been observed within any of the undecided sub-units on the inner shelf, resulting in more defined contourite structures.

It is difficult to determine whether the current velocity is different between the inner shelf and outer part of the shelf, due to some differences in the depositional environment. The western part of the inner shelf (Area 1) generally shows a larger build-up of mounded drift structures, which may suggest stronger bottom-currents here. On the outer shelf, there is moat structures deposited at different levels, moving upward onto the confinements of the Vøring Basin. This indicates that the contourite deposits on the outer shelf were more affected by changes in current pattern and sea-level oscillation.

5.2.4 Boundaries between the sub-units

The boundaries between sub-units K1-K6 on the outer shelf, as well as the unclassified sub-units on the inner part of the shelf, may represent a change in current- pattern, or velocity. Previous studies (Bohrmann et al., 1990) have found a change in sediment structure at the Vøring Marginal High during late Miocene to early Pliocene time. The accumulated sediments were characterized by shifts between carbonate- and opal-dominated sediments. This may be an indication of alternating periods of decreased surface water circulation with a relative isolation of deep water (opal-dominated), and periods of increased surface and deep water circulation (carbonate-dominated), possibly related to sea-level oscillation around the critical sill depth of the Greenland-Scotland Ridge (Bohrmann et al., 1990). Geochemical studies done by Bruns et al., (1998) shows shifts in both sediment-structure and sedimentation rate in the Vøring basin during Miocene and Pliocene. These shifts are greatly affected by

changes in ocean currents, due to water masses from different origin, vary in properties. This is strengthening the interpretation of alternating periods of deep water circulation during the deposition of the Kai formation. Because erosion, transport and deposition is related to current velocities and turbulence, gran size distribution should be sensitive to bottom current velocities.

5.2.5 Contourite drifts along the Norwegian continental margin further north and south

The contourite drift deposits observed on the Vøring margin, as well as in the Vøring basin have been identified as mounded elongated contourite drifts. Previous studies (Laberg et al., 2005a) show that there have been found similar contourite development from the northern North Sea basin and the northern Atlantic Ocean from the Miocene period and forwards. According to Laberg et al., (2005a), this might be an indication that the ocean currents affecting the deposits in the study area were part of a larger circulation system sharing properties with that of the present, with water masses flowing northeastward into the study area. Laberg et al., (2005b) found evidence for bottom-current controlled deposition and erosion, similar to the Vøring Plateau, southwest of the study area in the Rockall Trough and the Faroe-Shetland Channel. This is in unity with Stoker et al., (2002), who also found similar Neogene uplift, deep water erosion and contourite deposits in The Rockall Trough. Similar contourite drift systems can be found north of the study area, at the Lofoten margin. Laberg et al., (2001) has classified the Lofoten deposits to be mounded elongated drift systems, related to bottom water circulation. The growth of the contourite drifts are controlled by sediment availability, deriving from both winnowing of the shelf and upper slope, and ice sheets on the shelf when present. This study have many similarities to The Rockall Trough, with deposition in a synclinal basin/channel stratigraphy and confinements with relevant contourite drift structures towards the confinements.

The oceanic bottom-current pattern during Miocene and Pliocene share many similarities with present day oceanography. Ocean currents are observed to still flow at the flanks of the local anticlinal highs. This might be an indication that the Miocene uplift, which affected the study area as well as the surrounding areas (Lofoten, Rockall trough and the Faroe-Shetland Channel), laid the foundation for the oceanography off mid-Norway today. The lack of tectonic events since Miocene time, strengthen this theory. Miller and Tucholke (1983), as well as Bohrmann et al., (1990) confirms this, as they suggested that the deep-water circulation within the Norwegian-Greenland Sea was established in the middle Miocene.

5.2.7 Summary

The inner shelf comprises of a contouritic depositional pattern, with evidence of mounded elongated drifts. Multiple moat structures, with associating onlap reflection termination around the local anticlinal highs suggest that the contour-currents were following the flanks of these highs. The geometry of the contourite deposits, together with the direction of the found moat structures in the area suggest a generally north-going bottom current system.

Within the outer shelf area, the Kai formation can be separated into different sub-units, based on reflection pattern, -termination and -distribution. There have been found similar contouritic depositional pattern at the flanks of the local highs, as at the inner shelf. In the deeper basin part, more hemipelagic sedimentation environment is favored, due to the lack of current-related evidence. There is therefore difficult to determine the paleo-oceanography during the deposition of K1. Some moat structures have been found within K1, but enough to interpret a separate ocean current pattern. Therefore the paleo-oceanography is based on the oldest half of the Kai formation in the Vøring basin (K2-K6). K6 is heavily eroded in the basin, which makes the interpretation of the paleo-oceanography during the deposition of the youngest sediments of the Kai formation difficult here. Younger sub-units than K6 have been accounted for, but because they are heavily affected by erosional truncation, and only locally found in the southeastern part of Area 2, they will not be taken into consideration in the interpretation of the oceanic circulation pattern during the deposition of the Kai formation.

The local highs affecting the bottom current pattern is mostly found to have steep sides, which results in the bottom current pattern not changing much with time. At the southern escarpment of the Vøring basin, the confinement of the basin is not as steep, resulting in a prograding upslope system, where the bottom currents are moved upward the escarpment with time.

The inner shelf is in general more dominated by ocean current controlled sedimentation, compared to the outer shelf. Therefore the currents have been interpreted to be strongest inner part of the slope, just east of the HHA. This will be further discussed below.

5.3 Polygonal faulting within the Kai formation

There is found multiple small-offset faults in the Vøring basin, which have been identified as polygonal faults, which may have a relation to fluid expulsion. Brendt et al., (2003) found that the polygonal fault systems in the study area are not necessarily in relation to typical fluid flow indicators, but rather in relation with overburden glacial debris. This is in consistency with Chand et al., (2011), who found that the polygonal faults could be the result of major

overpressure buildup. The polygonal fault found in the study area is overburden by glacial debris from the Quaternary Naust formation. This may suggest in the sediment thickness of the Kai formation in the Vøring basin were larger during deposition in relation to present day. This is in unity with Chand et al,. (2011), who found evidence of porosity reduction in the Vøring basin, resulting in dewatering, diagenesis and normal compaction. Bryn et al., (2005) suggest that the rapid loading from the Naust glacial deposits will increase the fluid flow from the contourite drifts in the Kai formation, and therefore increase the pore pressure leading to a reduction in slope stability in the area.

The polygonal fault systems can only be located on the outer part of the shelf, in the Vøring basin (Area 2). There were not observed any evidence of polygonal faulting on the inner section of the Kai formation (Area 1), nor in the underlying Brygge formation here. As the Kai formation on the inner part of the shelf is underlying the thickest part of the Naust formation, there is reason to believe that the lack of polygonal faults in Area 1 is the result of a different sediment composition between the two areas. Polygonal faults generally occur in connection with the expulsion of fluids within the sediments, and can here be located in ooze sediments in the Kai formation. The inner part of the shelf may therefore not have any expulsion of fluids from the older, underlying sediments, or simply not be characterized by the same ooze-like deposits as further west in the Vøring basin.

Polygonal faults often occur frequently in fine grained sediment basin fills (Cartwright et al., 2003). The contraction of the Kai formation, which caused the faulting mechanism within the formation, is interpreted by Dewhurst et al. (1999) to have a connection to the amount of smectite within the sediment package. Further it is explained that the clayey ooze dominated Kai formation have a high smectite content in the Vøring basin, and are therefore able to frequently create faults at a large scale, which together with the compaction from the Naust formation creates polygonal faulting. Berndt et al., (2003) observed that the vertical extent of the polygonal faults is associated with the thickness of the host sediment package. Therefore, the vertically largest polygonal faults is found where the host Kai formation is at its thickest. The polygonal faults can, some areas in the Vøring basin, be observed to enter the bottommost sub-units of the Naust formation, which have a completely different sediment composition than the Kai and Brygge formations. This is interpreted to be the result of the rapid loading of the Naust formation. This is in unity with Gay and Berndt (2007) who suggested that the rapid loading from submarine slides may have reactivated the polygonal fault system, leading to an upward accumulation of the faults into the base Naust formation.

5.4 Ocean circulation in the study area during the deposition of the Kai formation

The deposition of the contouritic Kai formation has to a great extent been affected by anticlinal structures (anticlinal highs and basin escarpment) in the study area (Fig. 5-4-1). At the flanks of these highs, moat structures have been found, as well as elongated mounded

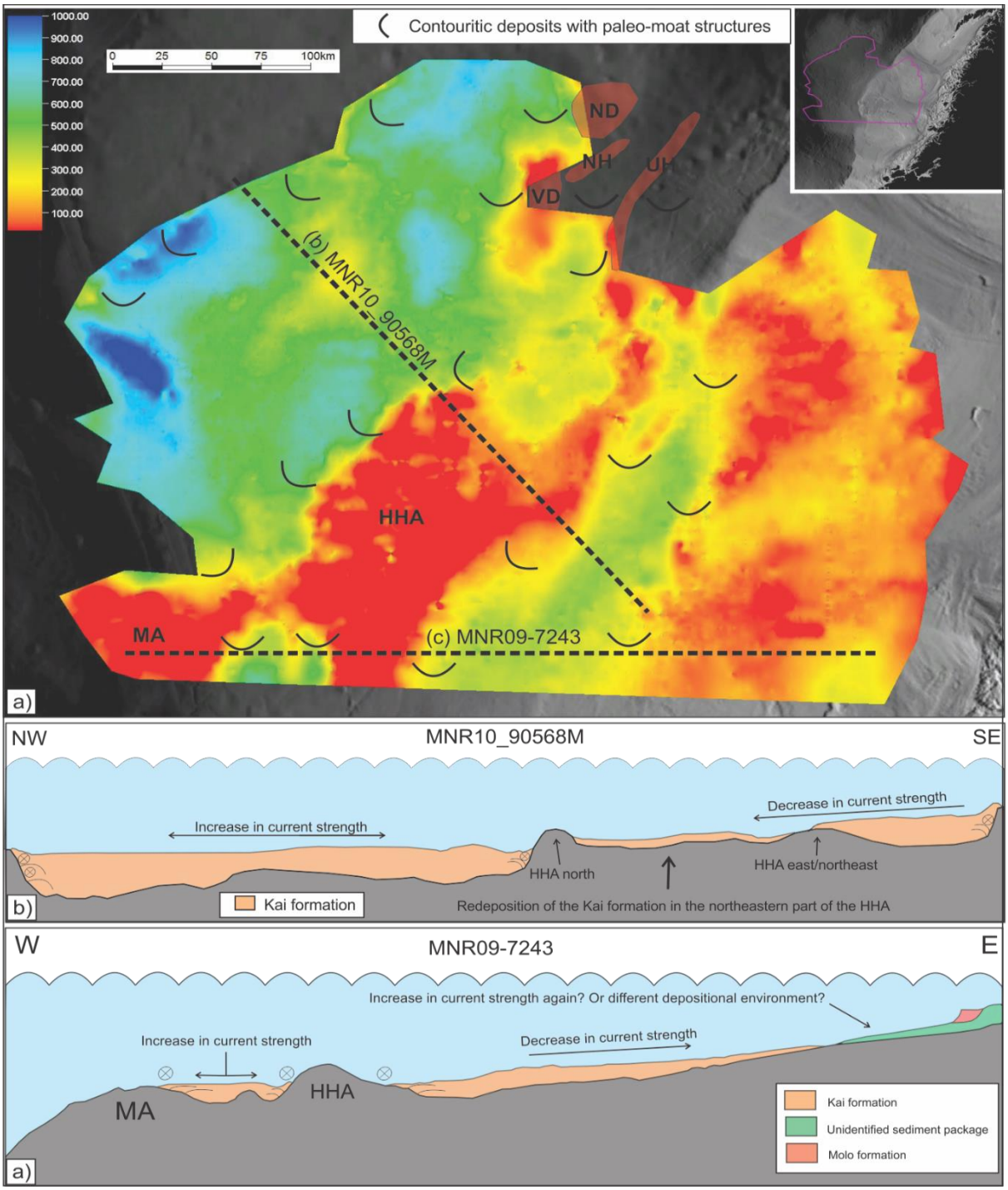

Figure 5-4-1: a) Thickness map of the Kai formation in the study area, with the location of the found moat structures. The red infillings at the northern part of the map shows structural elements which may have played a role in the oceanic circulation. b) Illustration of the seismic line MNR10_90568M with the distribution of the Kai formation in a NW/SE orientation throughout the study area. c) Illustration of seismic line MNR09-7243 with the distribution of the Kai- and Molo formation, as well as the unidentified sediment package in the easternmost part of the study area. The location of the seismic lines is displayed in a).

contourite structures, ending in onlapping reflection terminations. The non-deposition of contouritic sediments on the top of these highs confirms this hypothesis (Fig. 5-4-1).

The oceanic circulation in the study area is found to generally follow a northeast-flowing pattern, similar to the pattern found outside the present day coast of Norway (Laberg et al., 2005b; Stoker et al., 2005). It has been discussed that the interpreted current pattern here has a relation to similar bottom-current systems further south and north. Therefore it is reasonable to believe that the interpreted ocean-currents found in the study area, during the deposition of the Kai formation, is originating from the south and are transported out of the study area towards the north/northeast. This further suggest that the current pattern is entering the study area near the arches found the south (HHA and MA), as well as the inner part of the Vøring margin (Fig. 5-4-2). The outgoing bottom current pattern would then be located near the

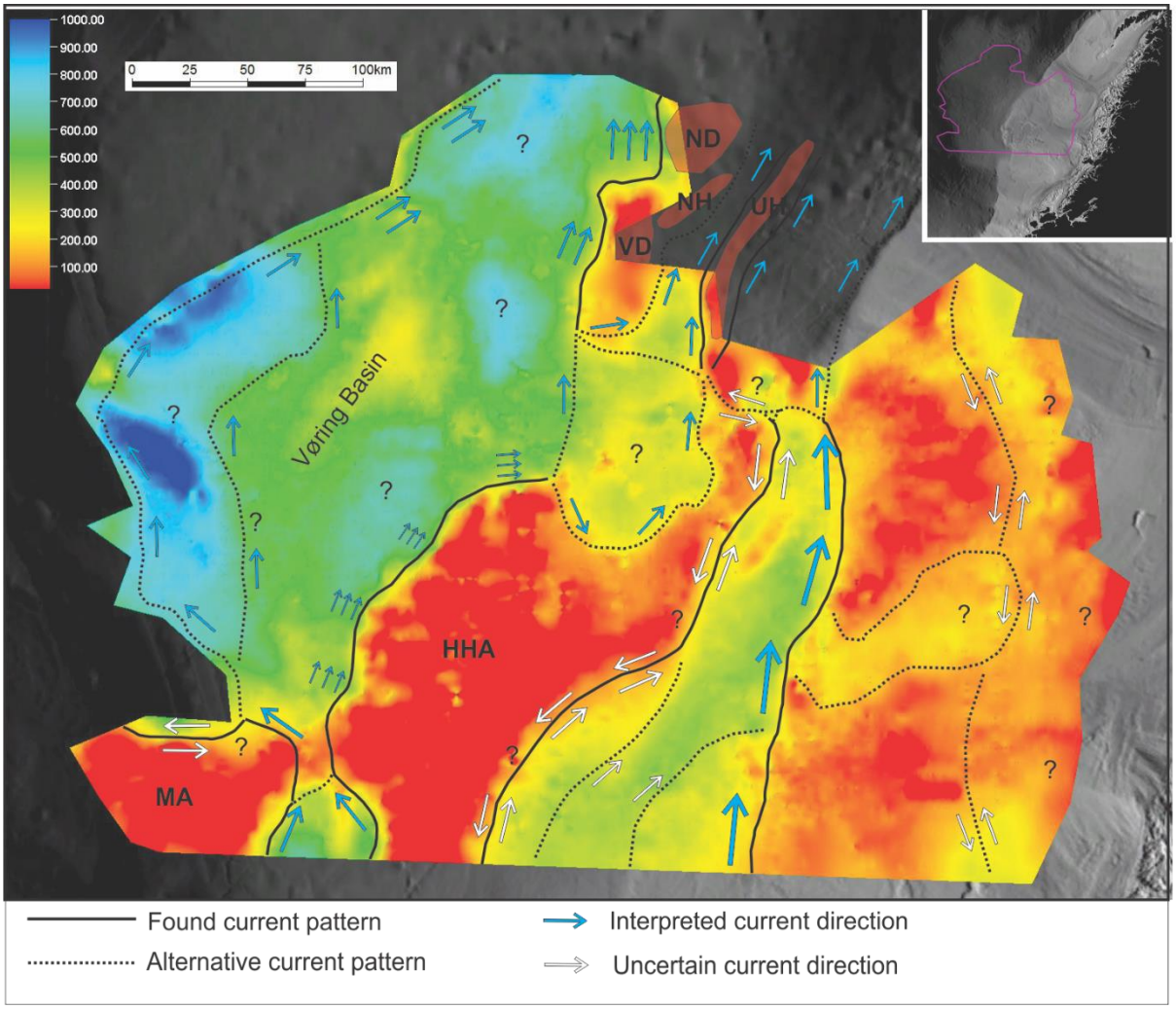

Figure 5-4-2: Thickness map of the Kai formation in the study area, with interpreted ocean circulation patterns and current flow direction. The red infillings at the upper part of the map shows structural elements which may have played a role in the north going oceanic circulation. Arrow size display an increase/decrease in current strength. Alignment of multiple arrows represent different generations of contourite deposits found at different locations upward the near high.

anticlinal highs in the northern part of the study area, as well as at the northern escarpment of the Vøring basin. The observed contour-indicating structures can help identify the pattern of the oceanic circulation, but not necessary the flowing direction of the currents. The general northward-flowing trend may therefore have some exceptions throughout the study area. A model of the oceanic circulation system during the deposition of the Kai formation have been made (Fig. 5.4.2). This study suggest a generally north/northeastern flowing system in the Vøring basin, with the largest currents located at the confinements of the basin, as well as around local anticlinal highs. Indications of contourite deposits have been found in the northwestern and southwestern part of the Vøring basin, with no clear contouritic evidence have been located in between, on the westernmost part of the Vøring Basin. Therefore multiple current patterns have been presented here.

On the inner shelf, it is also interpreted that the general flow direction is northwards, but due to compaction from local anticlinal structures in the northern part of the shelf, the flow pattern may turn southwards again. This is presented on Figure 5-4-2 as an uncertain flow pattern on the eastern flank of the Helland-Hansen Arch. North of the Helland-Hansen Arch the ocean circulation may deviate from the general trend, following the northeastern side of the arch, continuing northward towards the local domes and highs in the northern part of the study area. There have not been observed any structures suggesting the movement of the current here, but a higher deposition of contouritic Kai formation deposits than at the arches suggest that the area have been affected by bottom currents.

The eastern part of the study are lack evidence of bottom current activity. Still a sediment package possibly representing the Kai formation is found here. The lack of bottom current indications may be due to erosion from the overlying Naust formation. The Naust unconformity confirms that erosion were present during the deposition of the Naust formation, but how big impact the erosion had to the underlying sediments is unclear. The current velocity is interpreted to decrease towards this eastern part of the study area, which may suggest that the ocean currents in this area were too weak to deposit current related structures.

The Kai formation reaches approximately 200-300 ms (TWTT), which is similar to the thickness of the sediments around the Helland-Hansen Arch. If there were a north-flowing bottom current system here during the deposition of the Kai formation, it would strengthen

the interpretation that the vastness of the Naust formation have rerouted the present-day currents further west in the study area.

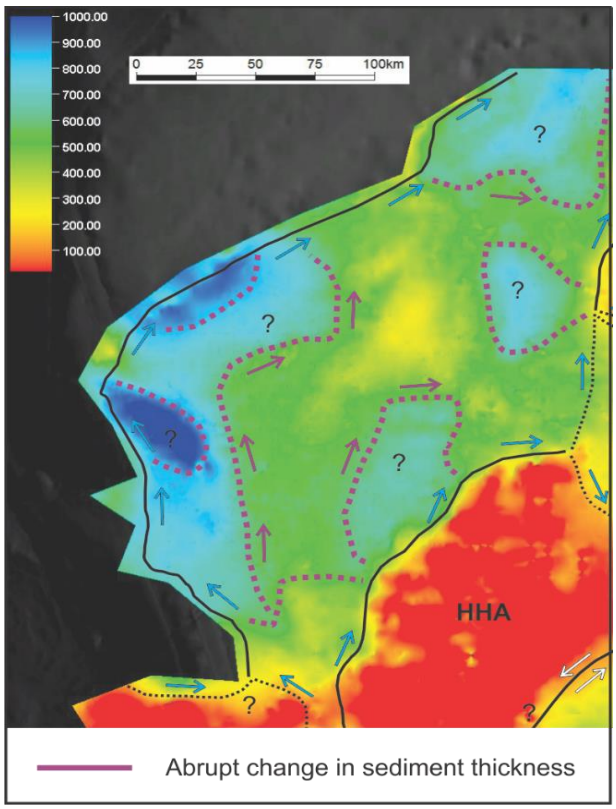

Figure 5-4-3: Outcrop of the Vøring basin region of the Thickness map, displaying changes in sediment thickness in relation to bottom currents in the area. Purple dotted lines display a pattern of abrupt changes in thickness of the Kai formation, which may be related to a change in current pattern.

In the Vøring basin, some abrupt changes in the sediment thickness have been accounted for (Fig. 5-4-3). The origin of these increases of the sediment thickness may be the result of bottom currents accumulating more sediments here. Another alternative is that the bottom currents in the Vøring basin at the time have eroded larger parts of the basin, which further implies that the currents with the highest velocity were located in the middle of the basin. There are no evidence to confirm this, and as the general trend of the currents were to follow the topographical heightening in the basin, this is a highly unlikely scenario. If the increase in sediment thickness were the result of accumulating bottom currents, it might be reasonable to assume that the abrupt changes symbolize different generations of contourite deposits. In the seismic data, there is observed current-influenced sediments on the inner part of the shelf, which indicates a current pattern further east than the pattern observed at present day. This implies that the topographical changes made by the Naust formation have had an impact on the pattern of the bottom currents off mid-Norway. This is in conformity with Laberg et al., (2005b), who suggested that the base Naust unconformity displays an abrupt change depositional environment, altering the oceanographic circulation.

The largest generation of contourite deposits have were found on the inner shelf. On the outer shelf, west of the HHA, multiple smaller generations were observed within the seismic data. This suggest a fairly steady accumulation of contourite deposits on the inner shelf, while a more changing system in favored on the outer shelf. The currents here were probably more affected by local tectonic changes, as well as sea-level oscillation. Sometime during the transition between Miocene and Pliocene a change to dominant hemipelagic sedimentation

occurred, indicating that the topographic control of the Vøring Plateau on the ocean currents was reduced (Laberg et al., 2005a). This might be the result of multiple generations of contouritic sediments building up at the flanks of the controlling anticlinal structures at the Vøring Plateau.

6. Summary and Conclusion

The Kai formation has been studied on the inner and outer shelf offshore Mid-Norway using 2D seismic data, correlated to some available wells. The overall aim was to increase our understanding of the depositional environment during the deposition of the Kai formation, in relation to the ocean circulation surrounding the Mid-Norwegian continental margin at the time. The main findings from this study are:

- The seismic signature on the inner shelf suggest the deposition of mounded elongated contourite drifts, with a thinning of the Kai formation towards the east.
- The seismic signature on the outer shelf suggest the deposition of multiple sub-units, representing changing intervals of current- pattern and strength, as well as possible sea-level oscillation.
- The seismic reflection pattern of the seismic subunits, as well as reflection termination towards the anticlinal structures (HHA and MA) in the area suggest sediments deposited from currents.
- Non-deposition of sediments on the local anticlinal highs (HHA and MA) suggest that the flow velocity of the bottom-currents in this area was too high for sediments to have been deposited.
- The ocean circulation during the deposition of the Kai formation follows the Vøring escarpment in the west-, the Helland-Hansen Arch in the middle-, and the shelf in the eastern part of the study area, with a general northeast flowing orientation. The ocean current pattern is clearly affected by anticlinal elevations in the study area.
- The deep-water circulation system in the study area, during Miocene-Pliocene, have many similarities with surrounding areas at the same time period (Lofoten-, Møre margin and the Rockall Trough), which suggest that the Vøring margin was related to the main ocean circulation system of the Norwegian – Greenland Sea at the time.
- The Kai/Molo relation in the eastern part of the study area is uncertain, but indication of a sediment package at the easternmost part of the area, with different sediment structure than the Molo formation, have been accounted for in the proposed model.
- The polygonal faults in the Vøring basin are related to dewatering, due to major overpressure buildup during the deposition of early Naust formation and/or the sediment composition (ooze deposits).

References

Andreassen, K. (2009). Lecture Notes for GEO-3123, Marine Geophysics. UiT, The Artic University of Norway.

Badley, M. E. (1985). Practical seismic interpretation. . *International Human Resources Development Corporation.*

Berndt, C., Bunz, S., & Mienert, J. (2003). Polygonal fault systems on the mid-Norwegian margin: a long-term source for fluid flow. *Subsurface Sediment Mobilization, 216*, 283-290.

Bohrmann, G., Henrich, R., & Thiede, J. (1990). Miocene to Quaternary paleoceanography in the northern North Atlantic: variability in carbonate and biogenic opal accumulations. *In: Bleil, U., Thiede, J (Eds.), Geological History of the Polar Oceans: Artic Versus Antarctic. Kluwer Academic Publishers, Netherlands*, 647-675.

Brekke, H. (2000). The tectonic evolution of the Norwegian Sea continental margin with emphasis on the Vøring and Møre basins. *Nbttvedt, A., et al., (Eds.), Dynamics of the Norwegian Margin, Spec. Publ. Geol. Soc. 167, 327–378.*

Brown, A. R. (1999). Interpretation of three-dimensional seismic data: American Association of Petroleum Geologist and the Society of Exploration Geophysics.

Bruns, P., Dullo, W.-C., Hay, W. W., Frank, M., & Kubik, P. (1998). Hiatuses on Vøring Plateau: sedimentary gaps or preservation artifacts? *Mar. Geol., 145*, 93-127.

Bryn, P., Berg, K., Stoker, M. S., Haflidason, H., & Solheim, A. (2005). Contourites and their relevance for mass wasting along the Mid-Norwegian Margin. *Marine and Petroleum Geology, 22*(1-2), 85-96.

Buiter, S. J. H., & Torsvik, T. H. (2014). A review of Wilson Cycle plate margins: A role for mantle plumes in continental break-up along sutures? *Gondwana Research, 26*(2), 627-653.

Cartwright, J., James, D., & Bolton, A. (2003). The genesis of polygonal fault systems: a review. *Subsurface Sediment Mobilization, 216*, 223-243.

Chand, S., Rise, L., Knies, J., Haflidason, H., Hjelstuen, B. O., & Boe, R. (2011). Stratigraphic development of the south Voring margin (Mid-Norway) since early Cenozoic time and its influence on subsurface fluid flow. *Marine and Petroleum Geology, 28*(7), 1350-1363.

Dahlgren, K. I. T., Vorren, T. O., & Laberg, J. S. (2002). Late Quaternary glacial development of the mid-Norwegian margin - 65 to 68 degrees N. *Marine and Petroleum Geology, 19*(9), 1089-1113.

Dahlgren, K. I. T., Vorren, T. O., Stoker, M. S., Nielsen, T., Nygard, A., & Sejrup, H. P. (2005). Late Cenozoic prograding wedges on the NW European continental margin: their formation and relationship to tectonics and climate. *Marine and Petroleum Geology, 22*(9-10), 1089-1110.

Dewhurst, D. N., Cartwright, J. A., & Lonergan, L. (1999). The development of polygonal fault systems by syneresis of colloidal sediments. *Marine and Petroleum Geology, 16*(8), 793-810.

Dowdeswell, J. A., & O Cofaigh, C. (2002). Glacier-influenced sedimentation on high-latitude continental margins: introduction and overview. *Glacier-Influenced Sedimentation on High-Latitude Continental Margins, 203*, 1-9.

Dowdeswell, J. A., Ottesen, D., & Rise, L. (2010). Rates of sediment delivery from the Fennoscandian Ice Sheet through an ice age. *Geology, 38*(1), 3-6.

Eidvin, T., Bugge, T., & Smelror, M. (2007). The Molo Formation, deposited by coastal progradation on the inner Mid-Norwegian continental shelf, coeval with the Kai Formation to the west and the Utsira Formation in the North Sea. *Norwegian Journal of Geology, 87*(1-2), 75-142.

Eidvin, T., Riis, F., & Rasmussen, E. S. (2014). Oligocene to Lower Pliocene deposits of the Norwegian continental shelf, Norwegian Sea, Svalbard, Denmark and their relation to the uplift of Fennoscandia: A synthesis. *Marine and Petroleum Geology, 56*, 184-221.

Eldholm, O., Tsikalas, F., & Faleide, J. I. (2002). Continental magin off norway 62-75N: Palaeogene tectono-magmatic segmentation and sedimentation. *Geological society London special Publication: Geological Society, London. In D. W. Jolley &*

B. R. Bell (Eds.), The North Atlantic igneous Province. "Stratigraphy, Tectonic, Volcanic and Magmatic Processes. Vol. 197, 39-68

Faleide, J. I., Vagnes, E., & Gudlaugsson, S. T. (1993). Late Mesozoic-Cenozoic Evolution of the South-Western Barents Sea in a Regional Rift Shear Tectonic Setting. *Marine and Petroleum Geology, 10*(3), 186-214.

Faleide, J. I., Solheim, A., Fiedler, A., Hjelstuen, B. O., Andersen, E. S., & Vanneste, K. (1996). Late Cenozoic evolution of the western Barents Sea-Svalbard continental margin. *Global and Planetary Change, 12*(1-4), 53-74.

Faleide, J. I., Tsikalas, F., Breivik, A. J., Mjelde, R., Ritzmann, O., Engen, O., . . . Eldholm, O. (2008). Structure and evolution of the continental margin off Norway and Barents Sea. *Episodes, 31*(1), 82-91.

Fronval, T., & Jansen, E. (1996). Rapid changes in ocean circulation and heat flux In the Nordic seas during the last interglacial period. *Nature, 383*(6603), 806-810.

Gay, A., & Berndt, C. (2007). Cessation/reactivation of polygonal faulting and effects on fluid flow in the Voring Basin, Norwegian Margin. *Journal of the Geological Society, 164*, 129-141.

Hjelstuen, B. O., Eldholm, O., & Skogseid, J. (1999). Cenozoic evolution of the northern Voring margin. *Geological Society of America Bulletin, 111*(12), 1792-1807.

Hjelstuen, B. O., Sejrup, H. P., Haflidason, H., Berg, K., & Bryn, P. (2004). Neogene and Quaternary depositional environments on the Norwegian continental margin, 62 degrees N-68 degrees N. *Marine Geology, 213*(1-4), 257-276.

Hjelstuen, B. O., Sejrup, H. P., Haflidason, H., Nygard, A., Ceramicola, S., & Bryn, P. (2005). Late Cenozoic glacial history and evolution of the Storegga Slide area and adjacent slide flank regions, Norwegian continental margin. *Marine and Petroleum Geology, 22*(1-2), 57-69.

Jansen, E., & Sjoholm, J. (1991). Reconstruction of Glaciation over the Past 6 Myr from Ice-Borne Deposits in the Norwegian Sea. *Nature, 349*(6310), 600-603.

Laberg, J. S., & Vorren, T. O. (1996). The Middle and Late Pleistocene evolution of the Bear Island Trough Mouth Fan. *Global and Planetary Change, 12*(1-4), 309-330.

Laberg, J. S., Dahlgren, T., Vorren, T. O., Haflidason, H., & Bryn, P. (2001). Seismic analyses of Cenozoic contourite drift development in the Northern Norwegian Sea. *Marine Geophysical Researches, 22*(5-6), 401-416.

Laberg, J. S., Dahlgren, K. I. T., & Vorren, T. O. (2005a). The Eocene-Late Pliocene paleoenvironment in the Voring Plateau area, Norwegian Sea - paleoceanographic implications. *Marine Geology, 214*(1-3), 269-285.

Laberg, J. S., Stoker, M. S., Dahlgren, K. I. T., de Haas, H., Haflidason, H., Hjelstuen, B. O., . . . Ceramicola, S. (2005b). Ceaozoic alongslope processes and sedimentation on the NW European Atlantic margin. *Marine and Petroleum Geology, 22*(9-10), 1069-1088.

Laberg, J. S., & Camerlenghi, A. (2008). The significance of contourites for submarine slope stability. In M. Rebesci & A. Canerkebghi (Eds.), *Contourites, Developments in Sedimentology* (Vol. 60, pp. 537-556).

Lundin, E., & Dore, A. G. (2002). Mid-Cenozoic post-breakup deformation in the 'passive' margins bordering the Norwegian-Greenland Sea. *Marine and Petroleum Geology, 19*(1), 79-93.

Løseth, H., & Hernriksen, S. (2005). A Middle to Late Miocene compression phase along the Norwegian passive margin. *In: Doré, A.G., Vining, B.A., (Eds.), Petroleum Geology: North-West Europe and Global Perspectives-proceedings of the 6th Petroleum Conferance*, 845-859.

Mangerud, J., Gyllencreutz, R., Lohne, Ø., & Svendsen, J. I. (2011). Glacial History of Norway. *In J. ehlers, P. l: Gibbard, & P. D. r. Hughes (Eds.),, Quaternary Glaciations Extent and Chronology* (Elsevier Science Limited), 279-298.

Martinsen, O. J., & Nøttvedt, A. (2007). The making of a land. *Norwegian Journal of Geology, 2. Edition*(Chapter 14.).

Miller, K. G., & Tucholke, B. E. (1983). Development of Cenozoic abyssal circulation south of the Greenland-Scotland Ridge. . *In: Bott, M. P. H et al., (EDS), Structural Development of the Greenland-Scotland Rigde. Plenum Publishing , pp. 449-589.*

Mitchum, R. M., Vail, J. P. R., & Sangree, J. B. (1977). Seismic Stratigraphy and Global Changes of Sea Level, Part 6: Stratigraphic Interpretation of Seismic Reflection Patterns in Depositional Sequences. In C. E. Payton (Ed.), *Seismic Stratigraphy - applications to hydrocarbon exploration* (Vol. 26). Tulsa, Oklahoma, U.S.A.: The American Association of Petroleum Geologists.

Nielsen, T., Knutz, P. C., & Kuijpers, A. (2008). Seismic Expression of Contourite Depositional System *Developments in Sedimentology* (Vol. 60): Geological Survey of Denmark and Greenland (GEUS), Øster Voldgade, Copenhagen, Denmark.

Nygard, A., Sejrup, H. P., Haflidason, H., & Bryn, P. (2005). The glacial North Sea Fan, southern Norwegian Margin: architecture and evolution from the upper continental slope to the deep-sea basin. *Marine and Petroleum Geology, 22*(1-2), 71-84.

Olsen, L., Sveian, H., Bergstrøm, B., & Rise, L. (2013). Quaternary glaciations and their variations in Norway and on the Norwegian continental shelf. *In Olsen, L.,Fredin, O. and Olesen, O. (eds.) Quaternary Geology of Norway, Geological Survey of Norway Special Publication, 13,*, pp. 27-78.

Ottesen, D., Rise, L., Rokoengen, K., & Sættem, J. (2001). Glacial processes and large-scale morphology on the mid-Norwegian continental shelf. *NPF Special Publication 10, 441–449.*

Ottesen, D., Dowdeswell, J. A., & Rise, L. (2005). Submarine landforms and the reconstruction of fast-flowing ice streams within a large Quaternary ice sheet: The 2500-km-long Norwegian-Svalbard margin (57 degrees-80 degrees N). *Geological Society of America Bulletin, 117*(7-8), 1033-1050.

Ottesen, D., Rise, L., Andersen, E. S., Bugge, T., & Eidvin, T. (2009). Geological evolution of the Norwegian continental shelf between 61 degrees N and 68 degrees N during the last 3 million years. *Norwegian Journal of Geology, 89*(4), 251-265.

Rebesco, M. (2005). Contourites. *In R.C. Selley, R.C. Cocks, L.R.M. Plimer (Eds.), Encyclopedia of Geology, vol. 4, Elsevier, Oxford (2005)*, pp. 513-527.

Rider, M. H., Kennedy, M., & Rider-French, C. (2011). *The geological interpretation of well logs*. Scotland: Rider-French.

Riis, F., Berg, K., Cartwright, J., Eidvin, T., & Hansch, K. (2005). Formation of large, crater-like evacuation structures in ooze sediments in the Norwegian Sea. Possible implications for the development of the Storegga Slide. *Marine and Petroleum Geology, 22*(1-2), 257-273.

Rise, L., Ottesen, D., Berg, K., & Lundin, E. (2005). Large-scale development of the mid-Norwegian margin during the last 3 million years. *Marine and Petroleum Geology, 22*(1-2), 33-44.

Rise, L., Ottesen, D., Longva, O., Solheim, A., Andersen, E. S., & Ayers, S. (2006). The Sklinnadjupet slide and its relation to the Elsterian glaciation on the mid-Norwegian margin. *Marine and Petroleum Geology, 23*(5), 569-583.

Rise, L., Chand, S., Hjelstuen, B. O., Haflidason, H., & Boe, R. (2010). Late Cenozoic geological development of the south Voring margin, mid-Norway. *Marine and Petroleum Geology, 27*(9), 1789-1803.

Rydningen, T. A., Vorren, T. O., Laberg, J. S., & Kolstad, V. (2013). The marine-based NW Fennoscandian ice sheet: glacial and deglacial dynamics as reconstructed from submarine landforms. *Quaternary Science Reviews, 68*, 126-141.

Stoker, M. S. (2002). Late Neogene development of the UK Atlantic margin. *In Dorè, A., Cartwright, J. A., Stoker, M.S., Vorren, T.O., Turner, J.P., White, N. (Eds.), Exhumation of the North Atlantic Margin: Timing, Mechanism and Implications for Petroleum Exploration, Geol. Soc. London Spec. Publ. 196, 313-329.*

Stoker, M. S., Praeg, D., Hjelstuen, B. O., Laberg, J. S., Nielsen, T., & Shannon, P. M. (2005). Neogene stratigraphy and the sedimentary and oceanographic development of the NW European Atlantic margin. *Marine and Petroleum Geology, 22*(9-10), 977-1005.

Storvoll, V., Bjorlykke, K., & Mondol, N. H. (2006). Velocity-depth trends in Mesozoic and Cenozoic sediments from the Norwegian Shelf: Reply. *Aapg Bulletin, 90*(7), 1145-1148.

Stow, D. A. V., Faugères, J.-C., Howe, J. A., Pudsey, C. J., & Viana, A. R. (2002). Bottom currents, contourites and deep-sea sediment drifts: current state-of-the-art. *In Stow, D.A.V., Pudsey, C.J., Howe, J.A., Faugères, J.A. & Viana, A.R. (eds): Deep-*

Water Contourite Systems: Modern Drifts and Ancient Series, Seismic and Sedimentary Characteristics., Geological Society, London, Memoirs, 22.

Svendsen, J. I., Alexanderson, H., Astakhov, V. I., Demidov, I., Dowdeswell, J. A., Funder, S., . . . Stein, R. (2004). Late quaternary ice sheet history of northern Eurasia. *Quaternary Science Reviews, 23*(11-13), 1229-1271.